Mohan Lal Kolhe *Editor*

Renewable Energy Systems and Sources

Proceedings of International Conference on Renewable and Clean Energy (ICRCE) 2023

Springer

Renewable Energy Systems and Sources

Mohan Lal Kolhe
Editor

Renewable Energy Systems and Sources

Proceedings of International Conference on Renewable and Clean Energy (ICRCE) 2023

Springer

Editor
Mohan Lal Kolhe
Smart Grid and Renewable Energy
Faculty of Engineering and Science
University of Agder
Grimstad, Norway

ISBN 978-981-99-6289-1 ISBN 978-981-99-6290-7 (eBook)
https://doi.org/10.1007/978-981-99-6290-7

This Springer imprint is published by the registered company Springer Nature Singapore Pte Ltd.
The registered company address is: 152 Beach Road, #21-01/04 Gateway East, Singapore 189721, Singapore

Paper in this product is recyclable.

Conference Committees

Conference General Chairs

Prof. Ryuichi Yokoyama, Waseda University, Japan
Prof. Akashi Shigeo, Tokyo University of Science, Japan

Conference Co-chair

Prof. Mingcong Deng, Tokyo University of Agriculture and Technology, Japan

Conference Program Chairs

Prof. Mohan Lal Kolhe, Universitetet of Agder, Norway
Prof. Dr. Lingai Luo, Polytech' Nantes—Université de Nantes, France
Prof. Shogo Nishikawa, Nihon University, Japan

Conference Program Co-chair

Prof. Masafumi Yamaguchi, Toyota Technological Institute, Japan

Conference Steering Co-chairs

Prof. Muhammad Arfin Khan Lodhi, Texas Tech University, USA
Prof. Yasuhiro Noro, Kogakuin University, Japan

Conference Publicity Chair

Assoc. Prof. Akira NISHIMURA, Mie University, Japan

Conference Technical Committees

Prof. Tarlochan Sidhu, University of Ontario Institute of Technology, Canada
Prof. Zhaoyun Zhang, Dongguan University of Technology, China
Prof. Marco Jung, Bonn-Rhein-Sieg University of Applied Sciences, Germany
Prof. Ir. Dr. Chong Wen Tong, University of Malaya, Malaysia
Prof. Adem Akpınar, Bursa Uludag University, Turkey
Prof. Dr. Mihaela Popescu, University of Craiova, Romania
Prof. Roberto Pfuyo, Universidad Nacional Tecnologica De Lima Sur, Peru
Prof. Ahmed M. El-Nahas, Menoufia University, Egypt
Prof. Dinesh Kumar Sharma, KK University, India
Assoc. Prof. Rosmadi Ghazali, Fakulti Sains Gunaan, Malaysia
Assoc. Prof. Shunichi Ohmori, Waseda University, Japan
Assoc. Prof. Diankai Qiu, Shanghai Jiao Tong University, China
Assoc. Prof. Pooya Davari, Aalborg University, Denmark
Assoc. Prof. Pierluigi Siano, University of Salerno, Italy
Assoc. Prof. Worachest Pirompugd, Burapha University, Thailand
Assoc. Prof. Rodney H. G. Tan, UCSI University, Malaysia
Assoc. Prof. Chu-Fen Li, National Formosa University, Taiwan
Asst. Prof. Sandra Hasanefendic, Vrije Universiteit Amsterdam, Netherlands
Asst. Prof. Ekkachai Sutheerasak, Burapha University, Thailand
Asst. Prof. Pirat Khunkitti, Khon Kaen University, Thailand
Dr. Noppakun Sangkhiew, Silpakorn University, Thailand
Dr. Smith Eiamsa-ard, Mahanakorn University of Technology, Thailand
Dr. Xinggang Yan, University of Kent, UK
Dr. Mahdi Majidniya, Université de Lorraine, France
Dr. Philippe Le-Huy, Hydro-Quebec Research Institute, Canada
Dr. Maziar Rastmanesh, Nautical Institue, Canada
Dr. Muhammad Imran Khan, Hamad Bin Khalifa University, Qatar
Dr. Sajid Muhaimin Choudhury, Bangladesh
Dr. Raik C. Orbay, Volvo Car Corporation, Sweden

Dr. Takuji Matsumoto, Kanazawa University, Japan
Dr. Tao Chen, University of Manitoba, Canada
Dr. Meiling Yue, Beijing Jiaotong University, China
Dr. Daniele Mestriner, University of Genoa with Regione Liguria and Toshiba S.P.A., Italy
Dr. I-Hsien Liu, National Cheng Kung University, Taiwan
Dr. Malka N. Halgamuge, Melbourne School of Engineering, Australia
Dr. Ir. Yuli Setyo Indartono, Bandung Institute of Technology, Indonesia
Dr. Poonam Sharma, Paradigm of Science Cultivation and Ingenious Cultivation Foundation, India
Dr. Chathura Ranasinghe, University of Moratuwa, Sri Lanka
Dr. Chokchai Chuenwattanapraniti, Burapha University, Thailand
Dr. Masoud Taghavi, Technical and Vocational University (TVU), Iran

Editorial

The development of sustainable energy systems will soon incorporate a sizable proportion of renewable energy technologies. The utilization of renewable energy technologies and resources has the potential to revolutionize how we produce and use energy, with substantial positive effects on the environment, the economy, and society. Even if there are obstacles to overcome, continuing to develop and invest in renewable energy technology is crucial to building a sustainable future for everyone.

The book voume 'Renewable Energy Systems and Sources,' Select Proceedings of International Conference on Renewable and Clean Energy (ICRCE) 2023, Special Volume of book series Springer Lecture Notes in Electrical Engineering (e-ISSN: 1876-1119) contains peer-reviewed select papers from the ICRCE 2023. The goal of this special book is to demonstrate advances in renewable energy systems that will contribute to sustainable development. The book chapters investigate cutting-edge solutions and best practices for renewable energy technology in order to meet the UN's SDG7 goal of "ensuring access to affordable, reliable, sustainable, and modern energy for all." Innovative system engineering techniques are included in this book for the techno-economic operation and integration of renewable energy sources. It addresses important topics such as energy network integration, dispatching of techno-economic power from renewable energy sources, operation of energy networks with growing penetration of renewable energy sources, energy efficiency, etc. The main aim of the book volume is to inform the readers about how net zero goals may be attained in practical applications by integrating renewable energy technology with energy conversion processes. Graduate students, academics, business professionals,

and policymakers interested in investigating the possibilities of energy technology in the creation of sustainable energy systems may find the book to be a helpful resource.

Grimstad, Norway Prof. Mohan Lal Kolhe

Preface

2023 13th International Conference on Renewable and Clean Energy (ICRCE 2023) was held in Tokyo, Japan during February 25–27, 2023, which is co-sponsored by Tokyo University of Science, Japan. It offered an ideal platform for presentation, discussion, criticism and exchange of innovative ideas and current challenges in the field of renewable and clean energy.

In consideration of health and safety for everyone, ICRCE 2023 is still made offline and online mixed. We feel pity that we cannot gather all together in Tokyo due to some travel restrictions. However, we worked hard to provide you with a high-quality conference as always, and with the hope that we can get your support.

The main theme of the conference is to address and deliberate on the latest technical status and recent trends in the research and applications of renewable and clean energy. The purpose of the conference is to provide an opportunity for the scientists, engineers, industrialists, scholars and other professionals from all over the world to interact and exchange their new ideas and research outcomes in related fields and develop possible chances for future collaboration. The conference is also aimed at motivating the next generation of researchers to promote their interests in renewable and clean energy.

The papers in the proceedings are accepted after being peer-reviewed by the conference technical committee, international reviewers based on the topic and quality. With the keynote speeches, invited speeches, oral sessions, we had an exciting program this year, which allowed participants to present and discuss the latest research and industrial developments in these fields.

On behalf of the organizing committee, we would like to deeply express our heartfelt appreciation to all our delegates, keynote speakers, invited speakers, session chairs, authors as well as all the committee members involved in the technical evaluation of conference papers and in the organization of the conference for their time, effort, and great contributions.

We also wish that this conference will be an unforgettable and wonderful experience for you.

Grimstad, Norway Prof. Mohan Lal Kolhe

Contents

Smart Grid and Power System Management

Online Optimal Resources Mix of Power System Using Dizzy Dragonfly Algorithm

Soraphon Kigsirisin

Abstract Online Resources Mix (ORM) consisting of wind turbine generators (WTGs), photovoltaics (PVs), battery energy storage systems (BESSs), fuel cell generators (FC), and the external sources play a vital role in supplying electricity to production processes of modern manufacturing plants. In this study, the power system of the two raw water stations (RWSs) at the Mahasawat Water Treatment plant (MHS) is studied and modified to utilize ORM. Then, developed from Dragonfly Algorithm (DA), Dizzy Dragonfly Algorithm (DDA) is proposed for dragonflies to follow the new movement characteristics to gain supreme performances in swarms. This aims to discover the excellent optimal power of ORM for RWSs through the minimization of the total cost of operation and maintenance, fuel, and electricity commercialization between RWSs and the external source, as the objective function of this study. The Time-of-Use (TOU) tariffs are considered on the commercialization cost. As a result, DDA provides the best total cost over the cost by DA and the other referred optimization algorithms.

Keywords Dizzy dragonfly algorithm · Electricity commercialization · Metaheuristic algorithm · Optimal resources mix · Time-of-use tariffs · Water treatment plant

1 Introduction

At present, power systems of recent manufacturing plants and residentials have been designed and constructed to generate and supply electricity to their production processes and loads, respectively. As in technological and friendly-environmental eras, those power systems utilize renewable energy such as WTGs, PVs, and BESSs, modern generators such as FC, and external sources for power generation [1, 2]. In this study, this utilization is called "Online Resources Mix (ORM)". The goals of utilizing ORM to power systems are to save power generation cost, reduce gas emission, and

S. Kigsirisin (✉)
Department of Corporate Innovation, Metropolitan Waterworks Authority, Bangkok, Thailand
e-mail: soraphon.works@gmail.com; soraphon.k@mwa.co.th

M. L. Kolhe (ed.), *Renewable Energy Systems and Sources*,
https://doi.org/10.1007/978-981-99-6290-7_1

make profits from electricity commercialization [3]. Without any ORM application in power systems, consumers must only buy electricity from external sources and pay high-electricity-cost bills unavoidably which results in loss of financial gains.

Mahasawat Water Treatment plant (MHS) is one of the Metropolitan Waterworks Authority, Thailand, water production plants. It has the responsibility to produce, transmit, and distribute quality water to customers in Bangkok, Nonthaburi, and Samutprakarn provinces with the maximum capacity of water production of around 1.6 million sq.m./day [4]. Water production processes in the MHS plant comprise the two raw water stations, the one water transmission station, the one water distribution station, and the filter and chemical buildings. For RWSs, they take in charge of pumping raw water up from a raw water canal to the MHS water production processes with the maximum power consumption of about five megawatts. Currently, RWSs have been supplied by external sources by an electricity supplier under the TOU tariffs. For this reason, RWSs are unmanageable for power and need to take enormous money to that supplier more than 50 million dollars per year.

For years, many researchers have invented and applied metaheuristic algorithms to solve such complex, non-convex, and non-linear problems in contemporary and modern power systems. For example, [5] applied Colliding Bodies Optimization Algorithm to solve optimal power flow problems on IEEE bus test systems. Regis et al. [6] performed Particle Swarm Optimization (PSO) to find out the optimal battery sizing for residential sectors. Yusri et al. [7] used Artificial Bee Colony Algorithm to discover the optimal sizing of PV panels in a case study. After that, original optimization algorithms were developed for agents to gain more exceptional performances in exploration and exploitation stages. The definitions of these stages can be read in [8]. The purpose of developed optimization algorithms is for agents to meet and provide excellent solutions to considered problems than solutions by their originals. For instance, [9] found a hybrid phasor PSO and gravitational search algorithm to unravel optimal power flow under WTGs and PVs utilization in a power generation section in the IEEE 30-bus test system. Khenissi et al. [10] invented hybrid PSO and genetic algorithm to obtain the PVs sizing connecting with the external sources.

One of the well-known swarm intelligence algorithms is Dragonfly Algorithm (DA). The author in [11] observed and converted the natural behaviors of dragonflies (agents) into mathematical equations for easy use to solve such complicated problems. In nature, dragonflies create swarms to gather with other dragonflies (friends) for groupings, to hunt the food source (a solution to a problem) for meals, and to avoid the enemy source for survivors. According to [12, 13], DA dragonflies have much efficient exploration performance. However, this study views that DA has disadvantageous features resulting in not meeting good food sources by dragonflies. Therefore, to eliminate these drawbacks, this study develops and proposes the new movement characteristics of dragonflies as the novel optimization technique, the so-called "Dizzy Dragonfly Algorithm". The movement characteristics of dragonflies in static and dynamic swarms are modified for getting greater exploration and exploitation performances to discover the most excellent food source in the search space. More details of DDA will be discussed in the following sections.

In this study, the main contributions are expressed as follows.

- Studying and modifying the power system of RWSs at MHS by the ORM utilization.
- Improving the performances of DA dragonflies by proposing many novel movement characteristics to dragonflies in static and dynamic swarms, so-called DDA.
- Simulating DDA to find out the optimal ORM for RWSs at MHS.
- Comparing and discussing the results by DDA with DA and the other referred optimization algorithms.

2 Online Resources Mix, Constraints, and Objective Function

In this section, equations of the ORM power generation are explained. Also, the power system constraints and the objective function of this study are formulated as mathematical equations.

2.1 Online Resources Mix

Wind turbine generator: Output power of WTGs depends on wind velocity as defined in (1) [9]. Hence, the total output power of a WTG is defined in (2).

$$p_{WTG}^{t} = \begin{cases} 0 & v^{t} \leq v_{\text{cut-in}}, v^{t} \geq v_{\text{cut-out}} \\ p_r \left(\frac{v^{t} - v_{\text{cut-in}}}{v_r - v_{\text{cut-out}}} \right) & v_{\text{cut-in}} < v^{t} < v_r \\ p_r & v_r, \leq v \leq v_{\text{cut-out}} \end{cases} \tag{1}$$

where, p_{WTG}^{t} denotes the output power generated by a WTG at time t (W); v^{t} denotes wind velocity at time t (m/s); $v_{\text{cut-in}}$ and $v_{\text{cut-out}}$ denote cut-in and cut-out wind velocity of a WTG, respectively (m/s); p_r denotes the rated power of a WTG (W).

$$P_{\text{WTG}}^{t} = \eta_{\text{WTG}} p_{\text{WTG}}^{t} N_{\text{WTG}} \tag{2}$$

where, P_{WTG}^{t} denote the total output power of WTGs at time t (W); N_{WTG} denotes the integer number of WTG in a considered system; η_{WTG} denotes the WTGs efficiency in percent.

2.1.1 Photovoltaic

Generated power by PVs rely on solar irradiance, ambient temperature, PV efficiency, and specifications as defined in (3) [14].

$$P_{\mathrm{PV}}^{t} = N_{\mathrm{PV}} P_{\mathrm{mod}} F F V_{y}^{t} I_{y}^{t} \tag{3}$$

where, N_{PV} denotes the integer number of PVs in a considered system; P_{mod} the capacity of a PV module; $F F$ denotes fill factor that can be calculated in (4); V_{y}^{t} and I_{y}^{t} can be found in (5) and (6), respectively.

$$F F = \frac{V_{\mathrm{MPP}} I_{\mathrm{MPP}}}{V_{\mathrm{oc}} I_{\mathrm{sc}}} \tag{4}$$

$$V_{y}^{t} = V_{\mathrm{oc}} - K_{v} T_{c} \tag{5}$$

$$I_{y}^{t} = s_{a}^{t}[I_{\mathrm{sc}} + K_{i}(T_{C}^{t} - 25)] \tag{6}$$

$$T_{C}^{t} = T_{A}^{t} + s_{a}^{t}\left(\frac{N_{OT} - 20}{0.8}\right) \tag{7}$$

where, T_{c}^{t} denotes cell temperature at time t (°C); T_{A}^{t} denotes ambient temperature at time t (°C); s_{a}^{t} denotes average solar irradiance at time t; N_{OT} denotes nominal operating temperature of cell (°C); I_{sc} denotes short circuit current (A); K_{i} denotes current temperature coefficient (A/°C); K_{v} denotes voltage temperature coefficient (V/°C); N_{PV} denotes the integer number of PV in a considered system; V_{oc} denotes open-circuit voltage (V); I_{MPP} denotes current at maximum power point (A); V_{MPP} denotes voltage at maximum power point (V);

2.1.2 Battery Energy Storage System

Unlike WTGs and PVs on power generation, BESSs can be charged for power storage from electricity supply and/or generators, be discharged for supplying power storage to loads, or be regardless of operation. Charging or discharging of BESSs is subject to power system conditions, and BESSs behaviors at a time, so-called "State of Charge at time t (SOC^{t})" [15]. SOC^{t} is defined in (8)–(10).

$$\text{If battery is charged}: \mathrm{SOC}^{t+1} = \mathrm{SOC}^{t} + \frac{\Delta t \times \eta_{\mathrm{ch}}}{E_{\mathrm{nom}}}\left(P_{\mathrm{ch}}^{t}\right) \tag{8}$$

$$\text{If battery is discharged}: \mathrm{SOC}^{t+1} = \mathrm{SOC}^{t} - \frac{\Delta t}{E_{\mathrm{nom}} \eta_{\mathrm{dis}}}\left(P_{\mathrm{dis}}^{t}\right) \tag{9}$$

$$\text{For do nothing} : \text{SOC}^{t+1} = \text{SOC}^{t} \tag{10}$$

where, P_{ch}^{t} denotes the charging power at time t (W); η_{ch} denotes the battery charging efficiency; Δt denotes the interval time (equal to 1 h in this study); E_{nom} denotes the battery system nominal energy (W); P_{dis}^{t} denotes the discharging power at time t (W); η_{dis} denotes the battery discharging efficiency in percent.

The total power of BESSs at time t (P_{BESS}^{t}) is defined in (11).

$$P_{\text{BESS}}^{t} = N_{\text{BESS}} p_{\text{BESS}}^{t} \tag{11}$$

where, p_{BESS}^{t} is equal to P_{ch}^{t} or P_{dis}^{t} in case of battery charging or discharging state, respectively (W); N_{BESS} denotes the integer number of BESSs in a considered system.

2.1.3 Fuel Cell Generator

FC generates electricity by a chemical reaction between hydrogen and oxygen. In this study, Protone Exchange membrane (PEM) fuel cell is used for the FC cells and overall efficiencies. The fuel cost of an FC can be calculated in (12) [3].

$$C_{\text{FC}} = C_{\text{nf}} \sum_{t} \frac{P_{\text{FC}}^{t}}{\eta_{\text{FC}}} \tag{12}$$

where, C_{FC} denotes the fuel cost of a FC ($/kWh); C_{nf} denotes the natural gas price for a FC ($/kWh); P_{FC}^{t} denote the output power at time t (W); η_{FC} denotes cell efficiency in percent.

2.2 Constraint

2.2.1 Power Balance

The power balance of a considered system is defined in (13)

$$P_{\text{WTG}}^{t} + P_{\text{PV}}^{t} + P_{\text{BESS}}^{t} + P_{\text{FC}}^{t} + P_{\text{buy}}^{t} - P_{\text{sell}}^{t} = P_{\text{Load}}^{t} \tag{13}$$

where, in this study, P_{BESS}^{t} is a negative value for BESSs charged for electrical storages, and positive value for BESSs discharging electricity to a system; P_{buy}^{t} and P_{sell}^{t} denote the buying and selling power from/to the external supplier (W), respectively.

2.2.2 State of Charge (SOC^t)

SOC^t Must be between $\text{SOC}^{\min}$ and $\text{SOC}^{\max}$ as defined in (14).

$$\text{SOC}^{\min} \leq \text{SOC}^t \leq \text{SOC}^{\max} \tag{14}$$

where, $\text{SOC}^{\min}$ and $\text{SOC}^{\max}$ denote the minimum and maximum SOC of BESSs in a considered system.

In this study, all BESSs must be only in a charging state or a discharging state. Therefore, this study defines Eq. (15) for preventing the immediate occurrence of both charging and discharging stages at the same time.

$$\text{ch}^t + \text{dis}^t \leq 1 \tag{15}$$

where, ch^t and dis^t denote the charging and discharging states of BESSs at time t, respectively.

2.2.3 Limits of Generator Numbers and Capacities

The optimal number of WTGs, PVs, and BEESs and the optimal output power of an FC are found out. Therefore, the boundary limits of ORM are determined below.

$$N_{\text{WTG}}^{\min} \leq N_{\text{WTG}} \leq N_{\text{WTG}}^{\max} \tag{16}$$

$$N_{\text{PV}}^{\min} \leq N_{\text{PV}} \leq N_{\text{PV}}^{\max} \tag{17}$$

$$N_{\text{BESS}}^{\min} \leq N_{\text{BESS}} \leq N_{\text{BESS}}^{\max} \tag{18}$$

$$P_{\text{FC}}^{\min} \leq P_{\text{FC}} \leq P_{\text{FC}}^{\max} \tag{19}$$

where, $N_{\text{WTG}}^{\max}$, $N_{\text{PV}}^{\max}$ and $N_{\text{BESS}}^{\max}$ denote the maximum integer number of WTGs, PVs, and BESSs, respectively. $P_{\text{FC}}^{\min}$ and $P_{\text{FC}}^{\max}$ denote the minimum and maximum power of an FC, respectively.

2.3 Mathematical Objective Function

The objective function of this study is to minimize the total cost of the two parts as defined in (20) (OF). The first part considers the cost of operation and maintenance of all generators (C_{OM}) which can be calculated in (21), and the cost of FC fuel

(C_{FC}). The other deems the electricity commercialization cost between RWSs and the supplier.

$$\text{min. OF} = (C_{OM} + C_{FC}) + \left(C_{buy} P_{buy} - C_{sell} P_{sell}\right) + pnf \tag{20}$$

where, C_{buy} and C_{sell} denote the buying and selling electricity costs from/to the supplier, respectively; pnf denotes the exterior penalty function factor used to preserve the boundary limits of variables (equivalent to 1e+10 for a variable breaking its limit) [16].

$$C_{OM} = C_{OM_{WTG}} P_{WTG} + C_{OM_{PV}} P_{PV} + C_{OM_{FC}} P_{FC} \tag{21}$$

where, $C_{OM_{WTG}}$, $C_{OM_{PV}}$ and $C_{OM_{FC}}$ denote the operation and maintenance cost of WTGs, PVs, and an FC, respectively. Note that, the operation and maintenance cost of BEESs is ignored, because this study utilizes operation and maintenance free BESSs).

3 Online Resources Mix, Constraints, and Objective Function

3.1 Dragonfly Algorithm

Primarily, the concepts of Dragonfly Algorithm (DA) are explained. DA is a kind of swarm computational algorithm mimicking and converting the natural behaviors of dragonflies into mathematical equations [11]. This conversion aims for easy use to solve such non-convex and complicated problems. In nature, dragonflies create swarms to collect friends to stay within their same swarms. The purpose of swarm creations is to hunt preys like mosquitoes as food sources (for meals), and to avoid enemies such as eagles (for their survivors). Dragonflies have two swarms, dynamic swarm, and static swarm as depicted in Fig. 1.

3.1.1 Dynamic Swarm

Dragonflies do not meet any food source in their swarms. They form their own swarms to convince and assemble with friends while flying. In this swarm, there are the two sorts as follows.

(a) A dragonfly meets at least one friend: When a dragonfly meets another friend, they gather to stay in the same swarm together to search for the food source. At this moment, dragonflies have the three behaviors as expressed below.

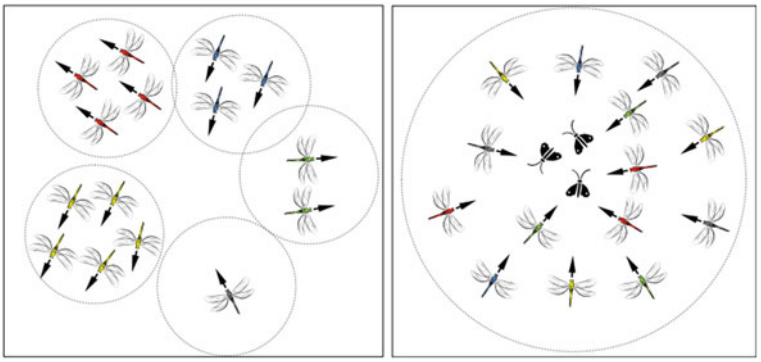

Fig. 1 **a** Dynamic swarm; **b** static swarm

1. Separation (SE_i),

$$SE_i = -\sum_{j=1}^{n_{\text{neigh}}} X_i - X_j \tag{22}$$

where n_{neigh} denotes the number of neighbors in its swarm; X_i denotes the current position of dragonfly i; X_j denotes the position of jth neighbor.

2. Alignment (AL_i),

$$AL_i = \frac{\sum_{j=1}^{n_{\text{neigh}}} \text{vel}_i}{n_{\text{neigh}}} \tag{23}$$

where vel_i denotes the velocity of jth neighbor.

3. Cohesion (CO_i),

$$CO_i = \frac{\sum_{j=1}^{n_{\text{neigh}}} X_j}{n_{\text{neigh}}} - X_i \tag{24}$$

The updated position of dragonfly i at Iter + 1 ($X_i^{\text{Iter}+1}$) is the summation between its position at Iter and step vector can be calculated as (25).

$$X_i^{\text{Iter}+1} = X_i^{\text{Iter}} + \Delta X_i^{\text{Iter}+1} \tag{25}$$

where, Iter denotes the simulation iteration number; $\Delta X_i^{\text{Iter}+1}$ denotes the step vector of d dragonfly i at Iter + 1 can be calculated as (26).

$$\Delta X_i^{\text{Iter}+1} = w\Delta X_i^{\text{Iter}} + (\text{seSE}_i + \text{alAL}_i + \text{coCO}_i) \tag{26}$$

where, w denotes the inertia weight; se, al, and co denote the separation, alignment, and cohesion factors, respectively. All of which can be calculated as defined in [11].

(1) A dragonfly does not meet any friend: Some dragonfly does not meet any friend. It independently flies to explore the food source by using the random walk strategy. This study calls it "levy flight dragonfly (LFD)". Because of the flying independence of LFD, it provides excellent exploration performance to DA. The updated position of a LFD can be defined in (27).

$$X_i^{\text{Iter}+1} = X_i^{\text{Iter}} + \text{Levy} \times X_i^{\text{Iter}} \tag{27}$$

where Levy denotes levy flight can be calculated as in (28).

$$\text{Levy} = 0.01 \times \frac{\text{rand}[0,1] \times \sigma}{|\text{rand}[0,1]|^{\frac{1}{\beta}}} \tag{28}$$

$$\sigma = \left(\frac{I^-(1+\beta) \times \sin(\frac{\pi\beta}{2})}{I^-(\frac{1+\beta}{2}) \times \beta \times 2^{(\frac{\beta-1}{2})}} \right)^{\frac{1}{\beta}} \tag{29}$$

$$I^-(x) = (x-1)! \tag{30}$$

where, β denotes a constant value.

(2) Swarm: A dragonfly meets the food source in its swarm. Then, it flies toward the food source and suddenly fly outward from the enemy source. Herein, dragonflies have more additional behaviors than dragonflies in dynamic swarms as expressed below.

4. Flying toward the food source (FO_i),

$$\text{FO}_i = X_{\text{FO}} - X_i \tag{31}$$

where X_{FO} denotes the ever-best position of the food source found.

5. Flying outward from the enemy source (EN_i),

$$\text{EN}_i = X_{\text{EN}} + X_i \tag{32}$$

where X_{EN} denotes the ever-worst position of enemy source come across.

The updated step vector can be calculated as defined in (33).

$$\Delta X_i^{\text{Iter}+1} = w\Delta X_i^{\text{Iter}} + (\text{seSE}_i + \text{alAL}_i + \text{coCO}_i + \text{foFO}_i + \text{enEN}_i) \tag{33}$$

where, fo and en denote the food and enemy factors, respectively, which can be calculated as defined in [11].

3.2 *Dizzy Dragonfly Algorithm*

Nevertheless, DA has weak features which limits dragonfly performances. Dragonflies lose opportunities to discover the greatest food source in the search space. Then, they obtain poor and inaccurate solutions to problems. Thereby, to eliminate these deficiencies, this study presents Dizzy Dragonfly Algorithm (DDA) by proposing the new movement characteristics for all dragonflies in static and dynamic swarms as follows.

3.2.1 LFD in Dynamic Swarm

Due to independent movements of LFDs as discussed in section III-A, LFDs use random parameters to update their positions. They move such undirected and long paths [13]. Disadvantageously, LFDs may not explore the excellent food source effectively. Therefore, this study proposes the four new movement characteristics for LFDs as follows.

(a) Flying toward a random friend (DDA_{LFD1}): In this characteristic, LFDs are commanded to fly toward a random friend to search for a good food source nearby. The equation of finding out a random friend (fr) and updated position of dragonfly i are defined in (34) and (35), respectively.

$$\text{fr} = \text{round}(1 + \text{rand}[0, 1] \times (n_{dr} - 1)) \tag{34}$$

$$X_i^{\text{Iter}+1} = X_i^{Iter} + \text{Levy} \times (X_{fr}^{Iter} - X_i^{Iter}) \tag{35}$$

where, $X_{\text{fr}}^{\text{Iter}}$ denotes the position of dragonfly fr at Iter.

(b) Flying outward from a random friend (DDA_{LFD2}): LFDs are ordered to fly outward from a random friend, which can be found in (34). This characteristic aims for LFDs to meet an excellent food source far away from a random friend. The updated position of LFDs is defined in (36).

$$X_i^{\text{Iter}+1} = X_i^{\text{Iter}} + \text{Levy} \times (X_{fr}^{\text{Iter}} + X_i^{\text{Iter}}) \tag{36}$$

(c) Flying toward the food source (DDA_{LFD3}): This characteristic is presented for LFDs to discover a better food source around the current food source. The updated position is defined in (37).

$$X_i^{\text{Iter}+1} = X_i^{\text{Iter}} + \text{Levy} \times (X_{\text{FO}}^{\text{Iter}} - X_i^{\text{Iter}}) \tag{37}$$

(d) Flying outward from the food source (DDA_{LFD4}): The objective of this characteristic is for LFDs to fly outward from the food source. Perhaps, the greater food source is located far away from the current food source. The updated position of LFDs is defined in (38).

$$X_i^{\text{Iter}+1} = X_i^{\text{Iter}} + \text{Levy} \times (X_{\text{FO}}^{\text{Iter}} + X_i^{\text{Iter}}) \tag{38}$$

In addition, this study uses a random parameter in the range [0, 1] (rand_{LFD}) to compete with the criteria of each characteristic for LFD i (LFD_i) to follow as defined in (39).

$$\text{LFD}_i = \begin{cases} \text{follow } DDA_{LFD1};\ \text{rand}_{\text{LFD}} < 0.25 \\ \text{follow } DDA_{LFD2};\ \text{rand}_{\text{LFD}} < 0.5 \\ \text{follow } DDA_{LFD3};\ \text{rand}_{\text{LFD}} < 0.75 \\ \text{follow } DDA_{LFD4};\ \text{else;} \end{cases} \tag{39}$$

(1) Dragonfly in static swarm: Due to the feature of swarm creations in DA, size of swarms is enlarging proportional to the number of simulation iterations. This causes dragonflies to be adhered in a static swarm which limits the exploration performance of DA. Therefore, this study proposes the four new movement characteristics of dragonflies in static swarms to boost the exploration performance as follows.

(a) Flying toward a random friend without concern of the enemy source (DDA_{ST1}): Dragonflies are controlled to fly toward a random friend only which are randomly fixed by (34). The step vector and the updated equation for this characteristic are defined in (40) and (25), respectively.

$$\Delta X_i^{\text{Iter}+1} = w\Delta X_i^{\text{Iter}} + (\text{seSE}_i + \text{alAL}_i + \text{coCO}_i + \text{fo}(X_{\text{fr}}^{\text{Iter}} - X_i^{\text{Iter}})) \tag{40}$$

(b) Flying outward from a random friend without concern of the enemy source (DDA_{ST2}): dragonflies are enforced to fly outward from a random friend only which is randomly designated by (34). In this characteristic, dragonflies may fly out of static swarms and act as an LFD. This increases the exploration performance. The step vector and the updated equation for this characteristic are defined in (41) and (25), respectively.

$$\Delta X_i^{\text{Iter}+1} = w\Delta X_i^{\text{Iter}} + (\text{seSE}_i + \text{alAL}_i + \text{coCO}_i + \text{fo}(X_{\text{fr}}^{\text{Iter}} + X_i^{\text{Iter}})) \tag{41}$$

(c) Flying toward the enemy source without concern of the food source (DDA_{ST3}): Theoretically in DA, the enemy source has been found and noted from worse to worst. This characteristic encourages dragonflies to fly toward the enemy source. Maybe, dragonflies fly out of a static swarm to stay in dynamic swarms. Also, a better food source is located near the enemy source. This characteristic aims for rising the exploration performance. The step vector and the updated equation for this characteristic are defined in (42) and (25), respectively.

$$\Delta X_i^{\text{Iter}+1} = w\Delta X_i^{\text{Iter}} + (\text{seSE}_i + \text{alAL}_i + \text{coCO}_i + \text{en}(X_{\text{EN}} - X_i))) \tag{42}$$

(d) Flying outward from the enemy source without concern of the food source (DDA_{ST4}): This characteristic encourages dragonflies to search for the more exceptional food source in which it is in the opposite side of the enemy source. Sometimes, dragonflies are outside a static swarm to rest in dynamic swarms. The step vector and the updated equation for this characteristic are defined in (43) and (25), respectively.

$$\Delta X_i^{\text{Iter}+1} = w\Delta X_i^{\text{Iter}} + (\text{seSE}_i + \text{alAL}_i + \text{coCO}_i + \text{en}(X_{\text{EN}} + X_i)) \tag{43}$$

(e) Flying toward the food source and suddenly outward from the enemy source (DDA_{ST5}): This is the original characteristic of dragonfly movement in DA as explained in section III-A. The step vector and the updated equation for this characteristic are defined in (33) and (25), respectively.

To apply the characteristics proposed above for dragonflies in static swarms, this study sets the criteria to all these characteristics and uses a random parameter in the range [0, 1] ($\text{random}_i^{\text{static}}$) for dragonfly i (X_i) to comply as defined in (44).

$$X_i = \begin{cases} \text{follow } DDA_{ST1};\ \text{random}_i^{\text{static}} < 0.2 \\ \text{follow } DDA_{ST2};\ \text{random}_i^{\text{static}} < 0.4 \\ \text{follow } DDA_{ST3};\ \text{random}_i^{\text{static}} < 0.6 \\ \text{follow } DDA_{ST4};\ \text{random}_i^{\text{static}} < 0.8 \\ \text{follow } DDA_{ST5};\ \text{else} \end{cases} \tag{44}$$

To get more efficient exploration and exploitation performances, the proposed characteristics in static swarms above are performed from the beginning of iterations to the half course of iterations. It is because the solution would be accurate by the DDA exploitation performance. Hence, the procedure of the DDA application is depicted as the flowchart in Fig. 2.

4 Time-of-Use Tariffs, Algorithm Parameters and ORM Specifications

4.1 Time-of-Use Tariffs

In this study, the power system of RWSs at MHS studied and modified to utilize ORM which is supplied by the external sources of a supplier. The TOU tariffs for RWSs by the supplier are subject to time and holidays. Details of the TOU tariffs are expressed in [17]. Power consumptions of RWSs from July 1st, 2020 to June

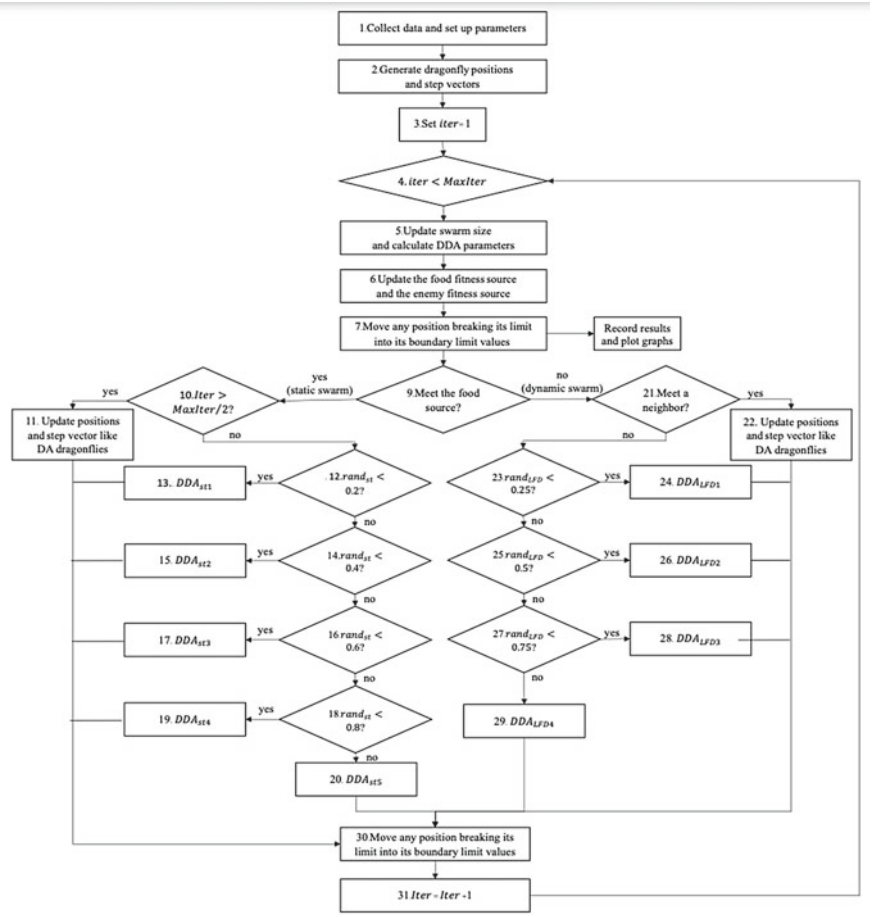

Fig. 2 The procedure of the DDA application

30th, 2021 are exampled to simulate and execute by DDA and the other referred optimization algorithms to find out the results of the objective function as in section II-C. RWSs only buy electricity from the supplier in case the total amount of power from WTGs, PVs, BESSs, and FC is lower than load consumptions at a time. In contrast, RWSs sell electricity to the supplier as per total amount of power from WTGs, PVs, BESSs, and FC is higher than load consumptions at a time. Note that there are no limits for power exchange and commercialization between RWSs and the supplier.

4.2 Algorithm Parameters

In this section, data and parameters for optimization simulations are expressed. Most of the DDA parameters are the same DA parameters in [11], besides the specific parameters of DDA such as the random parameters as mentioned in section III-B. In this study, the concepts and parameters of the referred IWO and PSO can be read in [18] and [19], respectively. Agent positions for all the optimization algorithms are expressed in (45).

$$X_i^{\text{Iter}} = [N_{\text{WTG}}, N_{\text{PV}}, N_{\text{BESS}}, P_{\text{FC}}^1, \ldots, P_{\text{FC}}^{8760}] \tag{45}$$

4.3 ORM Specifications

Data of wind velocity, solar irradiance, and temperature in an hour interval during the considered time are extracted from [20] and can be depicted in Fig. 3. SOC of batteries does not need to be equal to the initial state. The cost of operation and maintenance of ORM is referred to in [3]. The ORM specifications are tabulated in Table 1 [3, 14].

5 Algorithm Performance Test and Numerical Result

To test the performances of DDA, all the concepts and parameters of DDA, DA, IWO, and PSO are written on the platforms of the MATLAB 2021b program. All simulations are executed on MacBook Pro M1 with 8 GB of Memory. The number of agents for simulations by all the optimization algorithms is set to 20. The maximum number of iterations is determined to 100. At an initial step of all the optimization algorithm applications, positions of agents and all independent parameters are randomly generated.

As seen in Table 2, the optimal number of WTGs, PVs, and BESSs by DDA, DA, IWO, and PSO simulation applications are expressed. The optimal number of PVs of all the optimization algorithms is like each other. But the optimal number of WTGs and BESSs is different from each other. Figure 4 shows the optimal power of FC by DDA, DA, IWO and PSO simulations which is fluctuating and different from each other at hours. Figure 5 shows the optimal power of PVs, buying and selling power from/to the external source by the DDA simulation in the 8760 h and the first 200 h exampled. The optimal power of WTGs, BESSs, and FC by DDA simulation during the 8760 h and the first 200 h exampled is displayed in Fig. 6. It can be observed that ORM generates power within its limits. WTGs power is variedly generated in condition of wind velocity. PVs produce power during daytime. The summation of

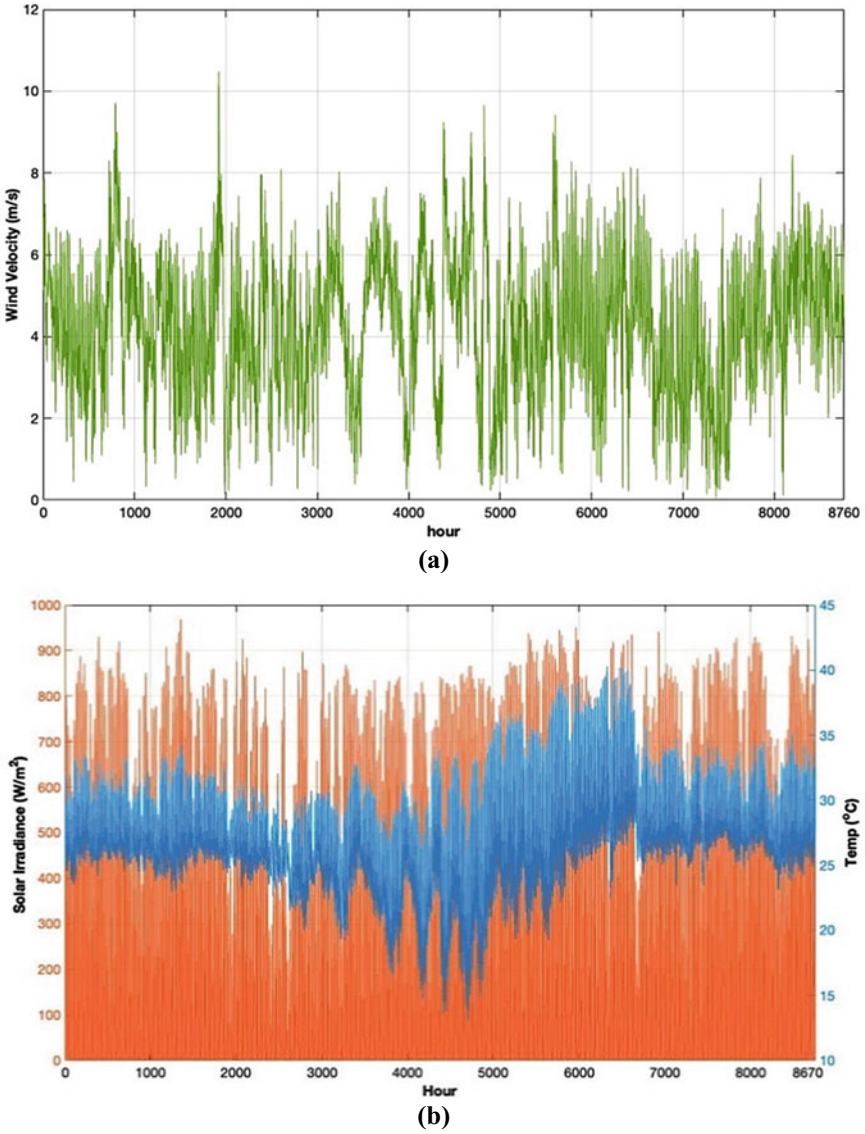

Fig. 3 **a** Wind velocity, **b** solar irradiance and temperature

all the ORM power is equal to the load consumption. At an hour, BESS power is charged for energy storage or discharged to the system. The power commercialization between RWSs and the external source occurs. RWSs can sell or buy power to/from the supplier which depends on the total amount of power generated by ORM. In other

Table 1 ORM specifications

WTG		PV	
Parameter	Value	Parameter	Value
V_n	11 m/s	V_{mpp}	28.36 V
V_{ci}	2.5 m/s	I_{mpp}	7.76 A
V_{co}	13	V_{oc}	36.96 V
p_r	200 kW	I_{SCn}	8.38 A
η_{WTG}	95%	K_v	0.1278
$N_{\text{WTG}}^{\text{min}}$	5	K_i	0.00545
$N_{\text{WTG}}^{\text{max}}$	20	N_{ot}	43
BESS		P_{mod}	220 W
SOC^{ini}	80%	$N_{\text{WTG}}^{\text{min}}$	5
SOC^{min}	20%	$N_{\text{WTG}}^{\text{max}}$	200
SOC^{max}	80%	**FC**	
E_{nom}	100 kW	$P_{\text{FC}}^{\text{min}}$	100 kW
$N_{\text{WTG}}^{\text{min}}$	5	$P_{\text{FC}}^{\text{max}}$	1,000 kW
$N_{\text{WTG}}^{\text{max}}$	100		

Table 2 Results of all the optimization algorithms

Parameters	IWO	PSO	DA	DDA
N_{WTG}	7	20	10	5
N_{PV}	200	200	200	200
N_{BESS}	22	5	5	5
$OF(\$)$	2,978,797.11	2,942,149.24	2,815,650.48	**2,633,741.77**

words, RWSs sell power to the supplier in case of power exceedingly generated by ORM and buy power from the supplier as per lack of power produced by ORM.

As a result, DDA obtains the total cost at $2,633,741.77 which is $181,908.71, $345,055.44, and $308,407.47 cheaper (better) than the total cost by DA, IWO, and PSO, respectively. Thanks to the much efficient exploration and exploitation performances of DDA in both static and dynamic swarms, DDA dragonflies have many movement characteristics to follow and fly over areas in the search space in static swarms or dynamic swarms. They are unadhered to flying toward the food source only in a static swarm and fly out of its static swarm to act as LFDs in dynamic swarms. With these proposed characteristics, DDA dragonflies can meet and provide the most excellent total cost over the cost by DA and the other referred optimization algorithms. Therefore, RWSs can utilize ORM in its system and save the total cost by the DDA application. Moreover, in discussion on the performances, the referred optimization algorithms apply the iteration numbers to order agents to be in the exploration or exploitation stages. For example, PSO reduces the inertia

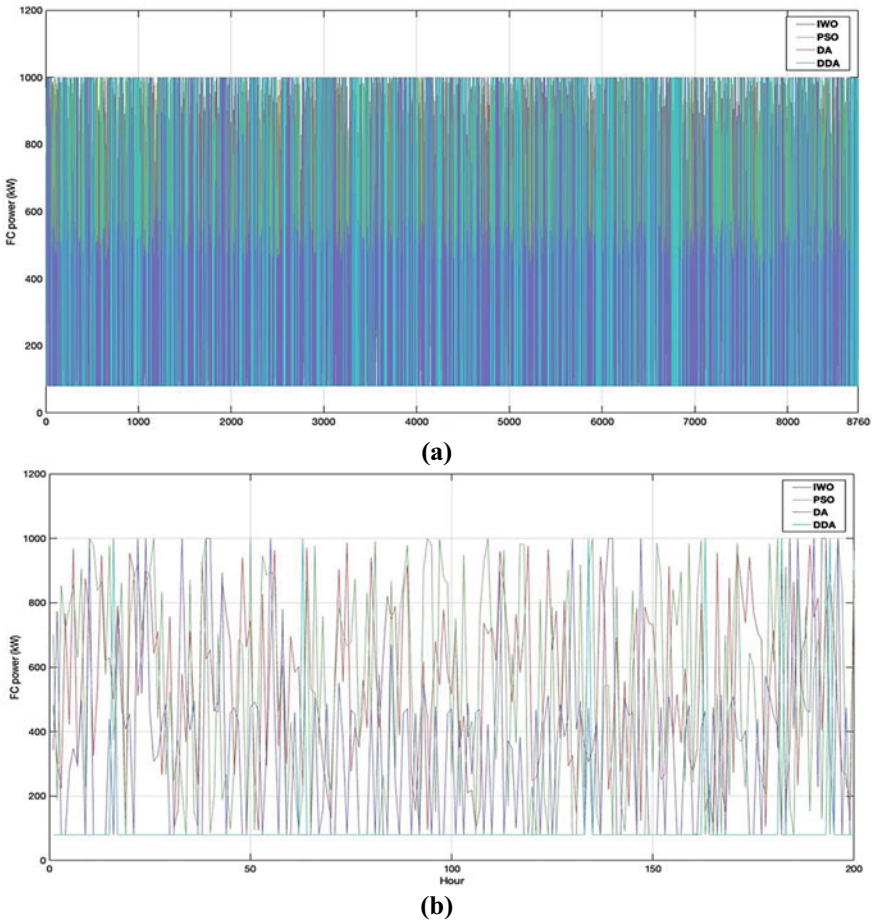

Fig. 4 Output power of FC by IWO, PSO, DA, and DDA **a** in 8760 h **b** in the first 200 h exampled

weight according to the number of iterations, which lessens the velocity of agents to enter the exploitation stage. PSO agents can move and discover the better results close to the position of the two best agents (personal and global best positions) at each iteration immediately which may be trapped in the local optima and provide not-best results to problems.

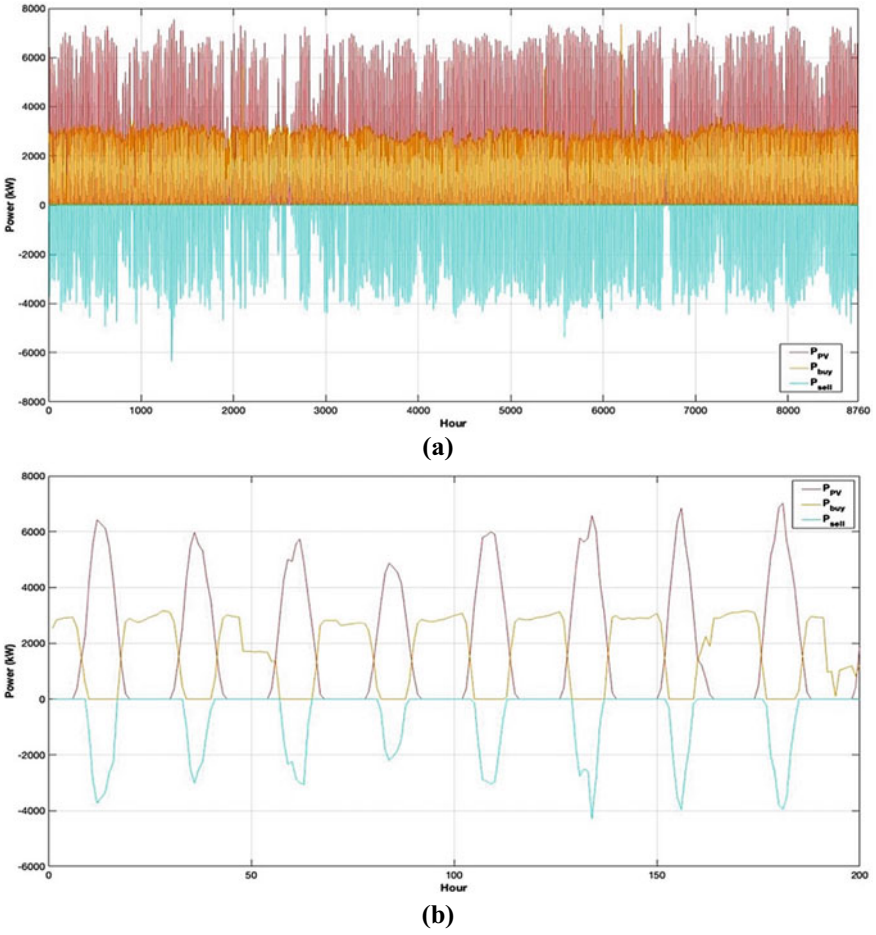

Fig. 5 The optimal power of PVs, buying and selling power from/to the external source by DDA **a** in 8760 h **b** in the first 200 h exampled

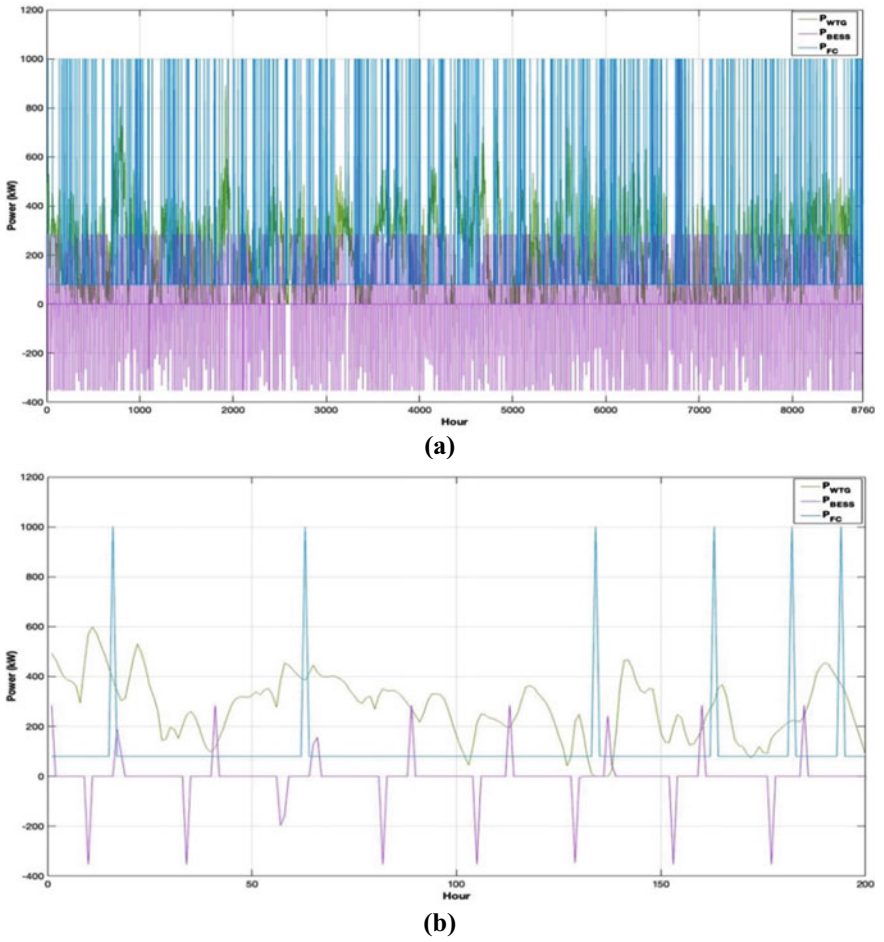

Fig. 6 The optimal power of WTGs, BESSs, and FC by DDA **a** in 8760 h **b** in the first 200 h exampled

References

1. Gamil, M.M., Lotfy, M.E., Hemeida, A.M., Mandal, P., Takahashi, H., Senjyu, T.: Optimal sizing of a residential microgrid in Egypt under deterministic and stochastic conditions with PV/WG/Biomass Energy integration **9**(3) (2021)
2. Wang, Z., et al.: Study on the optimal configuration of a wind-solar-battery-fuel cell system based on a regional power supply. IEEE Access **9**, 47056–47068 (2021). https://doi.org/10.1109/ACCESS.2021.3064888
3. Mohamed, F.A., Koivo, H.N.: System modelling and online optimal management of microgrid using mesh adaptive direct search. Int. J. Electr. Power Energy Syst. (2010). https://doi.org/10.1016/j.ijepes.2009.11.003
4. U. S. C. of Commerse: Metropolitan Waterworks Authority, Thailand (2013). www.energyxxi.org

5. Bouchekara, H.R.E.H., Chaib, A.E., Abido, M.A., El-Sehiemy, R.A.: Optimal power flow using an improved colliding bodies optimization algorithm. Appl. Soft Comput. J. (2016). https://doi.org/10.1016/j.asoc.2016.01.041
6. Regis, N., Muriithi, C.M., Ngoo, L.: Optimal battery sizing of a grid-connected residential photovoltaic system for cost minimization using PSO algorithm. Eng. Technol. Appl. Sci. Res. **9**(6), 4905–4911 (2019). https://doi.org/10.48084/etasr.3094
7. Yusri, M., Khalil, A., Peng, A.S.: Optimal sizing of stand-alone PV system using artificial bee colony algorithm. Int. J. Integr. Eng. **13**(5), 54–67 (2021). https://doi.org/10.30880/ijie.2021.13.07.007
8. Crepinsek, M., Liu, S.H., Mernik, M.: Exploration and exploitation in evolutionary algorithms: a survey. ACM Comput. Surv. (2013). https://doi.org/10.1145/2480741.2480752
9. Ullah, Z., Wang, S., Radosavljevic, J., Lai, J.: A solution to the optimal power flow problem considering WT and PV generation. IEEE Access (2019). https://doi.org/10.1109/ACCESS.2019.2909561
10. Khenissi, I., Fakhfakh, M.A., Sellami, R., Neji, R.: A new approach for optimal sizing of a grid connected PV system using PSO and GA algorithms: case of Tunisia. Appl. Artif. Intell. **35**(15), 1930–1951 (2021). https://doi.org/10.1080/08839514.2021.1995233
11. Mirjalili, S.: Dragonfly algorithm: a new meta-heuristic optimization technique for solving single-objective, discrete, and multi-objective problems. Neural Comput. Appl. (2016). https://doi.org/10.1007/s00521-015-1920-1
12. Kigsirisin, S., Miyauchi, H.: A modified dragonfly algorithm for economic load dispatch problems using isolated dragonfly control. In: CIGRE AORC 2020 (2020)
13. Aci, Ç.I., Gülcan, H.: A modified dragonfly optimization algorithm for single- and multiobjective problems using Brownian motion. Comput. Intell. Neurosci. (2019). https://doi.org/10.1155/2019/6871298
14. Teng, J.H., Luan, S.W., Lee, D.J., Huang, Y.Q.: Optimal charging/discharging scheduling of battery storage systems for distribution systems interconnected with sizeable PV generation systems. IEEE Trans. Power Syst. (2013). https://doi.org/10.1109/TPWRS.2012.2230276
15. Azaroual, M., Ouassaid, M., Maaroufi, M.: Optimum energy flow management of a grid-tied photovoltaic-wind-battery system considering cost, reliability, and CO2 emission. Int. J. Photoenergy (2021). https://doi.org/10.1155/2021/5591456
16. Coello, C.A.C.: Theoretical and numerical constraint-handling techniques used with evolutionary algorithms: a survey of the state of the art. Comput. Methods Appl. Mech. Eng. (2002). https://doi.org/10.1017/CBO9781107415324.004
17. T. Metropolitan Electricity Authority: Electricity tariffs (2018). www.mea.or.th
18. Xing, B., Gao, W.-J.: Invasive weed optimization algorithm, pp. 177–181 (2014)
19. Esmin, A.A.A., Coelho, R.A., Matwin, S.: A review on particle swarm optimization algorithm and its variants to clustering high-dimensional data. Artif. Intell. Rev. **44**(1), 23–45 (2015). https://doi.org/10.1007/s10462-013-9400-4
20. The power data access viewer (2022). https://power.larc.nasa.gov/data-access-viewer/

IOT-Enabled Blockchain-Based Intelligent Electric Charging Station

A. V. Rose and Priya G. Das

Abstract A wireless local area network (WLAN) is used to communicate between the smart intelligent electric charging station and the IOT cloud platform. The Backpropagation Artificial Neural Network (BPANN) in MATLAB is used to process vehicle data repositories that have been connected to the IOT analytics cloud platform. Using an FPGA controller and the launching pad LAUNCHXL-F28069M, the BPANN calculates the charging time and load need in accordance with which it sends signals to the solar grid tie system. The board used for the development is by Texas Instrument. The system is made to work together to maximize the use of grid energy. The technology will use solar energy when it is available to immediately charge the electric vehicle. If solar energy is not available, the system will be powered by the grid. The apparatus will also offer solar power to the grid when solar energy is available but there are no EVs plugged into the charging station. In this mode, the charging station will operate as a solar power plant that is connected to the grid. An interleaved boost converter is utilized in place of the transformer that is typically used to transmit low voltage solar energy to the grid. This modification results in a significant reduction in the system's overall cost and size. In order to further ensure cybersecurity, transactions are performed utilizing blockchain technology, which was created using Solidity on the Remix IDE Ethereum platform. To ensure that the charge history and data are preserved securely.

Keywords IOT · Blockchain · Intelligent electric charging station · Solar grid tie system · Cyber security · WLAN communication · Backpropagation · Artificial neural network

A. V. Rose (✉)
A P J Abdul Kalam Technological University, Thiruvananthapuram, Kerala, India
e-mail: 20m056@gmail.com

P. G. Das (✉)
NSS College of Engineering, Palakkad, Kerala, India
e-mail: priyadas27@gmail.com

M. L. Kolhe (ed.), *Renewable Energy Systems and Sources*,
https://doi.org/10.1007/978-981-99-6290-7_2

1 Introduction

Future smart grid and smart city visions envision the widespread use of electric vehicles that can be charged either on or off-board and run on an electric power source. Infrastructure for embryonic charging is a major barrier to widespread use of electric vehicles. The automobiles in the market as a result of the power demand that EVs will the grid is under stress. In this aftermath, a specific number of numerous stations for recharging electric vehicles in suitable places are necessary to install in order to recharge electric automobiles. In order to achieve this, a number of strategies have been provided by scientists. A crucial element of the charging station EVSE, or electric vehicle supply equipment, provides including sockets, electric energy is used to recharge electric vehicles. Depending on, outlets, connector, on-board or off-board charger the charging intensity used, charging levels and requirements are explained in the section that follows. Meter-equipped networked EV supply equipment is capable of a wide range of tasks, including "smart grid" applications. Charging stations need to be constructed in homes, offices, markets, and shopping centers in order to keep electric vehicles fueled up and operating dependably. The authors suggested that in order to develop smart recharging stations with good communication infrastructure—communication between utilities, substation control centers, charging stations, and electric vehicles—in view of grid stability and efficient energy consumption. Another idea for a smart charging station is offered that makes use of a high power factor PWM inverter, which is seen as a crucial piece of technology for the widespread adoption of electric vehicles [1]. In [2], three clearly defined charging techniques are provided. Additionally, recharging station study in relation to various EV charging parameters, traffic mobility factors, size of the energy storage, quality of service (QoS), cost factor, and best placement of smart charging station are being worked on [2, 3]. For quick charging of electric vehicles, an energy storage device based on ultra-capacitors has also been suggested [4]. Thus, work is being done to create a charging infrastructure that is reliable, strong, efficient, and affordable. Numerous strategies and techniques have been put forward in the wake of this to establish EV recharging stations [5]. This study examines and discusses the cutting-edge methods being created for EV charging stations. A framework for the best design and implementation of EV charging stations is offered after comparing several methods that have already been suggested. An intelligent bidirectional charging interface for electric vehicles is suggested, which is directly powered by PV-based renewable energy generation. It is outfitted with a specially designed multilevel power converter to supply the desired level of voltage rating to the vehicle charger and is mounted with an efficient communication bridge among all nodes of the system. The proposed system, which is crucial for describing the suggested strategy, is discussed in this paper. A wireless local area network (WLAN) is used to communicate between the smart intelligent electric charging station and the IOT cloud platform. The Backpropagation Artificial Neural Network (BPANN) in MATLAB is used to process vehicle data repositories that have been connected to the IOT analytics cloud platform. Using an FPGA controller and the launching pad LAUNCHXL-F28069M, the

BPANN calculates the charging time and load need in accordance with which it sends signals to the solar grid tie system. Board for development by Texas Instruments. The system is made to work together to maximize the use of grid energy. The technology will use solar energy when it is available to immediately charge the electric vehicle. If solar energy is not available, the system will be powered by the grid. The apparatus will also offer solar power to the grid when solar energy is available but there are no EVs plugged into the charging station. In this mode, the charging station will operate as a solar power plant that is connected to the grid. An interleaved boost converter is utilized in place of the transformer that is typically used to transmit low voltage solar energy to the grid. This modification results in a significant reduction in the system's overall cost and size. Additionally, transactions are performed utilizing Blockchain Technology, which was created using Solidity in the Remix IDE and Ethereum platform, to assure cybersecurity. So that the history of transactions and the charger data is safely kept.

2 Methodology

The station's lack of a means to forecast both the quantity of approaching vehicles and the characteristics of EVs, such as battery size and charging time, is an issue. Power distribution is a challenging need. There is no way to monitor the quality of the power customers receive. Effective EV load management requires smart energy management. Analytics, battery tracking, and even others lack cyber security for online payments. Through the navigation button, electric vehicles may find the closest charging station anytime a low battery warning appears while driving. Here, we will assume the charging station is wired to the grid and has solar power.

In Fig. 1, a system where an electric vehicle and a charging device share a data connection and the charging device shares a data connection with a charging operator is known as smart EV charging or intelligent charging. Smart charging allows the owner of the charging station to monitor, manage, and restrict the use of their devices remotely to reduce energy consumption, in contrast to conventional (or dumb) charging devices that aren't connected to the cloud. The sky is the limit when using cloud-based solutions (pun intended). Smart EV charging services are very customizable; you can easily add and remove elements to build a system that meets your requirements. Existing charging stations can also be modified and given new functions. Because of this, intelligent EV charging is also future-proof.

As the world continues to change, shifting needs and expectations will be translated into new features and added to the smart system. In Fig. 2, data repository of EV charging data is added to IOT platform and is provided using WLAN communication for system input. The system determines whether to connect solar panels to the grid or calculates current and future loads. Blockchain technology allows for cash transactions. In this case, we use the IOT platform NodeMCU, where we add the data repository to the cloud. Thingspeak serves as our cloud. Using a Wi-Fi module esp8266, we download data from the cloud to the system. The system performs

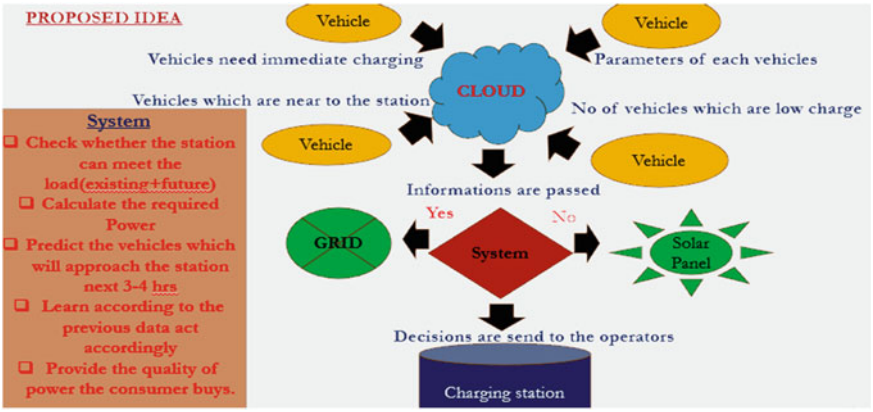

Fig. 1 Technological stack for proposed system

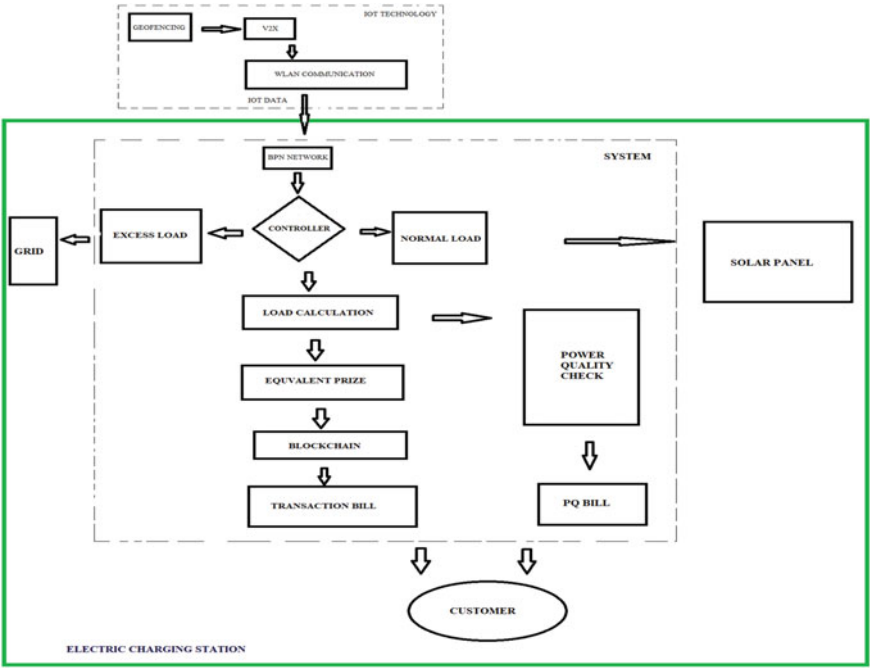

Fig. 2 Block diagram

grid synchronization, load calculations, and load forecasting. Transactions involving cash are conceivable by means of blockchain technology. The quality of power is also given to the consumer.

3 Intelligent Charging Station

Through the navigation button, electric vehicles may find the closest charging station anytime a low battery warning appears while driving. Here, we will assume the charging station is wired to the grid and has solar power [6]. A system where an electric vehicle and a charging device share a data connection and the charging device shares a data connection with a charging operator is known as smart EV charging or intelligent charging [7–9]. Smart charging allows the owner of the charging station to monitor, manage, and restrict the use of their devices remotely to reduce energy consumption, in contrast to conventional (or dumb) charging devices that aren't connected to the cloud. The sky is the limit when using cloud-based solutions (pun intended). Smart EV charging services are very customizable; you can easily add and remove elements to build a system that meets your requirements is shown in Fig. 3. Existing charging stations can also be modified and given new functions. Because of this, intelligent EV charging is also future-proof.

As the world continues to change, shifting needs and expectations will be translated into new features and added to the smart system. Electric vehicles with low-charge as well as those that approach the station using the navigation bar. IOT data are provided using WLAN communication for system input. In Fig. 4, it deals with a learning that is carried out on a multilayer feedforward neural network using the backpropagation technique. A collection of weights are learned iteratively to predict the class label of set. An input layer, one or more hidden layers, and an output layer make up a multilayer feed-forward neural network. Every layer is composed of units. The attributes that were measured for each training set correspond to the inputs to the network. The units that make up the input layer are simultaneously given the inputs. These inputs flow via the input layer before being simultaneously weighted

Fig. 3 Imported data in Thingspeak

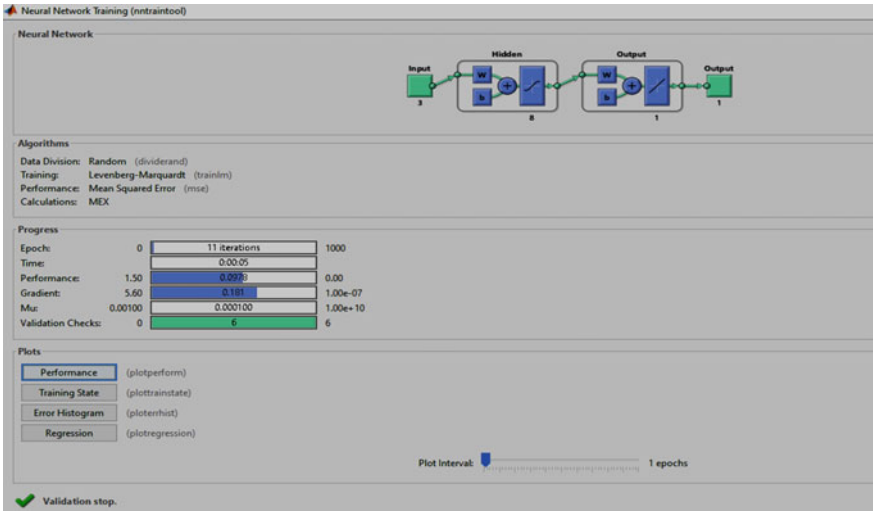

Fig. 4 Backprpogation ANN converges

and supplied to the hidden layer, a second layer of "neuronlike" units. Hidden layers are arbitrary, even though there is often only one utilized in practice. Figure 5 shows the convergence of the learning system at the 11th epoch. Units in the output layer are fed weighted outputs from the final hidden layer, which emits the network's prediction for certain tuples. The hidden layer units' outputs can be fed into the input of a subsequent hidden layer, and so forth. Even though there are typically only one used in practice, hidden layers are arbitrary. Units in the output layer, which emit the network's prediction for specific set, are fed weighted outputs from the final hidden layer. The system determines whether to connect solar panels to the grid or calculates current and future loads.

Blockchain technology allows for cash transactions, which is depicted in Fig. 6. Also provided to the customer is the quality of power [10, 11]. Any microcontroller can connect to your Wi-Fi network with the ESP8266 Wi-Fi Module, a self-contained SOC with an integrated TCP/IP protocol stack. Either an application can be hosted on the ESP8266 or all Wi-Fi networking tasks can be delegated to another application processor. An ESP8266 Wi-Fi module is a SOC microprocessor that is mostly utilized for the creation of end-point Internet of Things (IoT) applications. It is known as a standalone wireless transceiver and is very inexpensive. It is utilized to make it possible for various embedded system applications to connect to the internet.

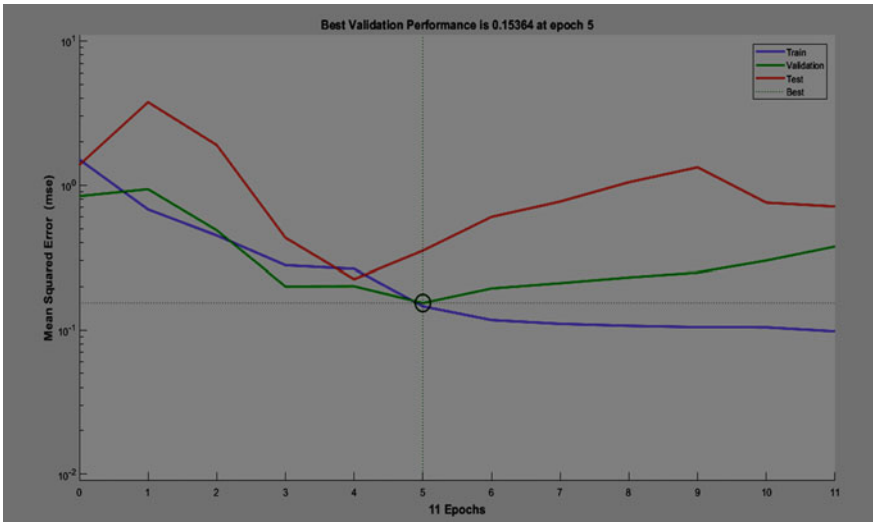

Fig. 5 Backpropagation ANN result

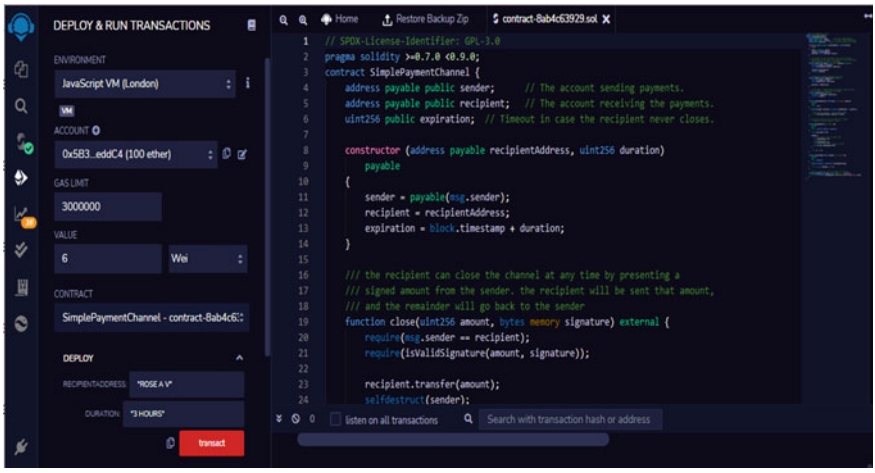

Fig. 6 Blockchain transaction script

4 Solar Grid Tie System

The PV array transforms solar energy into electrical energy, which is then sent to the interleaved boost converter. In Fig. 7 it illustrate the boosted voltage generated by the interleaved boost converter is then delivered to the battery utilized in an electric vehicle. After charging, a grid-tie inverter sends any extra power to the grid. In cases where using an electric vehicle is not practical, solar energy is sent into the grid.

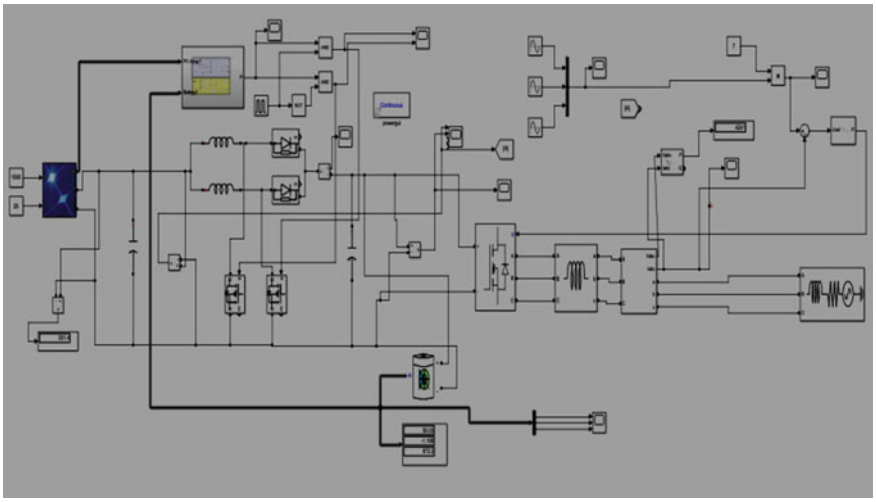

Fig. 7 MATLAB simulation of solar grid tie system

When solar electricity is not available but an electric vehicle can be charged, the grid provides the voltage to the car. When solar electricity is also available, electric vehicles are charged using solar panels. The solar input of 290 V is being boosted by the interleaved boost converter to 850 V and is shown in Fig. 8. Clearly shows the boosted output curve from the above-mentioned converter. This voltage is then fed to the battery. The PV array transforms solar energy into electrical energy, which is then sent to the interleaved boost converter. Figure 9 depicts the V-I and P-I characteristics of interleaved boost converter.

The battery system is made up of two parts: the battery MPPT and the battery controller circuit in Fig. 10. The MPPT technique is beneficial for maintaining a PV array's operation point at its maximum. Thanks to battery storage technology, utilities and operators of power systems can store energy for later use. SOLAR/PV ARRAY: Individual solar cells are layered in a repetitive matrix pattern to form a single solar array unit. This crucial process of turning solar energy into electrical energy is carried out by these solar arrays. Since these solar panels are connected to the interleaved boost converter through a capacitor, the voltage across the terminals of the device stays constant. On the other hand, the PV array's current and voltage depend on temperature and light exposure nonlinearly. As a result, to operate the module as efficiently as possible, the voltage and current must be continuously checked.

DESIGN OF SOLAR PANEL: Array data Parallel strings = 2.

Series-connected modules per string = 10.

Input Voltage = 29 × 10 = 290 V.

A battery energy storage system (BESS), an electrochemical device, charges (or collects) energy from the grid or a power plant and then discharges that energy later to create electricity or other grid services as required.

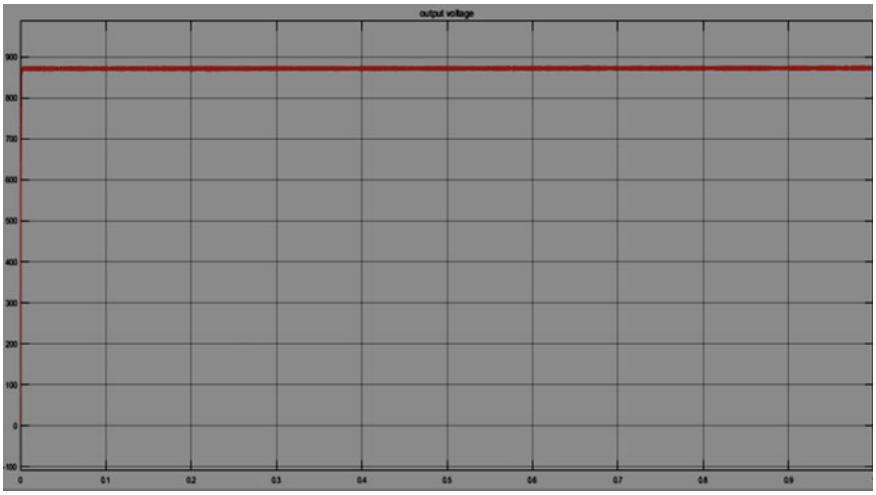

Fig. 8 V-T characteristics of Interleaved boost converter

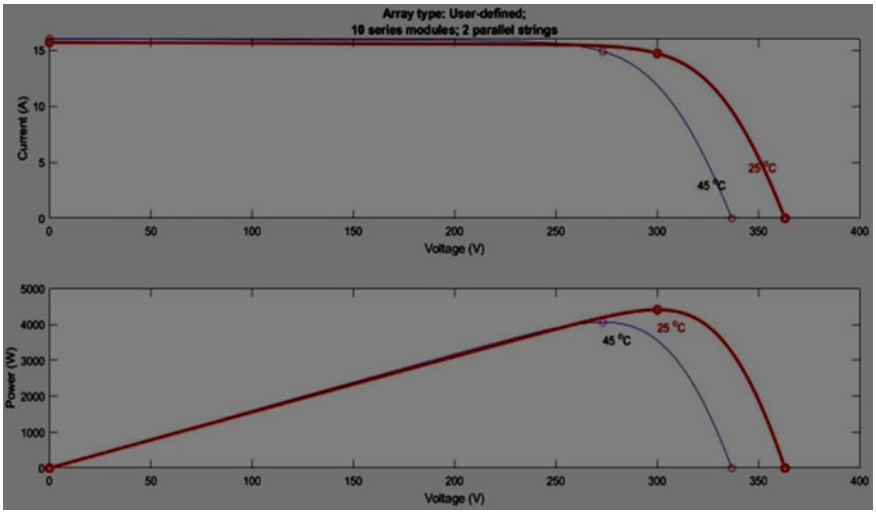

Fig. 9 I-V and P-V characteristics

Battery storage is one technological solution that could increase the flexibility of the power system and enable considerable levels of renewable energy integration. According to studies and real-world experience, high levels of renewable energy from variable renewable energy (VRE) sources can be safely and dependably incorporated into linked power networks without the need for new energy storage resources. In this instance, a PWM is created using a triangle signal and three sinusoidal waves. The inverter output was compared to a reference waveform that was created. Both graphs

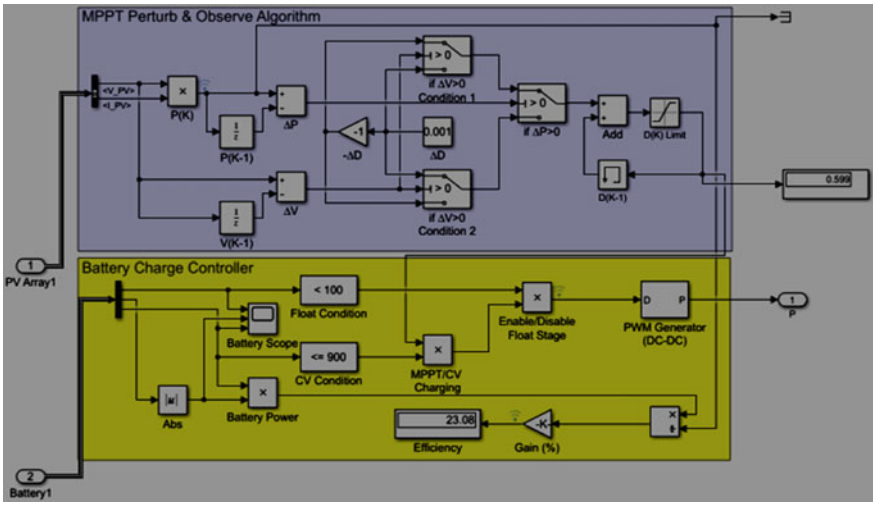

Fig. 10 MPPT and battery controller circuit

were compared as well as the grid's synchronism was investigated. Demonstrates the interleaved boost converter which supplies current to the grid.

So, after battery charging, any excess energy is sent to the grid and is shown in Fig. 11. Figure 12 depicts the reference waveform used for the purpose. The capacity to synchronize the output with a reference alternating amount is another feature of a grid-tie inverter. It takes in a DC voltage and produces an alternating amount. Green energy facilities that are linked to the public utility grid employ grid-tie inverters. Grid power and solar power conversion are always in step. The ability of the PV system to feed any additional energy produced into the grid is built into the system. This capacity improves the system's controllability and enables it to function successfully and adaptable in a variety of system operating scenarios. In order to feed electricity back into the electrical system, "synchronization" is an essential step.

The voltage, frequency, and phase angle differences between the respective phases of the generator output and grid supply must be as small as possible in order to ensure synchronization that is shown in Fig. 13. An alternating current generator must be synchronized with the grid prior to connecting. In order to distribute the electricity, it needs to operate at the same frequency as the network. Synchronization is necessary prior to connecting the generator to a grid. Synchronization can be done either manually or automatically. In order to stop voltage and frequency irregularities, synchronization serves the purposes of monitoring, accessing, enabling, and automatically taking control measures. The DC output from the PV array must be converted into AC power in order to be fed into the grid or to power the required loads. The battery's DC power must also be inverted before being used. Phase shift and a lock loop (PLL) are used to synchronize the grid after the inverter is linked to it. Power can be transferred from the grid section to the DC connection and vice versa. An inverter is located in between the AC and DC lines. It transforms the DC

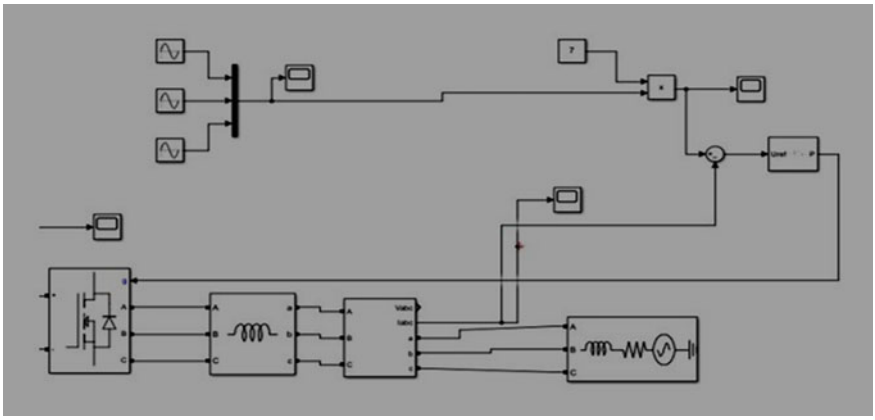

Fig. 11 Grid simulation

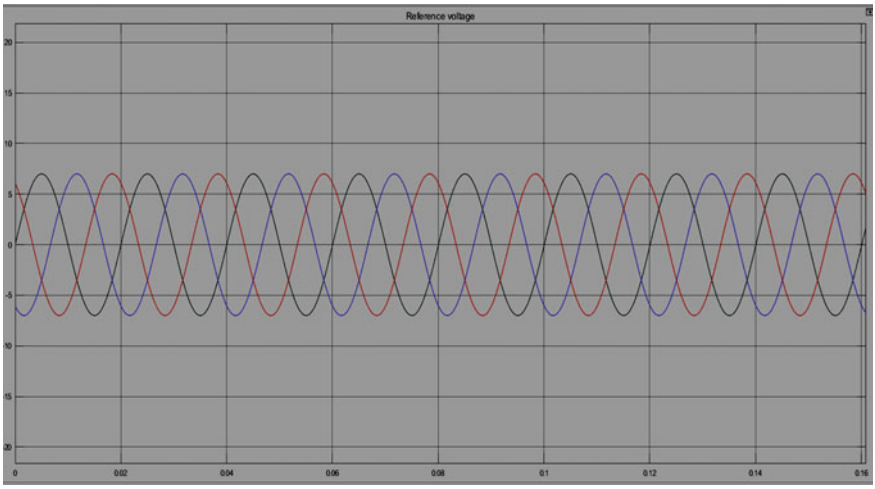

Fig. 12 Reference waveform

power from the PV side or the power that is drawing from the battery to AC to feed into the load or utility. Similar to this, before charging the storage battery, it rectifies grid AC electricity into DC power. The system's AC line is made up of the consumer loads and the utility grid, to which the entire system is connected.

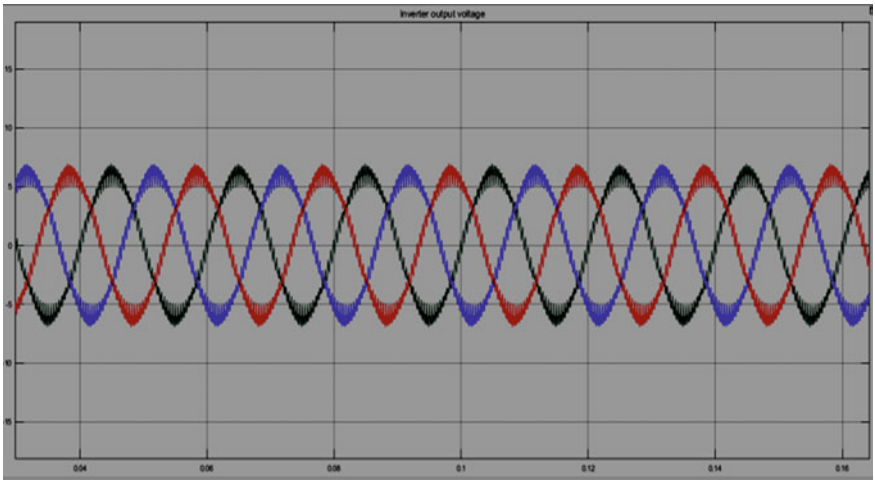

Fig. 13 Inverter output waveform

5 Hardware

The proposed system involves a smart, intelligent electric charging station that interacts with the IOT cloud platform via a wireless local area network (WLAN). You may gather, visualize, and investigate real-time data streams in the cloud with the ThingSpeak TM IoT analytics platform service.

ThingSpeak rapidly visualizes data that are transmitted by your devices to it. The ESP-12E module, which houses the ESP8266 chip with Tensilica Xtensa 32-bit LX106 RISC microprocessor which is depicted in Fig. 14, is included with the NodeMCU ESP8266 development board. This microprocessor has an adjustable clock frequency range of 80–160 MHz and supports RTOS. To store data and programs, NodeMCU contains 4 MB of Flash memory and 128 KB of RAM. It is perfect for IoT projects thanks to its high processing power, built-in Wi-Fi and Bluetooth, and Deep Sleep Operating capabilities. Assembling, visualizing, and analyzing real-time data streams in the cloud are possible with the help of the IoT analytics platform service ThingSpeak.

Data uploaded by users are instantly visualized via ThingSpeak. Data sent by your devices to ThingSpeak are instantly visualized by ThingSpeak. You can analyze and analyze data online as it comes in thanks to ThingSpeak's ability to run MATLAB code. For IoT systems that need analytics, ThingSpeak is frequently used for prototype and proof of concept solutions. The Internet of Things (IoT) aims to remotely connect objects for smooth operation. It fills the gap between data networks and device sensors. It gives information about the data that are used in the backend application. An IoT platform is a collection of parts that enables programmers to disperse applications, gather data from a distance, secure communication, and manage sensors. An IoT platform controls device connectivity and enables the

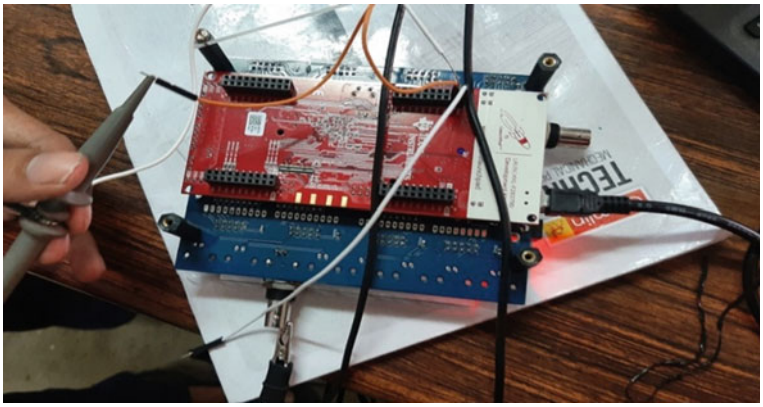

Fig. 14 FPGA controller and the launching pad LAUNCHXL-F28069M

creation of new mobile software apps by developers. It makes business transformation possible and makes it easier to collect data from gadgets.

It links many parts, ensuring a constant stream of communication between the gadgets. The IoT platform aids in better understanding client wants and makes it easier to create products that meet those needs. It gives businesses more operational intelligence and visibility, which facilitates better decision-making. Figure 15 illustrates inter-leaved DC-DC converters have a number of benefits over conventional boost converters, such as very little current ripple, excellent efficiency, and rapid dynamics. An interleaved converter, which has a better efficiency of roughly 98%, is used to enhance the output voltage to 800 V. Using an interleaving gadget can also help you feel less stressed and work more effectively. Interleaved boost PFC is the most popular power factor correction architecture. Figure 16 shows the experimental setup of inverter that is used for synchronization in lab. The rectifying diode bridge and boost converter are utilized in this system to convert AC voltage to DC voltage. After that, the boost converter raises the voltage. As a result, the current develops a sinusoidal wave and the output voltage ripple is reduced. One boost converter runs at a time as a result of pulses produced by the driver circuit. Since the interleaved boost converter combines two boost converters, one of them is turned on during the positive half cycle and the other during the negative half cycle. The inductors get short-circuited when the MOSFET is triggered. High-speed switching results from the gate receiving a PWM pulse. The inductor is charged at the moment of the short. These result in the MOSFET opening, doubling the inductor charge. The capacitor is then used to discharge this. In order to prevent voltage return flow, a diode is positioned in the path. Therefore, voltage increases as a result of rapid speed switching. Figure 17 shows the hardware setup.

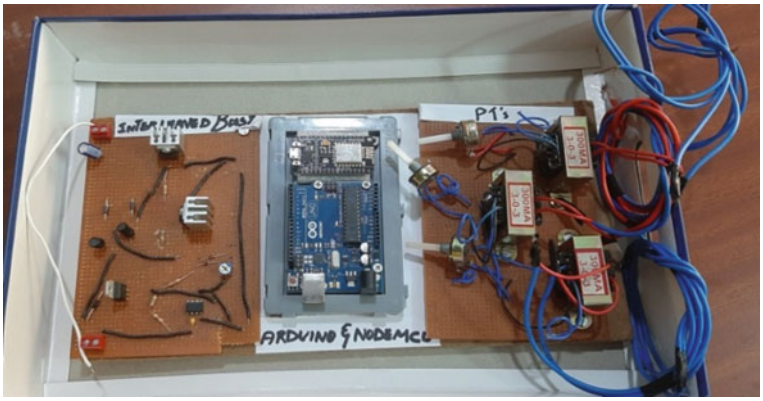

Fig. 15 Interleaved boost controller

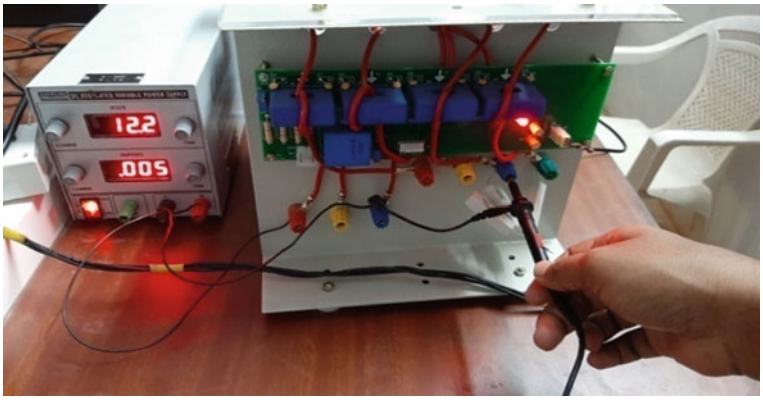

Fig. 16 Inverter

Fig. 17 Hardware setup

6 Conclusion

A wireless local area network (WLAN) was used to connect the smart intelligent electric charging station to the IOT cloud platform. Additionally, vehicle data repositories were added to the IOT analytics cloud platform and analyzed using Backpropagation Artificial Neural Networks (BPANN) in MATLAB. The BPANN uses the launching pad LAUNCHXLF28069M to determine the charging time and load demand before sending signals to the solar grid tie system. Board for development by Texas Instruments. A solar-powered electric vehicle charging station is designed, planned, and put into operation. The requisite voltage rating is obtained using an interleaved boost converter. MATLAB-Simulink is used to simulate the interleaved boost converter, and the results are shown. Later, the findings are examined, and the functioning model is created using the discovered simulation settings. MATLAB-Simulink is used to build and simulate grid-tie inverters in order to synchronize the transmission of surplus energy to the grid. Along with MPPT, a battery system is incorporated to store the energy for later usage. The amount of ripples produced was lessened with the aid of the interleaved boost converter. As a result, a solar-powered electric vehicle charging station that is more effective and environmentally benign is created. Additionally, transactions are conducted using Blockchain Technology, which was created using Solidity in the Remix IDE Ethereum platform, to ensure cybersecurity. As a result, the transaction history and billing information are safely kept. In the future, geofencing will be established at smart, intelligent electric charging stations using GPS tracking. This virtual perimeter has a 7 km radius and surrounds the charging station. This fictitious geofence boundary tracks and detects the presence of electric vehicles in real time. Additionally, automatic system operation can be offered. Additionally, blockchain integration is possible. As a result, all live data are safely preserved.

Acknowledgements The authors would like to thank the financial support under KSCSTE-SARD scheme and MODROB scheme for the purchase of lab equipments.

References

1. Smart Charging Infrastructure for Electric Vehicles Azhar Ul-Haq, Concettina Buccella, Carlo Cecati, Hassan A. Khalid Department of Industrial and Information Engineering and Economics, University of L'Aquila, and DigiPower s," r. l. Via G. Gronchi, pp. 18–67100.
2. A. Hess, M. Francesco, M. Reinhardt, C. Casetti, "Optimal deployment of charging stations for electric vehicular networks", in Proc. of the First Work. on Urban Net., ACM, New York, USA, pp. 1–6, 2012
3. Z. Fan, "Distributed charging of PHEVs in a smart grid," in Proc. IEEE Int. Conf. Smart Grid Communications, Brussals, pp. 255-260, Oct. 2011
4. J. Song, A. Toliyat, D. Turtle, A. Kwasinski, "A Rapid charging station with an ultracapacitor energy storage system for plug-in electrical vehicles," in Proc. of Elect. Machines and Systems, Incheon, USA, pp. 2010

5. Z. Sahinoglu, Z. Tao, K. H. Teo, “Electric vehicles network with nomadic portable charging stations”, IEEE Vehicular Technology Conf., Ottawa, Canada, pp. 1 - 5, Sep. 2010
6. P. Bose and P. Sivraj, “Smart charging infrastructure for electric vehicles in a charging station,” in 2020 4th International Conference on Intelligent Computing and Control Systems (ICICCS), 2020. 7
7. Fard, A.Y., Shadmand, M.B.: Multitimescale three-tiered voltage control framework for dispersed smart inverters at the grid edge. IEEE Trans. Ind. Appl. **57**(1), 824–834 (2021)
8. N. Fareed and M. V. M. Kumar, “Single stage grid tied solar PV system with a high gain bi-directional converter for battery management,” in 2020 International Conference on Power Electronics and Renewable Energy Applications (PEREA), 2020.
9. J. Silva et al., “Fast-model predictive control for a grid-tie photovoltaic system,” in IECON 2020 The 46th Annual Conference of the IEEE Industrial Electronics Society, 2020.
10. J. Liu, H. Zhang, L. Zhen, “Blockchain technology in maritime supply chains: applications, architecture and challenges,” Int. J. Prod. Res., pp. 1–17, 2021.
11. Kaushal, R.K., Kumar, N., Panda, S.N.: Blockchain technology, its applications and open research challenges. J. Phys. Conf. Ser. **1950**(1), 012030 (2021)

The Substation Construction Project Location Selection in Thailand by Using TOPSIS Technique

Arwut Jatephook, Choosak Pornsing, Noppakun Sangkhiew, Arisa Sanonok, Peerapop Jomthong, and Putpipong Laikrathok

Abstract Electricity is necessary for human life and is a major driver of economic growth. The demand for electricity has been rising continuously. An effective and sufficient power transmission infrastructure is required to deliver high-quality, reliable, and sustainable electricity. Therefore, the purpose of this paper is to select a location for substation construction project in Thailand. Based on a survey of the various landmarks, 10 alternative locations for the substation's construction are suitable locations. There are Krathum Baen 6, Krathum Baen 7, Tha Sai 2, Tha Muang 2, Tha Maka 2, Ban Pong 3, Bang Lane 2, Samut Sakhon 10, Samut Sakhon 11, and Om-Noi 5. Four criteria to be considered in the selection of the location of the substation construction project are determined as power consumption, the number of system problems time, the number of outages electricity meters, and electricity bills. The TOPSIS technique is conducted for calculation. The findings demonstrate that substation construction project that decision-makers must consider is the number of system problems time. The suitable locations are Om-Noi 5 and Bang Lane 2, Tha Maka 2, respectively.

Keywords Sustainable · TOPSIS · Electric power · Location selection

A. Jatephook (✉) · C. Pornsing · N. Sangkhiew · A. Sanonok
Department of Industrial Engineering and Management, Faculty of Engineering and Industrial Technology, Silpakorn University, Nakhon Pathom 73000, Thailand
e-mail: Jatephook_A@silpakorn.edu

P. Jomthong
Department of Biomedical Engineering, Faculty of Health Sciences, Christian University, Nakhon Pathom 7300, Thailand

P. Laikrathok
Provincial Electricity Authority Area 3 (Central), Nakhon Pathom 73120, Thailand

M. L. Kolhe (ed.), *Renewable Energy Systems and Sources*,
https://doi.org/10.1007/978-981-99-6290-7_3

1 Introduction

Electrical power is essential for human life and contributes to multidimensional change. The path of electric power development continues with a mechanism of quality creation that relies on a variety of fuel sources that are linked together through the electricity transmission system. Electricity transmission system is crucial in delivering electricity from power plant to consumers [1], ensuring that people have access to fundamental service. All regions of Thailand will experience wealth thanks to an effective electric power transmission infrastructure, which will also produce dependable economic stability for long-term investment decisions.

The Power Development Plan (PDP) 2018–2037 states that Thailand's demand for power has been steadily rising, leading the necessary organizations to provide more capacity. The Electricity Generating Authority of Thailand (EGAT), the Metropolitan Electricity Authority (MEA), and the Provincial Electricity Authority (PEA), which are all responsible for the transmission and distribution of electricity in Thailand, must make plans for generating enough electricity to meet demand and have reliable delivery systems in place. However, the distribution of electricity to users has restrictions on the delivery distance for places remote from the power plant. The transmission of electricity over long distances will experience voltage drops that cannot provide the customer with enough electricity. For this reason, a substation is required to connect the power plant to the customer in order to reduce losses during the distribution to the user.

The substation is outfitted with tools for controlling voltage, the flow of electrical energy, and short-circuit protection for cutting off transmission lines from the power grid. The primary purpose of substations is to generate and change voltage levels in order to transfer and distribute electrical energy. In an effort to create a more effective domestic electricity transmission system, Thailand approves a numerous of substation development projects each year. Therefore, it is vital to rank each project in order of significance before building substation, and expanding electrical distribution systems in the most critical area first. Nowadays, project planning relies on the expertise of experts in combination with forecasting methods to make planning decisions, thus lacking clarity on the factors that need to be considered.

In this paper aims to study the factors used to determine and prioritize power substation construction projects with TOPSIS techniques. This will help determine which factors are the most important and which should be considered first, or which factors need to be studied thoroughly. The rest of this manuscript is organized as follows: Sect. 2 describes the research methodology, including data collection, and data analysis. Section 3 proposes the results. Conclusions are finally presented in Sect. 4.

2 Methodology

This study considers the relevant factors for prioritizing substation construction projects within the Central Region of Thailand based on TOPSIS techniques to propose as a guideline for planning 10 pending substation construction projects as shown in Table 1, which is detailed as follows.

2.1 Data Collection

The primary data were obtained by interviewing 15 experts with more than 16 years of working experience and being in departments directly involved in the construction of substations. We will briefly explain the principles of priority comparison with TOPSIS methods and decision-making criteria so that experts can accurately and accurately assess the importance weight. The experts provided the information that came from five departments, namely, the Electricity Supply Analysis and Planning Department, Electrical Planning Department, Substation Construction Project Management Department, and Customer Relations Department. The secondary data were collected from Annual Performance Report, website, or news. See the collected and already calculated data in Table 2.

2.2 Data Analysis

Data analyze use Microsoft Excel to calculate according to the TOPSIS technique to prioritize substation construction projects. The calculation process is as follows:

(1) Technique for Order Preference by Similarity to Ideal Solution (TOPSIS)

Table 1 List of substation construction projects

No	Substation
A1	Krathum Baen 6
A2	Krathum Baen 7
A3	Tha Sai 2
A4	Tha Muang 2
A5	Tha Maka 2
A6	Ban Pong 3
A7	Bang Lane 2
A8	Samut Sakhon 10
A9	Samut Sakhon 11
A10	Om-Noi 5

Table 2 The collected data

Location\criteria	Power consumption	The number of system problems time	The number of outages of electricity meters	Electricity bill
A1	122,732,083.81	0	46,875	437,078,150.06
A2	122,732,083.81	0	46,875	437,078,150.09
A3	234,421,719.51	1	80,702	822,913,828.78
A4	10,397,295.65	1	24,301	37,373,973.20
A5	23,940,635.03	0	29,468	79,296,595.63
A6	32,940,635.03	7	47,706	120,052,949.63
A7	51,793,422.00	0	22,661	176,046,645.07
A8	234,421,719.51	1	80,702	822,913,828.78
A9	234,421,719.51	1	80,702	822,913,828.78
A10	111,901,036.30	0	76,206	402,577,235.50

TOPSIS was first developed by Hwang Ching-Lai and Kwangsun Yoon in the 1980 [2]. TOPSIS is one of the Multiple Criteria Decision Making [3, 4]. The basic concept is determining the best alternative that is the shortest distance from the positive ideal solution (PIS) [5] and the farthest distance from Negative Ideal Solution (NIS) [6, 7]. TOPSIS is a tool that assists in ranking alternatives according to the information used to evaluate each one. Therefore, TOPSIS is appropriate for decision-making based on quantitative standards that allow for the evaluation of numerical alternatives. The TOPSIS calculation steps as follows [7]:

Step 1: Normalized Decision Matrix $R = [r_{ij}]_{m\times n}$ with $i =, \ldots, m$ and $j = 1, \ldots, n$ as

$$r_{ij} = \frac{x_{ij}}{\sqrt{\sum x_{ij}^2}} \tag{1}$$

Step 2: The objective criteria weight (W_j) of each criterion is calculated. This study also uses entropy weight method, which is a typical diversity-based weighting method. We calculate attribute weights based on the diversity of attribute data among the alternatives. Entropy weight method is frequently used as the weight determination method for TOPSIS [7]. W_j is calculated as follows:

Calculate entropy measure of every index using the following equation

$$P_{ij} = \frac{x_{ij}}{\sum_j x_{ij}} \tag{2}$$

$$E_j = -K\sum\nolimits_{j=1}[P_{ij} \times \mathrm{In}\, P_{ij}] \text{ where } K = \frac{1}{\mathrm{In}(m)} \tag{3}$$

Define the divergence through:

$$\text{div}_j = 1 - E_j \tag{4}$$

Obtain the normalized weights of indices:

$$W_j = \frac{\text{div}_j}{\sum_j \text{div}_j} \tag{5}$$

Step 3: Calculate the Weighted Normalized Decision Matrix using the following equation:

$$V_{ij} = w_j r_{ij}, \forall i \in \{1, \ldots, m\}, \forall j \in \{1, \ldots, n\} \tag{6}$$

Step 4: Identify the positive ideal solutions; A^+ (benefits) and negative ideal solutions A^- (costs):

$$V^+ = (V_1^+ + V_2^+, \ldots, V_m^+) \tag{7}$$

$$V^- = (V_1^- + V_2^-, \ldots, V_m^-) \tag{8}$$

where A_j^+, A_j^- are defined as in (9) and (10)

$$A_j^+ = \{\left(\max_i v_{ij}, j \in J_1\right), (\min_i v_{ij}, j \in J_2)\} \tag{9}$$

$$A_j^- = \{\left(\max_i v_{ij}, j \in J_1\right), (\min_i v_{ij}, j \in J_2)\} \tag{10}$$

and J_1 and J_2 represent the criteria benefit and cost, respectively.

Step 5: Calculate the separation measures as:

$$d^+ = \sqrt{\sum (v_{Aj} - v_j^+)^2}, \forall_j \in \{1, \ldots, n\} \tag{11}$$

$$d^- = \sqrt{\sum (v_{Aj} - v_j^-)^2}, \forall_j \in \{1, \ldots, n\} \tag{12}$$

Step 6: Calculate the relative closeness to the ideal solution as:

$$\frac{d_i}{d_i^+ + d_i^-}, \forall i \in \{1, \ldots, m\} \tag{13}$$

Note that $C_i = 1$ if $A_i = A^+$ and $C_i = 0$ if $A_i = A^-$

(2) Selection Criteria

Table 3 List of selection criteria

Number	Criteria	Description
C1	Power consumption	Maximum concurrent power consumption as measured by meter
C2	The number of system problems time	The number of times an electrical system malfunctioned
C3	The number of outages electricity meters	The number of electricity meters that will be impacted by a power outage
C4	Electricity bill	Average monthly electricity income

The criteria used for priority in this paper are straightforward and reliable due to the selection process use interviewing experts in the relevant field who are real practitioners. The criteria consist of four criteria: Power consumption (C1), the number of system problems time (C2), the number of outages electricity meters (C3), and electricity bill (C4), as shown in Table 3.

3 Results and Discussions

The factors listed in Table 3 are studied to be used as criteria for prioritizing substation construction projects. We calculated priority values according to the TOPSIS technique with Microsoft Excel to prioritize each guideline. Which criteria have the highest value will matter the most. On the other hand, which criteria have the lowest value will matter the least, and the sum of all the resulting weighted values must be equal to 1.

According to the TOPSIS procedure in the previous section, the normalized matrix is shown in Table 4. The objective criteria weight derived from the entropy weight method are shown in Table 5. The relative closeness to the ideal solution is calculated. Then, the alternatives according to the relative closeness are ranked as shown in Table 6.

According to the values of closeness coefficients of the 10 substation construction projects, the construction project of Om-Noi 5 substation should be carried out first with the highest TOPSIS index value of 0.99941, followed by Bang Lane 2, Tha Maka 2, Krathum Baen 6, Krathum Baen 7, Tha Muang 2, Ban Pong 3, Tha Sai 2, and Samut Sakhon 10, and Samut Sakhon 11 with the same priority weight value of 0.77868, respectively. In light of the objective criteria weight, C2 is the weight that raises the most concern among the other three criteria. Overall, taking into account the other weights, the construction of the Om Noi 5 project should go ahead first, while the Samut Sakhon 10 and Samut Sakhon 11 projects should be constructed as the last.

Table 4 The normalized matrix

Location\Criteria	C1	C2	C3	C4
A1	0.267	0.000	0.254	0.270
A2	0.267	0.000	0.254	0.270
A3	0.509	0.137	0.438	0.508
A4	0.023	0.137	0.132	0.023
A5	0.052	0.000	0.160	0.049
A6	0.070	0.962	0.259	0.074
A7	0.112	0.000	0.123	0.109
A8	0.509	0.137	0.438	0.508
A9	0.509	0.137	0.438	0.508
A10	0.243	0.000	0.413	0.248

Table 5 The objective criteria weight

Criteria	C1	C2	C3	C4
Weight	0.2451	0.2714	0.2387	0.2448

Table 6 Rank the preference order

Alternatives	TOPSIS index	Rank
A1	0.95291	4
A2	0.95011	5
A3	0.77868	8
A4	0.90248	6
A5	0.97330	3
A6	0.86028	7
A7	0.99292	2
A8	0.77868	9
A9	0.77868	10
A10	0.99941	1

4 Conclusions

According, the findings of the research and analysis of factors influencing the decision to rank the substation construction projects using the TOPSIS technique, the factors influencing the consideration of four factors are power consumption (C1), the number of system problems over time (C2), the number of outages electricity meters (C3), and electricity bill (C4). C2 is the most concerning factor with a threshold weight of 0.2714, followed by C1, C4, and C3, respectively. The results showed that the construction of Om Noi 5 substation should be carried out first, followed by Bang

Lane 2, Tha Maka 2, Krathum Baen 6, Krathum Baen 7, Tha Muang 2, Ban Pong 3, Tha Sai 2, and Samut Sakhon 10, and Samut Sakhon 11, respectively, which ranks 1–3 in accordance with the Provincial Electricity Authority's operational plan.

The factors taken into account in this analysis can be utilized as decision-making input when deciding how to order substation construction projects. The TOPSIS technique can also be used for other tasks in the future.

Acknowledgements This article was supported in part by the Silpakorn University Research, Innovation and Creative Fund.

References

1. Roszkowska, E.: Multi-criteria decision making models by applying the TOPSIS method to crisp and interval data. Multi. Crit. Decis. Mak./Univ. Econ. Katowice **6**, 200–230 (2011)
2. Zhao, D., Li, C., Wang, Q., Yuan, J.: Comprehensive evaluation of national electric power development based on cloud model and entropy method and TOPSIS: a case study in 11 countries. J. Clean. Prod. **277**, 123190 (2020)
3. Dymova, L., Sevastjanov, P., Tikhonenko, A.: An approach to generalization of fuzzy TOPSIS method. Inf. Sci. **238**, 149–162 (2013)
4. Jayant, A., Sharma, J.: A comprehensive literature review of MCDM techniques ELECTRE, PROMETHEE, VIKOR and TOPSIS applications in business competitive environment. Int. J. Curr. Res. **2**, 65461–65477 (2018)
5. Yoon, K.P., Hwang, C.L.: Multiple Attribute Decision Making: An Introduction. Sage Publications, Thousand Oaks, CA (1995)
6. Krohling, R.A., Pacheco, A.G.: A-TOPSIS–an approach based on TOPSIS for ranking evolutionary algorithms. Procedia Comput. Sci. **55**, 308–317 (2015)
7. Shahroudi, K., Tonekaboni, S.M.S.: Application of TOPSIS method to supplier selection in Iran auto supply chain. J. Glob. Strat. Manag. **2**, 123–131 (2012)

Numerical Investigation of Wind-Induced Vibration and TMD Damping Effect of the Large-Span Transmission Tower-Line System

Yanji Li, Wenxiao Qian, Guoqiang Zhang, Xinwei Zhang, Quan Chen, and Huawei Niu

Abstract The large-span transmission tower-line system's response to wind-induced vibration and vibration control are the main subjects of this paper. The first step is to establish the single transmission tower (STT) model and the transmission tower-line system (TTLS) model, and the dynamic response of the system is analyzed accordingly. Then, the numerical method is used to investigate how the tuned mass damper (TMD) affects the top vibration response of the tower-line system. Based on the dynamic characteristics, the results demonstrate a significant similarity between the transmission tower-line system and the single tower. Additionally, when the TMD's mass ratio is set to 2%, the developed TMD does have some impact on the tower-line system's in-plane bending vibration. The acceleration (STD) reduction rate is proved bigger than 30%, while the displacement (STD) reduction rate is about 10%.

Keywords The large-span transmission tower-line system · Numerical simulation · Wind-induced vibration · Vibration control · TMD

Y. Li · W. Qian · X. Zhang
State Grid East Inner Mongolia Electric Power Co., Ltd, Hohhot, China

G. Zhang
China Electric Power Research Institute, Beijing, China
e-mail: zhangguoqiang@epri.sgcc.com.cn

Q. Chen · H. Niu (✉)
College of Civil Engineering, Hunan University, Changsha, China
e-mail: niuhw@hnu.edu.cn

Q. Chen
e-mail: Chen1998@hnu.edu.cn

M. L. Kolhe (ed.), *Renewable Energy Systems and Sources*,
https://doi.org/10.1007/978-981-99-6290-7_4

1 Introduction

Due to the characteristics of high height, low self-resonance frequency, and heavy load, the large-span transmission towers are extremely sensitive to wind loads. As a matter of fact, wind damage accidents of transmission towers occur occasionally both at home and abroad, which not only seriously affects the normal social production and life but also represents a serious threat to people's lives and the security of their property. Therefore, in recent years, more and more scholars have devoted a lot of energy to the research of the transmission towers about wind-induced vibration response and wind-induced vibration control.

In accordance with the respective characteristics of the background response and the resonance response of the tower-line coupled system, Guo et al. [1] further investigated the frequency-domain simplified analysis approach of the tower-line system about wind-induced vibration response. Evaluating whether the stiffness of the transmission lines was taken into account or not, Irvine [2] performed a finite element dynamics analysis of the single transmission tower. With the use of closed-form solutions and wind tunnel experiments, Zhang et al. [3] investigated on the three-dimensional dynamic reaction of three types of transmission lines (I, V, and strain) bundled with an insulator. Ghazal et al. [4] used computer software (ADINA and SAP2000) to investigate the effect of transmission lines response and the transmission tower-line system on a steel lattice transmission tower under heavier wind load. Zhao et al. [5] conducted a field test of a TTLS prototype in order to thoroughly examine the vibration behavior of conductors with and without ice coatings. In their wind tunnel tests for a STT and a TTLS under uniform flow field and turbulent flow field, Deng et al. [6] used the 500 kV Jiangyin large-span tower as their engineering background. They discovered that the frequency of conductor vibration was primarily low-frequency vibration, whereas the frequency of tower vibration was relatively high. Also, as wind speed increased, the first fourth modes' response dominated the power spectrum, and the spectral component grew rich. The TTLS's nonlinear effect grew. Using a wind tunnel air-elastic model with a scale ratio of 1:40, Chen et al. [7] investigated the wind-induced vibration response of the STT during weather winds and typhoons. By using a numerical approach, Lan et al. [8] investigated the effectiveness of the viscous damper in reducing wind-induced vibration, including the layout of the viscous damper and damping index, taking the 1000 kV substation frame with large scale as research project. Lei et al. [9] developed a non-contact eddy current tuned mass damper (ECTMD) for the broken transmission lines impact and wind-related damage to transmission tower structure, and proved the omnidirectional damping effect of the method through numerical simulation and wind tunnel test. The effect of mass ratio, frequency ratio, and damping ratio on the damping effect of the large-span STT TMD was confirmed by numerical simulation for Tian et al. [10].

The large-span STT and TTLS's dynamic characteristics, wind-induced vibration response, and vibration control require rigorous investigation. This research examines the reaction of the large-span TTLS to wind-induced vibration and the TMD

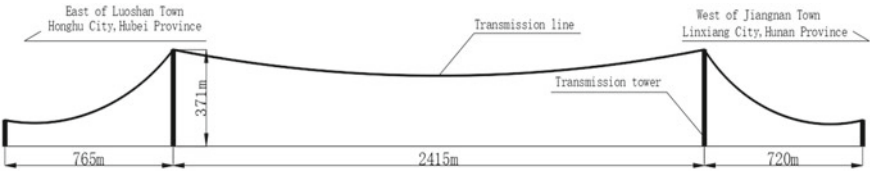

Fig. 1 The TTLS spacing distribution diagram

damping effect using a 1000 kV UHV AC transmission as the engineering background. The large-span transmission tower is divided into two banks, with the left bank located in the east of Luoshan Town, Honghu City, Hubei Province, and the right bank located in the west of Jiangnan Town, Linxiang City, Hunan Province. The main span distance is 2415 m, and the span distribution is 765–2415–720 m. The nominal height of the large-span tower is 297.5 m, while the whole tower is 371 m. The detailed layout is shown in 0 (Fig. 1).

2 Dynamic Characteristics Analysis

2.1 Single Transmission Tower (STT)

Firstly, the finite element program ANSYS was used to create the STT model depicted in 0. Among them, the transmission tower's major components, which were simulated by the Beam188 unit, are Q345, Q420 steel pipe, and angle iron; Beam4 unit was used to simulate part of the diagonal braces and horizontal braces; the four knots at the bottom of the tower were consolidated with the earth (Fig. 2).

In Table 1 and 0, the vibration characteristics and their descriptions of the STT's first fifth modes are displayed (Fig. 3).

2.2 Tower-Line System (TTLS)

In actual operation, the TTLS includes transmission lines and insulators in addition to the STT. For the entire TTLS, problems such as insulator suspension failure, line break failure, and line icing that could arise cause the presence of transmission lines need to be taken into account, and the way in which the transmission lines react to the main tower will also have a complex impact [11]. Therefore, on the basis of subsection II-A (STT's model), the "two towers and three lines" TTLS finite element model was established, and the specific details of the finite element model are shown in 0 (Fig. 4).

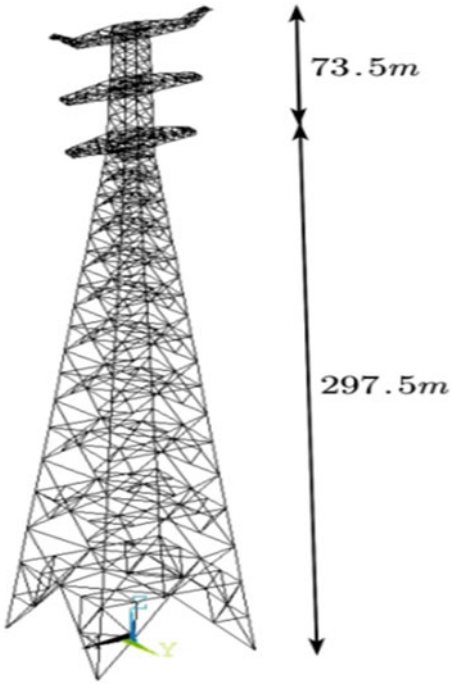

Fig. 2 The STT finite element model

Table 1 Description of the first fifth modes of the STT

Modes order	Frequency (Hz)	Modes mass (kg)
1	0.350	486,624
2	0.351	484,971
3	0.840	465,036
4	0.854	403,698
5	0.895	73,560

The first fifth modes of the STT in a TTLS are essentially the same as those of the STT if one disregards the low-frequency vibration of the transmission lines and takes the mode form of the tower as the primary research object. Table 2 displays a comparison of the STT and tower-line systems' first fifth modes.

Basically consistent with the research result of Yu's [12], the TTLS's first fifth modes' self-resonance frequency is slightly reduced compared with the STT because the influence of the transmission lines on the quality contribution of the TTLS is greater than the contribution of stiffness.

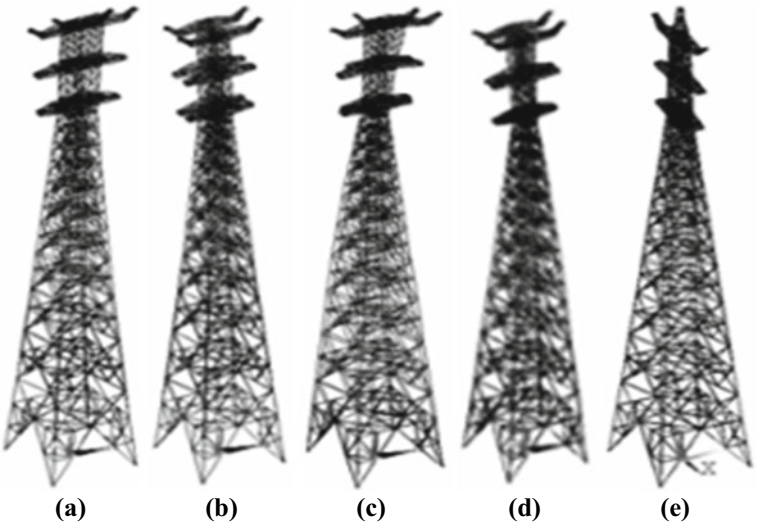

Fig. 3 The first fifth modes diagram of the STT: **a** the first mode; **b** the second mode; **c** the third mode; **d** the fourth mode; **e** the fifth mode

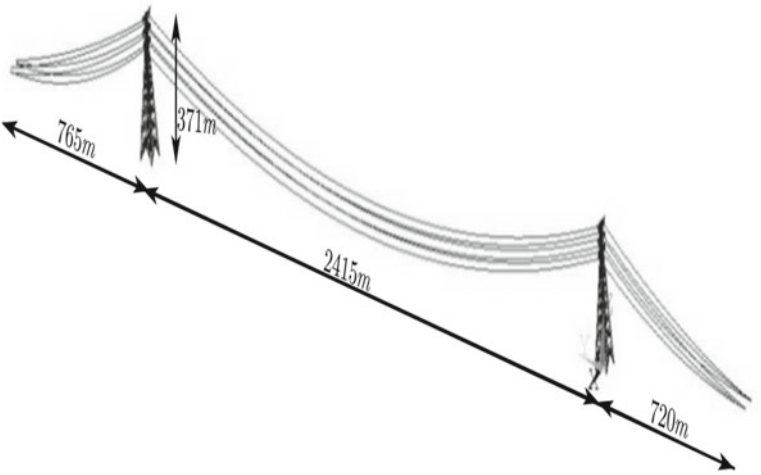

Fig. 4 The "two towers and three lines" finite element model

Table 2 Comparison of the dynamic characteristics of TTLS and STT

Modes order	STT frequency (Hz)	TTLS frequency (Hz)	Difference (%)
1	0.350	0.324	7.429
2	0.351	0.324	7.692
3	0.840	0.784	6.667
4	0.854	0.800	6.323
5	0.895	0.819	8.492

3 Wind-Induced Vibration Response Analysis

3.1 Wind Load Simulation and Loading

Firstly, the pulsating wind speed time history was generated using the harmonic synthesis method proposed by Shinozuka et al. [13] and Deodatis [14]. The resulting time history curve and power spectrum curves are presented in 0 (Fig. 5).

The finite element software ANSYS was used to load the derived pulsing wind time history into the TTLS finite element model for the wind-induced vibration response analysis. The transmission tower was separated into 22 pieces from top to bottom, and the appropriate wind speed was taken within each segment for loading since wind speeds varied at different altitudes. 0 depicts the loading point or section (Fig. 6).

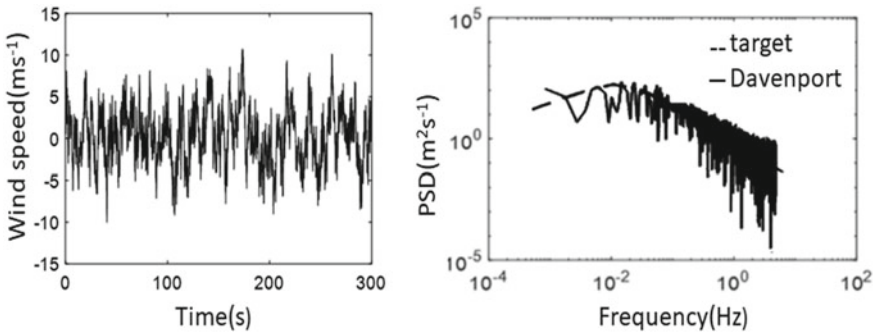

Fig. 5 Pulsating simulation results of TTLS: **a** Time history of pulsating wind; **b** Power spectrum of pulsating wind

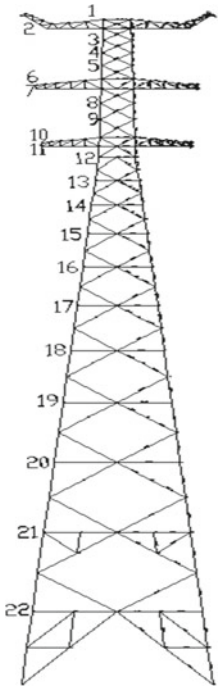

Fig. 6 Schematic diagram of the pulsating wind loading point

3.2 The Wind-Induced Vibration Response

A total of 61 nodes on the 22nd floor of the transmission tower were pulsated wind loading along the transmission lines (0° wind direction) and vertical the transmission lines (90° wind direction), then transient analysis was performed with ANSYS. 0 displays the outcomes of extracting the displacement and acceleration response at the top of the TTLS (Fig. 7).

It is clear that the response values are bigger in the direction along the transmission lines because the windward area in that direction is larger than it is in that direction of the vertical transmission lines. In Table 3, the data of the results are provided.

At the same time, the Fourier transform was applied to the time history curves of the wind-induced vibration response along the transmission lines and vertical the transmission lines at the top of the TTLS, and the spectrum curves are drawn in 0 (Fig. 8).

From 0, under wind load, the excellent frequencies of the TTLS's first and second modes are essentially equivalent to the self-resonant frequencies of the structure's first and second modes. That is, the in-plane bending vibration of the first and second modes (mainly the first mode) primarily dominates the response of the TTLS in both directions.

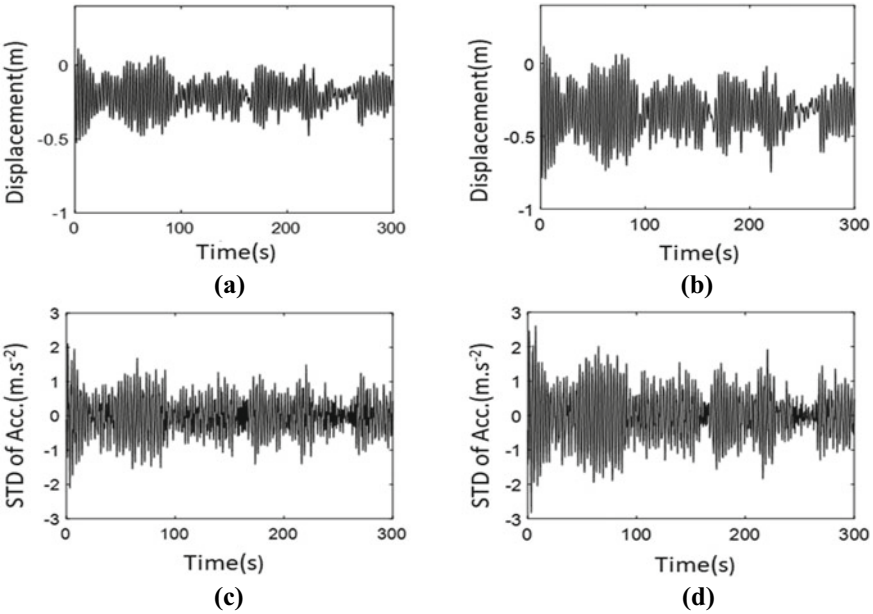

Fig. 7 The wind-induced vibration response results of TTLS: **a** Displacement results vertical the transmission lines; **b** Displacement results along the transmission lines; **c** Acceleration results vertical the transmission lines; **d** Acceleration results along the transmission lines

Table 3 The results of wind-induced vibration response for TTLS

Wind direction (°)	Maximum of displacement (m)	Standard of displacement (m)	Average of displacement (m)	Maximum of acceleration ($m\ s^{-2}$)	Standard of acceleration ($m\ s^{-2}$)
0	−0.794	0.395	0.334	2.834	0.756
90	−0.527	0.245	0.208	2.109	0.564

4 TMD Design and the Research of TMD Damping Effect

4.1 TMD Design

During the working process, the conductor plate of the eddy current damper does not contact with the magnet, which is an ideal damping method without friction and wear. When the mass block is moving, the magnetic inductive line movements are cut, and the magnetic flux in the conductor plate changes, resulting in eddy currents; the damping force is created when the magnetic fields created by the permanent magnet and the eddy current interact. In the whole process of the conductor plate movement, the conductor plate's kinetic energy is first transformed into electric energy, which

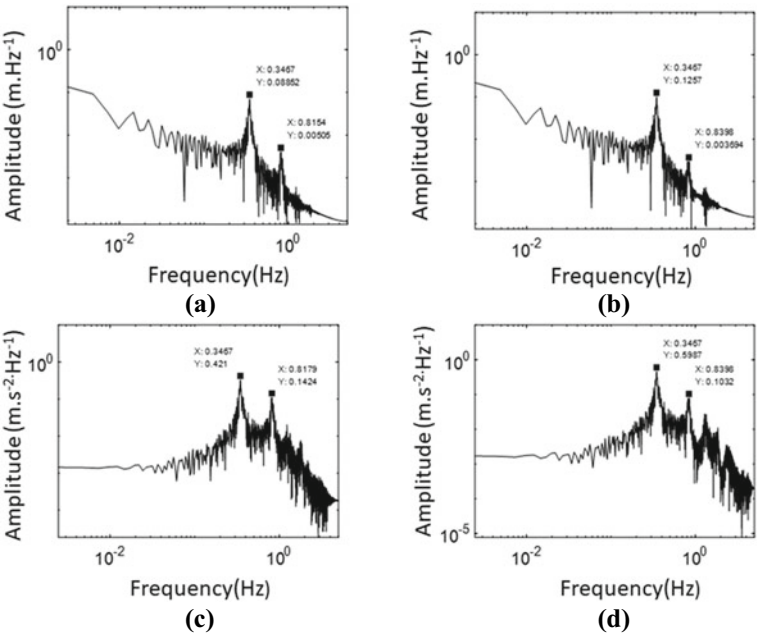

Fig. 8 The wind-induced vibration response spectrum curves of TTLS: **a** displacement spectrum curve vertical the transmission lines; **b** displacement spectrum curve along the transmission lines; **c** acceleration spectrum curve vertical the transmission lines; **d** acceleration spectrum curve along the transmission lines

is subsequently transformed into internal energy through the ampere-force working, so as to achieve energy dissipation.

Three factors, mass ratio, frequency ratio, and damping ratio generally affect how well TMD controls vibration. Equations (1) and (2), which make use of Den Hartog's [15] formula, were used to determine the optimal parameters, the optimal frequency ratio and the optimal damping ratio of TMD.

$$f_{\mathrm{TMD}} = f/(1+\mu) \tag{1}$$

$$D_{\mathrm{opt}} = \left[\frac{3\mu}{8(1+\mu)}\right]^{1/2} \tag{2}$$

where f is the frequency of the modes that TMD controls. From subsection III-B, the main modes of wind-induced vibration in the TTLS are the first two modes in both directions (along the transmission lines and vertical the transmission lines) of the structure, and these two modes are also the controlled target when designing eddy current TMD. Where D, μ are damping and mass ratio for TMD, respectively.

And μ can be calculated by Eq. (3).

Table 4 TMD design results for the TTLS

Mass ratio (%)	Mass of TMD (kg)	Frequency of TMD (Hz)	Damping of TMD (%)
2.000	9979.000	0.327	8.417

$$\mu = m_{\mathrm{TMD}}/m_S \tag{3}$$

where m_{TMD}, m_S are the modal mass for TMD and the research structure, respectively.

According to the dynamic characteristics analysis of the TTLS and Eqs. (1)–(3), TMD parameters in Table 4 can be obtained when the mass ratio is 2%.

4.2 The Research of TMD Damping Effect

4.2.1 Installation and Numerical Simulation of Eddy Current TMD

Generally, the maximum displacement location of the mode that is to be controlled is often where TMD is installed. In this study, the first mode of the target modes of the TTLS is in-plane bending (among the transmission lines and vertical the transmission lines), and the top displacement is the biggest. Therefore, TMD is hence mounted on the transmission tower's summit. Furthermore, the suspension point is split into two pieces to address the issue of too much local force while taking into account the viability of actual technical installation and structural force. 0 depicts the eddy current TMD installation diagram (Fig. 9).

Combin14 unit, which has one-dimensional, two-dimensional, or three-dimensional axial or torsional capabilities, was used to simulate spring-dampers with one-dimensional tensile and compressive effects in the finite element software ANSYS. Since the spring-damper system had no mass, the Mass21 unit was used to represent the structural particle.

4.2.2 The Damping Effect of Eddy Current TMD

After simulating the installation of eddy current TMD in the finite element model, a series of transient analysis of pulsating wind under the same working conditions as in subsection III-B were carried out. The numerical simulation calculated results were compared with those without TMD and the drawing was as 0 (Fig. 10).

It can be seen from 0 that after the installation of TMD, the displacement response and acceleration response along the transmission lines and vertical the transmission lines at the top of the TTLS were reduced to some extent, among which the standard reduction rate of acceleration was more than 30%, and the standard reduction rate of displacement was about 10%. The specific vibration damping effect data are shown in Table 5.

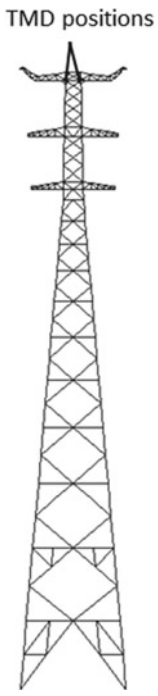

Fig. 9 Installation diagram of the eddy current TMD

5 Conclusions

The following are the main conclusions from the finite element analysis and numerical calculation of the TTLS of a 1000kV UHV AC transformation project:

(1) The TTLS's vibration modes are essentially the same as those of a single tower, but because transmission lines and other structures are present, the frequency of the TTLS is about 7% lower.
(2) The structural wind-induced vibration response is primarily based on the in-plane bending vibration of the first and second modes of the structure (mainly the first mode), and the wind-induced vibration response of the TTLS along the transmission lines is greater than that of the vertical transmission lines.
(3) The eddy current TMD (2% mass ratio) designed for the first second modes of the TTLS has some effect on controlling the wind-induced vibration of the structure, and the acceleration (STD) reduction rate is proved bigger than 30%, while the displacement (STD) reduction rate is about 10%.

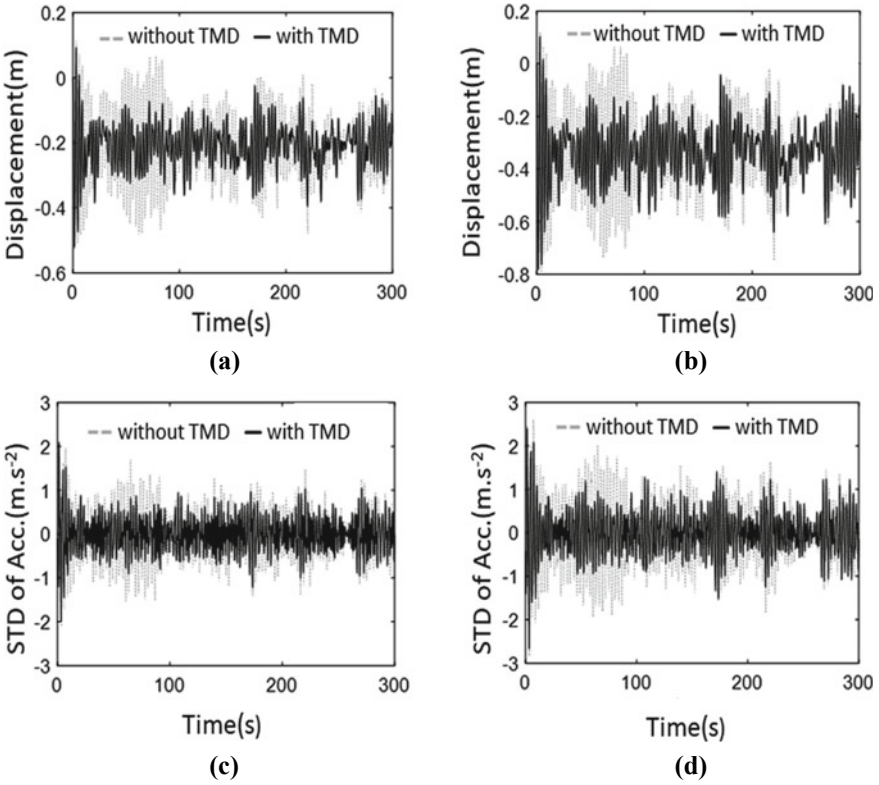

Fig. 10 The comparison results with or without TMD: **a** displacement results vertical the transmission lines; **b** displacement results along the transmission lines; **c** acceleration results vertical the transmission lines; **d** acceleration results along the transmission lines

Table 5 The tower-line system wind-induced vibration reduction rate summary

Item	0°	90°
Standard of displacement without TMD (m)	0.245	0.395
Standard of displacement with TMD (m)	0.212	0.352
STD reduction rate of displacement (%)	13.369	10.926
Standard of acceleration without TMD (m s^{-2})	0.564	0.756
Standard of acceleration with TMD (m s^{-2})	0.384	0.499
STD reduction rate of acceleration (%)	31.783	33.973

References

1. Guo, Y., Sun, B., Ye, Y., Lou, W., Shen, G.: Frequency-domain analysis on wind-induced dynamic response and vibration control of long span transmission line system. Acta Aerodyn. Sin. **27**(3), 288–295 (2009)
2. Irvine, H.M.: Cable Structure, pp. 468–479. The MIT Press, Cambridge (1981)
3. Zhang, Z., Wang, D., Wang, T., Yu, Z., Huang, Z., Zhang, D.: Aeroelastic wind tunnel testing on the wind-induced dynamic reaction response of transmission line. J. Aerosp. Eng. **34**(1), 04020105 (2021)
4. Ghazal, T., Elkassas, E., El-Masry, M.I.: Conductive cables vibrations effect on lattice steel transmission towers. J. Steel Struct. & Constr. **5**(1), 1–7 (2019)
5. Zhao, G., Lu, Z., Wang, X., Peng, Y., Chang, S.: Full scale experiment for vibration analysis of ice-coated bundled-conductor transmission lines. Struct. Eng. **26**(1), 336–352 (2021)
6. Deng, H., Zhu, S., Chen, X., Wang, Z.: Wind tunnel investigation on model of long span transmission line system. J. Tongji Univ. **31**(2), 132–137 (2003)
7. Chen, F.B., Yan, B.W., Weng, L.X., Cai, Q.R., Li, Q.S.: Wind tunnel investigations of aeroelastic electricity transmission tower under synoptic and typhoon winds. J. Aerosp. Eng. **34**(1), 1–13 (2021)
8. Lan, B., Yan, K.: Wind-induced vibration control for substation frame on viscous damper. Struct. Eng. **62**(3), 1303–1315 (2020)
9. Lei, X., Xie, W., Nie, M., Niu, H., Chen, J., Wang, Y.: Development and application of a new type of TMD in transmission tower vibration reduction. J. Vib. Shock **38**(13), 73–80 (2019)
10. Tian, L., Zeng, Y., Galvín, P.: Parametric study of tuned mass dampers for long span transmission tower-line system under wind loads. Shock Vib. **2016**, 1–11 (2016)
11. Liu, Z., Liu, Z.: Nonlinear finite element method for form-finding analysis of transmission line. J. New Ind. **3**(7), 50–58 (2013)
12. Yu, Z.: Wind simulation and coupled wind-induced vibration research of large span transmission tower-line systems. Ind. Constr. **44**(s1), 503–508 (2014)
13. Shinozuka, M., Yun, C.B., Seya, H.: Stochastic methods in wind engineering. J. Wind Eng. Ind. Aerodyn. **36**, 829–843 (1990)
14. Deodatis, G.: Simulation of ergodic multivariate stochastic processes. Eng. Mech. **122**(8), 778–787 (1996)
15. Den Hartog, J.P.: Mechanical Vibrations, pp. 126–131. Dover Publications, New York (1947)

Clean Energy Power Generation and Pollution Emissions from Engine

Geothermal Energy: Energy Alternative to Combat Frosts and Cold Spells in Perú

Diana Castillon Huayhua, Junior H. Nieto Lapa, and Steve D. Camargo Hinostroza

Abstract In recent years, frosts and cold spells have been more prolonged and have caused an increase in respiratory diseases, death of livestock, food shortages, and crop losses, especially in the high Andean areas. Therefore, this research was proposed to evaluate geothermal energy as an alternative to combat frosts and cold spells in Peru, this was done with information from ministries, important representative institutions, or attached to the above and scientific articles on the subject, taking into account the economic, social, and environmental. The results show that there is a high geothermal potential, concentrated in the south of our country, with an electrical generation capacity of 3000 megawatts. The Schumann and Quello Apacheta projects are currently the most advanced and will have an initial investment of more than US$ 1000 million and an initial production of approximately 500 MW. The contributions that the use of geothermal energy will provide will be the generation of jobs, massive heating, cheap energy, zero emissions, it is not susceptible to meteorological changes, improves food conservation, and could add economic growth of 0.7–1.9% per year to the regions that host these geothermal power plants. Therefore, geothermal energy is a renewable natural resource due to the heat reserve stored inside the earth, where its efficiency, inexhaustibility, environmental friendliness, low cost, and durability make it a viable energy alternative to combat frosts and cold spells in Peru.

Keywords Geothermal energy · Frosts · Peru · Geothermal potential

1 Introduction

In the last two decades of this century, according to Rivera Delgado et al. (2021), the studies of energy transition and the role that innovation and technology play in the development of solutions energy and development of countries (mainly emerging economies) have claimed great importance in the research field of development, innovation systems, transitions to sustainability, and energy systems [1]. Hence, the

D. C. Huayhua (✉) · J. H. Nieto Lapa · S. D. Camargo Hinostroza
Continental University, San Carlos, 1980 Huancayo, Peru
e-mail: 75516910@continental.edu.pe

M. L. Kolhe (ed.), *Renewable Energy Systems and Sources*,
https://doi.org/10.1007/978-981-99-6290-7_5

energy demand is increasing in line with the increase in the consumption of goods and services, however, in the attempt to meet and satisfy these needs has led to overexploitation of fossil fuels for the production and distribution of these. As a result, concern has arisen about environmental care, because productive systems work with traditional energy resources and, given the limited ecological capacity we have, it is necessary to implement new clean energies. The earth possesses an enormous amount of these energetic resources (30 million Terawatts) [2], however, one of the bigger problems that faced humanity is the obtainment and transformation of these resources.

Energy is known for its indispensability for social, industrial, and economic development. Energy is the source that allows us to achieve high productivity values and economic growth, the industry currently uses large amounts of energy, mainly of the electrical type, therefore, industries require abundant energy, served at home, with adequate prices, which are safe, efficient, that do not run out and do not pollute the environment [3] and meeting these growing needs energy and protect the environment is one of the challenges facing the world; in our case, we have many different renewable sources, including geothermal [4].

On the other hand, in Peru, year after year, frosts and cold spells hit the high Andean areas of the country. CENEPRED estimates that, for this present year, more than 3.7 million hectares of crops (13% more than last year) are at risk of being exposed to low temperatures, and a few 550 districts in 17 regions of the country in high risk and very large of exposure in July and August. The largest number of hectares threatened itself find in the regions of Puno, Ayacucho, Arequipa and the great number of crops threatened them two first together with Ancash [5]. In addition, it is added that there are more than 7 million Peruvians, 663 thousand of whom live in the group of persons of very high risk and more than 6.5 million people are in the group high risk under the influence of the low temperatures, where influenza and pneumococcal is principals diseases more frequent and is vaccinations have not exceeded 30% [6], whatever thus increasing the vulnerability and risk of contracting respiratory diseases.

According to Rumbo Minero, (2020), geothermal energy is a cleaner alternative for ensuring sustainable electricity supply. Since geothermal energy uses steam that resides of the way naturally below the earth and then re-inject it after use, this generates a closed and sustainable cycle of electricity production. The world's first geothermal power plant began operating in 1913 and today, more than 100 years later, is still producing power. Well-managed, a geothermal reservoir could be inexhaustible [7].

For all the above mentioned, Peña Jumpa, (2014) frosts and friajes are common phenomena during the winter in the Peruvian Andes, causing the death of thousands of animals, destruction of homes, damage to health and family economy of people, which leads us to reflect on the need for the right to heating [8]. Therefore, this research aims to describe geothermal energy as an energy alternative to combat the frosts and cold that year after year hit our high Andean areas of our country.

2 Materials and Methods

2.1 Search Criteria

The search for information took into account the reliability of the pages or databases consulted, such as Google Scholar, Scielo, Springer Link, Scopus, among others and approved theses, as well as the journal ranking databases such as SCIMAGO.

On the other hand, when evaluating the social, economic, and environmental impacts of geothermal energy, we have taken into account laws, regulations, and relevant information provided by the virtual platforms of the Ministries involved in our research, as well as the most renowned newspapers in our country and abroad that show the energy potential of geothermal energy in Peru.

2.2 Frosts and Fringes

According to Editorial EC, 2022, Frost occurs when temperatures drop below 0 °C, this conception corresponds to meteorological frosts, but agrometeorological frosts, is the decrease in air temperature falls to critical values, which kills plant tissue. In the case of agrometeorological, frost depends on the critical temperature level of each crop and can be greater than 0 ºC [9]. Frosts have already hit much of the country's Andean highlands, causing an increase in respiratory diseases linked to the coronavirus (COVID-19) pandemic, with the most affected regions being Puno, Arequipa, Tacna, Moquegua, Cusco, Ayacucho, Huancavelica, Pasco, Junín, and Apurímac.

EC Newsroom, 2022, describes that the cold begins with moderate to heavy rains, thunderstorms, and winds in a south-to-north direction. The maximum temperatures will be lower due to cloudiness, therefore, these rains advance leaving the sky almost clear, to clear the southern jungle and the presence of cold air caused the temperature to drop significantly in a few hours [9], frosts occur about 6–10 times a year, and the duration of these frosts lasts from 3 to 7 days, in many extreme cases up to 10 days.

2.3 Geothermal Potential in Perú

In the field of energy production, we have an impressive water potential, along with natural gas more than 90% of electricity is produced, but we also have other promising sources such as geothermal heat, which comes from the heat of the interior of the earth [4], these geothermal deposits are originally found in hot springs and geysers.

Peru has abundant geothermal resources, where Master Plan estimates that Peru has geothermal potential to generate 3,000 MW distributed in thermal fields in the south of the country (60%). Therefore, Peru has implemented an integrated plan to

develop geothermal energy and contribute 1,000 MW of electricity by 2030 [10, 11]. This energy production will be constant and uninterrupted over time, since no other renewable energy (solar or wind), can be kept in operation for long periods since they suffer too many interruptions, mainly weather conditions. In addition, many experts say that geothermal energy is more efficient in the long term and thus provides greater energy security.

For Gonzales, 2022, Peru with its geothermal potential, can produce 3,000 MW, which is equivalent to 50% of the electricity currently produced throughout the country, this is due to our strategic and privileged location on the Pacific Ring of Fire [7]. As well as our country there are many others that have the same or even greater geothermal potential and reasons such as the growing energy needs have prompted Quaise Energy, they are embarking on an ambitious project; develop the deepest hole in the earth to extract geothermal energy [12] (see Fig. 1).

Normal geothermal development is concentrated in dry steam and hot steam systems; however, the enormous heat content of the Earth's interior is contained in dry rocks [13]. Therefore, Arequipa is one of the regions that intends to develop and explore the potential of renewable energy, this has generated public interest in promoting private investment for the exploration and exploitation of geothermal resources. Among the places of interest, we find that the Chivay—Pinchollo geothermal field has great potential, a generation power generation potential of 150 MW, the highest in the country, while the area can produce around 500 MW [14].

3 Results and Discussions

3.1 Social Impact

Peru has at least 44,000 population centers distributed in 17 regions of the country, where frost and cold hit in different ways. According to the National Center for Disaster Risk Estimation and Reduction (Cenepred), attached to the Ministry of Defense, 7 million 162,648 people are at a special level of vulnerability [6], where they suffer food shortages, loss of crops, loss of livestock, among others. Being the number of Peruvians vulnerable to low temperatures is very high, therefore, it is proposed the implementation of geothermal power plants, to achieve a widespread application in outdoor heating, homes, ponds or aquaculture centers and livestock centers.

According to the PNER, it diagnoses that Peru shows different special peculiarities such as; the remoteness, poor accessibility to localities, low consumption and low economic income make it impossible to use massive heating of large areas [15]. Under the deployment of renewable energy resources and emerging technologies will impact the development of the world, especially emerging market economies, provided that the development of appropriate technological solutions leads to greater prosperity

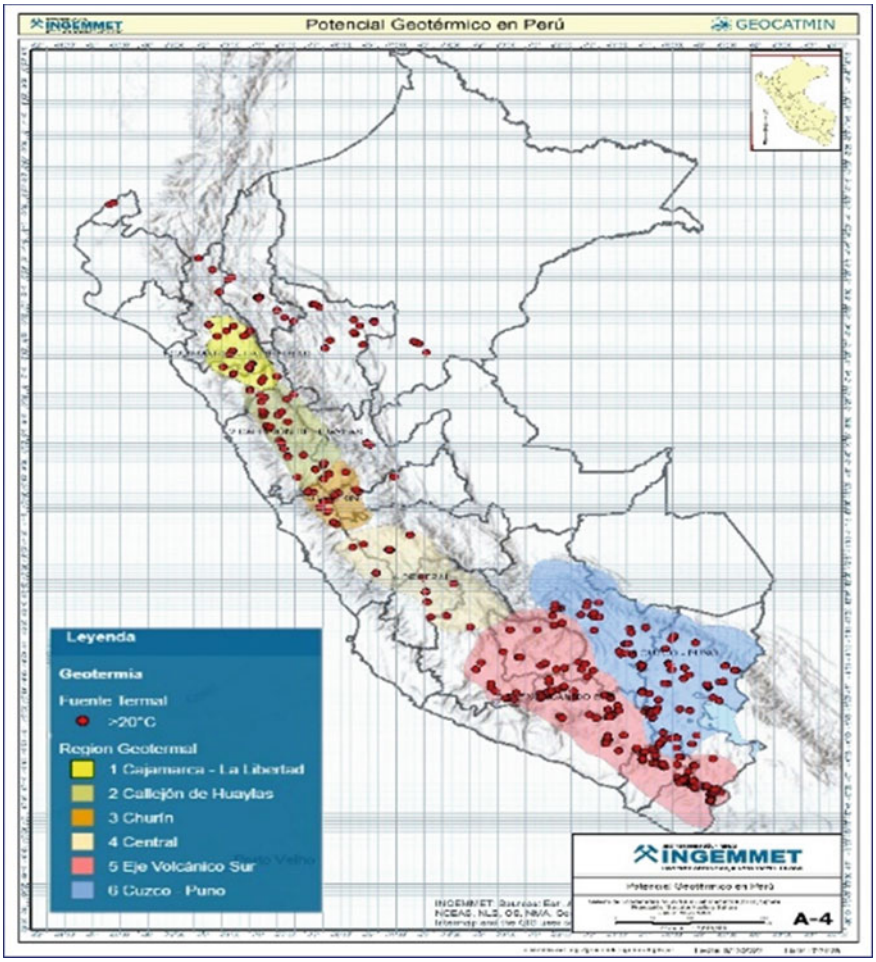

Fig. 1 Distribution of geothermal potential in Peru. *Source* Energy and Mines Sector-INGEMMET (2022). *Note* **a** Distribution of thermal source and thermal region in Peru. **b** Distribution of geothermal areas in the southern region of the country

in society, creating new jobs and improving the quality of life [7]. According to the workers' unions, in Peru, the energy transition is necessary and just for life, humanity, the planet and nature, however, they must be done with a fair process that does not deprive workers of their jobs, especially in the mining, oil, fishing sector, etc. [16], in Peru, Supreme Decree No. 003-2022 has already been approved, where the climate emergency is declared of national interest and making it essential to face it. In turn, the health crisis experienced has taught us that a country will not be able to walk without its workers and in the energy transition it must be carried out with the participation of its workers and society itself.

According to Perego (2021), in the last decades, geothermal energy has proven to be a reliable and efficient technology to provide heat and/or cooling to both residential and non-residential buildings, including industrial or research facilities, the clearest example being the ELI-NP "extreme light infra-structure" plant in Magurele, Romania, these systems were mostly used in cold climates [17], this European experience encourages the development of this type of technology in the high Andean zones of our country. It is a very reliable, effective, and low-cost alternative to combat the frosts and cold spells that occur year after year, which will benefit more than 7 million Peruvians who live in critical conditions, mostly due to the increasing frost and cold spells.

3.2 Environmental Impact

The energy transition (ET) is a way to decarbonize the world's energy systems, transforming them into carbon-free systems [1]. Geothermal power plants have become a renewable, environmentally friendly, and clean resource and are gradually being recognized, accepted, and valued [18] because they are very environmentally friendly.

Geothermal energy is a clean and renewable resource with abundant reserves, wide distribution and stable temperature, its development and use play an essential role in saving energy, reducing emissions and protecting the environment [18]. That said, renewable energies (solar and wind) are very susceptible to weather changes, however, geothermal energy is a more reliable, safe, affordable, and sustainable alternative capable of providing energy continuously and can be used worldwide and its implementation will contribute to minimizing the emission of greenhouse gases (GHG), thus mitigating climate change [19]. Geothermal projects are increasing in our country, for example, the regions of Arequipa, Trujillo and Loreto mainly, the latter has a project under evaluation, where specialists say that the non-consumption of fuels, makes it a sustainable alternative for the environment and most importantly, it will help reduce the conservation of the Amazon [20].

In 2020, the MINEM reports that in Peru the electricity demand amounted to 52,713 gigawatt-hours (GWh), in addition, around 5% has already been incorporated for the generation of electricity from renewable sources [4], also, in addition, geothermal energy is represented as an ecological alternative in energy production [7], since the source of heat emitted from the earth's core is inexhaustible and permanent. It should also be added that due to climate change there have been variations in rainfall patterns, which means that it will probably rain too little or rain too much and, in both cases, in both cases, this directly affects the performance of hydropower plants [21].

This year several geological and geophysical studies carried out in the Peruvian offshore would reveal the geothermal potential in oil basins in the north of the country, specifically in the Trujillo Basin, since a high heat flow has been discovered in formations related to methane hydrates. According to this study, a geothermal gradient of

up to 100 °C has been found and it is configured as an alternative to giving a second life to the oil platforms that are installed and thus add to the energy transition [22].

It is normally considered that the use of geothermal energy does not cause any environmental impact, however, according to Bussotti (1997) who has compiled the description of several authors who have investigated the possible effects of emissions on terrestrial ecosystems, they have reported that the damage is macroscopic in the trees growing around the geothermal power plants that were examined for this study, which basically consists of yellowing and necrosis of the leaf margins. The authors attribute it mostly to the action of boron, these damages are localized and affect only trees growing no more than a few tens of meters from the power plants [23].

3.3 Economic Impact

For Falen (2021), the government's investment in the fight against frost and cold will reach about S/524 million this year. According to the Multisectoral Plan for these events, this figure exceeds those registered between 2014 and 2019, however, it is lower than the budget approved during 2020 (S/670 million) and 2021 (S/994 million) [24], also, according to the Ministry of Development and Social Inclusion (MIDIS), some 18 million soles were allocated this year to social programs for interventions to protect users from exposure to frost and cold in the high Andean and jungle areas, in order to protect health [25].

According to La Vega Polanco (2021), geothermal energy is a resource that can attract significant investments. Peru plans to invest more than US$ 1,000 million in the construction of two geothermal plants in Arequipa (Achumani) and Moquegua (Quello Apacheta) with an initial capacity of 500 MW [4]. For Rumbo Minero (2020), the fact that Peru has a development potential of 3,000 MW makes it a very attractive country for this type of investment, which has a positive in the economy [8], many experts assure that the initial investment for the development of projects of this type is very high, however, they also indicate that the investment for this type of projects should be in the medium and long term.

Peru's economy has been plunged into a deep sea of doubt. First, even with the impact of the pandemic, combined with a series of bad public policy proposals has had a negative impact on confidence, reducing private investment [4]. According to the Central Bank, there will be no growth in 2022 and only moderate growth in 2023, however, if the government does this, there will be a great opportunity to restructure investments by promoting renewable energies and especially, investment in geothermal energy [11], in addition, according to Tuesta, investments in geothermal plants of US $ 1000 million may generate 0.7–1.9% of annual economic growth to the Arequipa region, likewise, it is estimated that there will be an impact on poverty reduction of 0.2–0.5 percentage points each year [4].

Geothermal energy could be used for air-conditioning of tourist hotels and could include a thermal hot baths service in an environmentally friendly way, and it could even be up to 20% cheaper than fossil fuels such as fuel oil or diesel [26], however,

according to Oviedo, if these proposals are implemented, the positive impact on tariffs will be significant, since there will be a reduction of between 6 and 7% for the end consumer [21]. Acevedo also explains that the Achumani project has a potential of 700 MWh and the first 100 MWh will cost between US$ 100 each, and the rest will be at market price [27], currently, the cost per MWh varies from US$ 25 to US$ 30, and the initial costs will compensate for the non-burning of fossil fuels and diesel.

4 Conclusions

The study shows that the geothermal potential in Peru is high, mainly due to its volcanic activity, with regions such as Puno, Arequipa, Moquegua, Ayacucho, Puno, and Pasco as the main areas of high viability to develop projects for the implementation of geothermal power plants, making it a usable resource for various activities throughout society, However, its energetic potential and availability in the Peruvian territory make it a renewable resource, since as the use of the resource increases, as it is estimated in the future, there will not be a decrease in its availability, and it is also environmentally friendly.

In the economic field, geothermal energy will contribute to a substantial increase in the economic growth of each region and consequently of the country. Reliability, inexhaustibility, durability, and low cost invite private investments to implement geothermal power plants to supply electricity to food industries, safe and natural heating, air conditioning of large areas and its non-susceptibility to weather changes make it an inexhaustible and safe energy source. Many experts assure that geothermal energy, due to its reliability, will be profitable in the short and long term, being the initial stage the most expensive, however, in the medium and long term, it could be up to 20% cheaper than traditional energies.

In the social field, the use of geothermal energy in Peru opens many employment centers in an amount of approximately 70,000 in the initial stage, according to many experts, and these will increase as the implementation, operation, and massification of geothermal energy are carried out, thus contributing to the reduction of unemployment and poverty rates at the national level. In addition, geothermal energy will help many high Andean areas with a very high vulnerability to low temperatures, to air-condition their areas, promote the creation of nurseries, intensify aquaculture, provide heating, among others, preventing the growth of the mortality rate in infants and older adults, massive deaths of livestock, loss of crops and food shortages.

References

1. Rivera Delgado, D., Díaz López, F.J., Carrillo González, G., Rivera Delgado, D., Díaz López, F.J., Carrillo González, G.: Transición energética, innovación y usos directos de energía geotérmica en México: un análisis de modelado temático. Probl. Desarro **52**(206), 115–141 (2021). https://doi.org/10.22201/IIEC.20078951E.2021.206.69713
2. Pous, J., Jutglar, L.: Energía geotérmica. CEAC, Barcelona (2004). https://books.google.com.pe/books?id=4DcMwnKF4wwC&printsec=frontcover&dq=energia+geotermica&hl=es&sa=X&redir_esc=y#v=onepage&q=energia%20geotermica&f=false. Accessed 05 Dec 2022
3. Llorrenc Guilera, A.G.: La industria 4.0 en la sociedad digital. Marge Books, Barcelona (2019). https://ebookcentral.continental.elogim.com/lib/unicont/reader.action?docID=5758826&query=energia+geotermica. Accessed 04 Dec 2022
4. de la Vega Polanco, M.: Perú tiene potencial en la geotermia para suministrar energía eléctrica. El Peruano, Lima, 23 February 2021. https://elperuano.pe/noticia/115835-peru-tiene-potencial-en-la-geotermia-para-suministrar-energia-electrica. Accessed 05 Dec 2022
5. Ciriaco Ruiz, M.: Heladas y friaje: Más de 3,7 millones de hectáreas de cultivo están en riesgo por las bajas temperaturas. Diario: El Comercio, NOTICIAS EL COMERCIO PERÚ, Lima, 05 July 2022. https://elcomercio.pe/peru/heladas-y-friaje-mas-de-37-millones-de-hectareas-de-cultivo-estan-en-riesgo-por-las-bajas-temperaturas-senamhi-cenepred-ecdata-noticia/. Accessed 09 Dec 2022
6. Bazo Reisman, A.: Heladas y friaje: Más de 7 millones de peruanos entre los más vulnerables ante las bajas temperaturas. Diario: El Comercio, NOTICIAS EL COMERCIO PERÚ, Lima, 03 July 2022. https://elcomercio.pe/peru/heladas-y-friaje-mas-de-7-millones-de-peruanos-entre-los-mas-vulnerables-ante-las-bajas-temperaturas-vacunacion-invierno-cenapred-ecdata-noticia/. Accessed 09 Dec 2022
7. Minero, R.: Potencial geotérmico peruano equivale al 50% de la electricidad que producimos. Rumbo Minero Internacional, 13 February 2020. https://www.rumbominero.com/peru/noticias/energia/potencial-geotermico-peruano-equivale-al-50-de-la-electricidad-que-producimos/. Accessed 05 Dec 2022
8. Peña Jumpa, A.: Heladas, Granizadas, Nevadas, Friajes y el Derecho a la Calefacción en los Andes. Agro Enfoque **29**(192), 53–54 (2014). https://pwebebsco.continental.elogim.com/ehost/detail/detail?vid=3&sid=90314f44-3084-4f3c-b5d6-b1362ad243cd%40redis&bdata=Jmxhbmc9ZXMmc2l0ZT1laG9zdC1saXZl#AN=95395316&db=a9h. Accessed 09 Dec 2022
9. Redacción EC: ¿Qué son las heladas, nevadas y friajes? Senamhi te precisa los conceptos. Diario: El Comercio, NOTICIAS EL COMERCIO PERÚ, Lima, 30 June 2022. https://elcomercio.pe/lima/sucesos/invierno-2022-que-son-las-heladas-nevadas-y-friajes-senamhi-te-precisa-los-conceptos-frio-enfermedades-respiratorias-rmmn-noticia/. Accessed 09 Dec 2022
10. Ministerio de Energia y Minas (MINEM): Plan maestro para el desarrollo de la energia geotermica en el Peru, February 2012
11. Tuesta, D.: Sobre volcanes, energía y crecimiento sostenible. Diario: El Comercio, NOTICIAS EL COMERCIO PERÚ, Lima, 02 October 2022. https://elcomercio.pe/economia/peru/david-tuesta-sobre-volcanes-energia-y-crecimiento-sostenible-consejo-privado-de-competitividad-noticia/. Accessed 05 Dec 2022
12. Gonzales, R.: Planean hacer el agujero más profundo de la Tierra para extraer una energía ilimitada. La Republica, Lima, 12 March 2022. https://larepublica.pe/ciencia/2022/03/11/planean-hacer-el-agujero-mas-profundo-de-la-tierra-para-extraer-una-energia-ilimitada-energia-geotermica/. Accessed 05 Dec 2022
13. Fink, D.G., Wayne, B.H., Carroll, J.M.: Manual Practico de Electricidad Para Ingenieros: Tomo 3, vol. 3, 11th edn. REVERTE S. A., Barcelona (1984). https://books.google.com.pe/books?id=0MvCfacWoLcC&pg=RA9-PA11&dq=energia+geotermica&hl=es&sa=X&ved=2ahUKEwis3qi6o-T7AhWcLrkGHRhPC0wQ6AF6BAgJEAI#v=onepage&q=energia%20geotermica&f=false. Accessed 05 Dec 2022

14. Jorquera, C.: Arequipa en Perú, busca potenciar energía geotérmica. Piensa en GEOTERMIA, 01 August 2017. https://www.piensageotermia.com/arequipa-en-peru-busca-potenciar-energia-geotermica/. Accessed 05 Dec 2022
15. Direccion General de Electrificacion Rural: Plan Nacional de Electrificación Rural 2021–2023. Lima, Lima, December 2020
16. Jara, M.: Transición energética justa con trabajo digno, la demanda en Perú. Inter Press Service: Periodismo y comunicacion para el cambio global, Lima, 08 September 2022. https://ipsnoticias.net/2022/11/transicion-energetica-justa-con-trabajo-digno-la-demanda-en-peru/. Accessed 05 Dec 2022
17. Perego, R., Pera, S., Boaga, J., Bulgheroni, M., Dalla Santa, G., Galgaro, A.: Thermal modeling of a Swiss urban aquifer and implications for geothermal heat pump systems. Hydrogeol. J. **29**, 2187–2210 (2021). https://doi.org/10.1007/s10040-021-02355-7/Published
18. Hou, J., Luo, X., Zhang, L.: Establishment of evaluation model for shallow geothermal energy resource development potential based on characteristic of geotemperature. Earth Sci. Res. J. **24**(3), 312–320 (2020). https://doi.org/10.15446/esrj.v24n3.89513
19. Vega-Garzon, L.P., Parra Ramos, J.A., García Sarmiento, M.P., Ruiz Gaitán, M.A., Pedraos Juya, L.A.: Use of geothermal energy in the food industry: a review. Revista Ingenierías Universidad de Medellín **21**(40), 67–86 (2022). https://doi.org/10.22395/rium.v21n40a5
20. Jorquera, C.: Resumen webinar: Perspectiva tecnológica de energía geotérmica para Loreto, Perú. Piensa en GEOTERMIA, 09 August 2022. https://www.piensageotermia.com/resumen-webinar-perspectiva-tecnologica-de-energia-geotermica-para-loreto-peru/. Accessed 05 Dec 2022
21. Lozano Alfaro, V.: Energías renovables: cambio necesario con visión de futuro para asegurar sostenibilidad. El Peruano, Lima, 05 December 2022. http://www.elperuano.pe/noticia/198353-energias-renovables-cambio-necesario-con-vision-de-futuro-para-asegurar-sostenibilidad. Accessed 05 Dec 2022
22. Jorquera, C.: Webinar: La geotermia podría alargar la vida de las plataformas petroleras off shore del Perú, 14 de Junio. Piensa en GEOTERMIA, 14 June 2022. https://www.piensageotermia.com/webinar-la-geotermia-podria-alargar-la-vida-de-las-plataformas-petroleras-off-shore-del-peru-14-de-junio/. Accessed 05 Dec 2022
23. Bussotti, F., Cenni, E., Cozzi, A., Ferretti, M.: The impact of geothermal power plants on forest vegetation. A case study at Travale (Tuscany, central Italy). Environ. Monit. Assess. **45**, 181–194 (1997)
24. Falen, J.: Recursos aprobados para enfrentar las heladas y el friaje serán los más bajos de los últimos tres años. Diario: El comercio, NOTICIAS EL COMERCIO PERÚ, Lima, 17 July 2021. https://elcomercio.pe/peru/recursos-aprobados-para-enfrentar-las-heladas-y-el-friaje-seran-los-mas-bajos-de-los-ultimos-tres-anos-informe-bajas-temperaturas-invierno-covid-19-ec-data-noticia/. Accessed 09 Dec 2022
25. Redaccion EP: Medidas frente a heladas y friaje. Diario Oficial El Peruano, Lima, 23 June 2022. https://elperuano.pe/noticia/162127-medidas-frente-a-heladas-y-friaje. Accessed 11 Dec 2022
26. Anonymous: Entregan concesiones para explotar energía geotérmica en cinco estados: [1]. Business and Economics, Mexico, 22 July 2015. https://www.proquest.com/docview/1698014887/F690BB6605FD4073PQ/5?accountid=146219. Accessed 04 Dec 2022
27. Caretas: Energía geotérmicalCalor de Tierra. Ilustracion Peruana CARETAS, Lima, 22 October 2022. https://caretas.pe/medio-ambiente/energia-geotermica-calor-de-tierra/. Accessed 05 Dec 2022

Selecting the Raw Material Plant of Biomass Power in the Northeastern Region of Thailand Using AHP and Fuzzy TOPSIS

Noppakun Sangkhiew, Choosak Pornsing, Shunichi Ohmori, and Peerapop Jomtong

Abstract The world is facing an energy crisis. Many nations have changed to producing power using a variety of renewable energy sources, including agricultural waste (biomass). Raw materials are one of the key elements for biomass power plants and must be properly chosen. This paper is the application of the Analytic Hierarchical Process (AHP) and Fuzzy Technique for Order Preference by Similarity to Ideal Solution (Fuzzy TOPSIS) for selecting the raw material plant of biomass power in the northeastern region of Thailand. The AHP is conducted to calculate the weights, and the fuzzy TOPSIS is conducted to rank three biomass raw material alternative plants based on the criteria. There are eight criteria that affect the success of biomass power plants: price, shipping costs, potential, diversity, stability, quality, and raw water. The result shows that specialists are most concerned about price and quality. Therefore, Plant A is ranked first in this study, which is in line with the major criteria of concern. It is reasonable and related because the price of raw materials must be suitable for the quality of the raw materials.

Keywords Biomass power · Fuzzy TOPSIS · AHP · Climate change

N. Sangkhiew (✉) · C. Pornsing
Department of Industrial Engineering and Management, Silpakorn University, Nakhon Pathom 73000, Thailand
e-mail: Meja.noppakun@gmail.com

S. Ohmori
Graduate School of Creative Science and Engineering, Waseda University, Tokyo 169-8050, Japan

P. Jomtong
Department of Biomedical Engineering, Faculty of Health Sciences, Christian University, Nakhon Pathom 73000, Thailand

M. L. Kolhe (ed.), *Renewable Energy Systems and Sources*,
https://doi.org/10.1007/978-981-99-6290-7_6

1 Introduction

Currently, the world is facing an energy crisis, which is either caused by the climate change, a sudden surge in demand, or war. As a result, there is an ongoing global fuel shortage. The global fuel price index increased by 100 points between August 2021 and March 2022. Meanwhile, the 2022 annual weighted price index for energy is expected to increase by nearly 50 points compared to 2021 [1]. It's not just about the price, but also the environmental impact. In particular, the accumulation of carbon dioxide in the atmosphere causes a greenhouse reaction.

According to the International Energy Agency (IEA) World Energy Outlook 2021 report, the electricity sector is the largest source of global CO2 emissions today and accounts for about 44% of energy sector emissions [2, 3]. Multiple factors, such as the type of conversion technology, plant efficiency, fuel type and quality, fuel transport distance, and local conditions (such as wind and solar resources), among others, affect the GHG emissions produced during the generation of electricity [4]. Energy resources are used in electricity generation, which is primarily fossil fuels like coal, oil, and natural gas. Significant problems including air pollution, high carbon emissions, and inadequate power supply security have been brought on by an over-reliance on fossil fuels for power generation [5].

In Thailand, the main source of electricity generation is fossil fuels, which are still insufficient for their use. The highest domestic power demand in 2021 was 31,023 megawatts (MW), an increase of 2.2% compared to the peak power demand of the previous year [6]. Therefore, it is necessary to find a near-depleted energy solution to rising electricity demands. Because if energy runs out, it will cause various economies to stagnate in terms of trade, investment, communication, transportation, etc.

The Thai government sector encouraged the private sector to invest in renewable energy or renewable energy within the country. The biomass power plant is one of the projects supported by the government. In order to obtain enough renewable energy for use, Thailand has studied and researched various technologies for turning biomass into biomass energy. The combustion biomass power plant uses agricultural waste or industrial production waste such as rice husks, bagasse, rice straw, palm bunches, and wood chips as fuel to produce electricity and steam. The working principle is similar to the thermal power plant. However, biomass is used as a combustion fuel to generate heat in steam generation.

One of the problems with biomass energy use is an insufficient amount of biomass to produce electricity. When looking for other types of biomass or from other sources to supplement, there will be problems in various matters as follows: (1) transportation costs; (2) high cost of technology applicable to many biomass fuels; and (3) high risk of collecting biomass in sufficient quantity from various sources. In addition, raw material criteria must also be considered, such as the raw material price, the energy potential of the raw material, the raw material quality, the raw material stability, and others.

There are quite a few biomass power plants in the northeastern region of Thailand, and there is a high demand for the raw materials needed to make fuel. So

that entrepreneurs can choose the right and quality raw material plants. This paper is the application of Analytic Hierarchy Process (AHP) and Fuzzy Technique for Order Preference by Similarity to Ideal Solution (Fuzzy TOPSIS) for selecting the raw material plant of biomass power in the Northeastern region of Thailand. The remainder of this paper is structured as follows in Sect. 2, where we present details on the AHP and Fuzzy TOPSIS, which is the principle method of our calculation. In Sect. 3, we show the results of selecting the raw material plant. Finally, conclusions are drawn in Sect. 4.

2 Methodology

In this paper, AHP was conducted to determine weights for the success criteria of biomass power plants. FUZZY TOPSIS was then conducted to compare biomass raw material plants. Then we will get suitable raw material plants in the northeastern region of Thailand.

2.1 Analytical Hierarchy Process (AHP)

Thomas Saaty introduced the Analytical Hierarchy Process (AHP). This approach compares every criterion of each alternative. The basis of the AHP is the pair-wise comparison model, which determines the weights of every unique criterion [7].

AHP calculation procedure

Step 1: Determine the criteria and sub-criteria for the decision hierarchy while considering the research objective.

Step 2: Using the basic scale of pair-wise comparison, create a set of all judgements in the comparison matrix where the set of elements is already compared.

Step 3: The corresponding Eigenvectors to the maximum Eigenvalues of comparison can be calculated to determine the relative weight of various factors.

Step 4: Verify the consistency of judgments across the Consistency Index (*CI*) and the Consistency Ratio (*CR*).

$$CI = \frac{\lambda_{\max} - n}{n - 1} \tag{1}$$

where $\lambda_{\max}$ is the Eigenvalue corresponding to the matrix of pair-wise comparisons and n is the number of elements being compared.

Consistency ratio (*CR*) is defined as:

$$CR = \frac{CI}{RI} \tag{2}$$

where *RI* is a random consistency index.

In general, a *CR* value of less than 0.1 is acceptable; if not, pair-wise comparisons should be revised to reduce incoherence.

2.2 The Fuzzy TOPSIS for Group Decision Making

According to TOPSIS's fundamental principle, the chosen alternative should be the closest to the positive-ideal solution and the farthest from the negative-ideal solution. The positive-ideal solution maximizes the criteria for benefits while minimizing the criteria for costs. On the other hand, the negative-ideal solution optimizes the cost criteria while minimizing the benefit criteria [8].

Group decision-making is the method of selecting a solution or solutions to a problem using data offered by several decision-makers. When DMs are operating in a fuzzy environment or when their understanding of the subject being studied is insufficient [9].

Fuzzy TOPSIS calculation procedure

Step 1: Select the linguistic ratings for the alternatives and the criterion.

Step 2: The fuzzy decision matrix should be created.

The fuzzy decision matrix will be obtained with m rows and n columns, where n is the number of criteria and m is the number of alternatives. The matrix is Eq. (3) where $\tilde{x}_{ij}$ is calculated as follows:

$$\tilde{x}_{ij} = \frac{1}{k}(\tilde{x}_{ij}^{1} \oplus \cdots \oplus \tilde{x}_{ij}^{k}) \tag{3}$$

Note that $\tilde{x}_{ij}^{k}$ is the performance rating of the ith alternative, A_i, with respect to the jth criterion, c_j evaluated by kth, decision-maker and $\tilde{x}_{ij}^{k} = (l_{ij}^{k}, m_{ij}^{k}, u_{ij}^{k})$.

Step 3: The normalization of the fuzzy decision matrix $\tilde{R}$ is shown as

$$\tilde{R} = [\tilde{r}_{ij}], i = 1, 2, \ldots, m \text{ and } j = 1, 2, \ldots, n \tag{4}$$

$$\tilde{r}_{ij} = \left(\frac{l_{ij}}{u_j^+}, \frac{m_{ij}}{u_j^+}, \frac{u_{ij}}{u_j^+}\right) \tag{5}$$

$$\tilde{r}_{ij} = \left(\frac{l_j^-}{u_{ij}^+}, \frac{l_j^-}{m_{ij}^+}, \frac{l_j^-}{l_{ij}^+}\right) \tag{6}$$

where $u_j^+ = \max_i \{u_{ij} | i = 1, 2, \ldots, n\}$—benefit criteria.

and $l_j^- = \min_i \{l_{ij} | i = 1, 2, \ldots, n\}$—cost criteria.

Step 4: Calculate the weighted normalized fuzzy decision matrix. The weighted normalized value v_{ij} is calculated as follows:

$$\tilde{V} = [\tilde{v}_{ij}]_{\text{mxn}}, i = 1, 2, \ldots, m \text{and} j = 1, 2, \ldots, n \tag{7}$$

where

$$\tilde{v}_{ij} = \tilde{r}_{ij} \otimes \tilde{w}_{ij}, i = 1, 2, \ldots, m \text{and} j = 1, 2, \ldots, n \tag{8}$$

Step 5: Both the positive and the negative-ideal solutions will be Determined. Due to the inclusion of the positive triangular fuzzy numbers in the range [0, 1], the fuzzy positive-ideal solution (FPIS A+) and the fuzzy negative-ideal solution (FNIS A−) can be defined as

$$A^+ = \left(\tilde{v}_1^+, \tilde{v}_2^+, \ldots, \tilde{v}_n^+\right) = \left\{\max_i \tilde{v}_{ij} | (i = 1, 2, \ldots n)\right\} \tag{9}$$

$$A^- = \left(\tilde{v}_1^-, \tilde{v}_2^-, \ldots, \tilde{v}_n^-\right) = \left\{\min_i \tilde{v}_{ij} | (i = 1, 2, \ldots n)\right\} \tag{10}$$

Step 6. Calculate the distances of each initial alternative to FPIS A+ and FNIS A−.

The equations that can be used to determine how far from each alternative is from the fuzzy positive ideal reference point and fuzzy negative ideal reference point, respectively, as follows

$$d_i^+ = \sqrt{\frac{1}{3}\sum_{j=1}^{n}\left(\tilde{v}_{ij} - \tilde{v}_j^+\right)^2} \tag{11}$$

$$d_i^- = \sqrt{\frac{1}{3}\sum_{j=1}^{n}\left(\tilde{v}_{ij} - \tilde{v}_j^-\right)^2} \tag{12}$$

Step 7. The closeness coefficient should be calculated. The proximity coefficient for each alternative should be determined (CC) as

$$CC_i = \frac{d_i^-}{d_i^+ + d_i^-}, i = 1, 2, \ldots, m \tag{13}$$

Step 8. According to their relative closeness, the alternatives are ranked. The best alternatives are those that have a higher value of C_i and therefore should be chosen because they are closer to the positive-ideal solution.

2.3 The Criteria

In this study, the criteria that affect the success of biomass power plants are extracted from a literature review. To compare the raw material plant of biomass power in Thailand, several attributes were chosen as comparison criteria:

C1—Price, defined as the raw material price.
C2—Shipping costs, defined as raw material shipping costs.
C3—Potential, defined as the energy potential of the raw material.
C4—Diversity, defined as variety of fuel raw materials.
C5—Stability, defined as the climate-related stability of raw materials.
C6—Quality, defined as the quality of the raw materials.
C7—Raw water, defined as the quality of the amount of raw water used in the production process.

2.4 The Alternatives of Raw Material Plant of Biomass Power in Thailand

According to the Electricity Generating Authority of Thailand, the Northeastern region of Thailand has more companies that generate electricity using biomass than any other area in Thailand. In these plants, most of the raw materials used in biomass power plants are bagasse. Therefore, the sugar factory that supplies bagasse to the biomass power plant is the raw material source that we have chosen. The choice of biomass raw materials plant was selected from 3 plants in the northeastern province as Table 1.

Table 1 The choice of biomass raw materials plant

Plant	Information
A	Registered Capacity 20,582 Tons Cane/day Distance from Bangkok to Factory 600 km
B	Registered Capacity 30,000 Tons Cane/day Distance from Bangkok to Factory 562 km
C	Registered Capacity 24,000 Tons Cane/day Distance from Bangkok to Factory 650 km

3 Results

3.1 Weight of Criteria Evaluation

Thomas Saaty proposed the judgment scale as follows: 1—equally important; 3—weakly more important; 5—strongly more important; 7—demonstrably more important; 9—absolutely more important. The values in between (2, 4, 6, and 8) represent compromise judgments. The results of a pair-wise comparison of each of the seven criteria listed are shown in the preference matrix from Table 2. The weight value and importance of the criteria are shown in Table 3.

The sequence of factors affecting the success of biomass power plants was obtained from the application of an analytical hierarchical method as shown in Table 3. We found that entrepreneurs gave the most importance to the price of raw materials. The second is quality, and the third is energy potential.

Table 2 Preference matrix

Criteria	C1	C2	C3	C4	C5	C6	C7
C1	1	7	5	9	5	3	9
C2	1/7	1	1/3	4	1/3	1/5	4
C3	1/5	3	1	5	1/2	1/4	5
C4	1/9	1/4	1/5	1	1/5	1/7	2
C5	1/5	3	2	5	1	1/3	1
C6	1/3	5	4	7	3	1	1
C7	1/9	1/4	1/5	1/2	1	1	1
Total	2.98	10.23	22.20	16.67	3.87	12.83	30.00

Table 3 The weight criterion

Criteria	C1	C2	C3	C4	C5	C6	C7	The weight criterion
C1	0.477	0.359	0.393	0.286	0.453	0.506	0.391	40.923
C2	0.068	0.051	0.026	0.127	0.030	0.034	0.174	7.291
C3	0.095	0.154	0.079	0.159	0.045	0.042	0.217	11.304
C4	0.053	0.013	0.016	0.032	0.018	0.024	0.087	3.463
C5	0.095	0.154	0.157	0.159	0.091	0.056	0.043	10.790
C6	0.159	0.256	0.314	0.222	0.272	0.169	0.043	20.511
C7	0.053	0.013	0.016	0.016	0.091	0.169	0.043	5.717
Total	1	1	1	1	1	1	1	100.000

3.2 Alternatives Evaluation

Surveys were employed in this study to gather information from Biomass Power Plant Entrepreneurs in the northeastern province. Respondents were asked to rate on a five-point Likert scale varying from "Strongly disagree" (1) to "Strongly agree" (5). As a result, triangular distribution is conducted for calculation. Although it cannot predict the actual distribution of random variables, it is a very helpful technique to convey uncertainty [10]. The aggregated triangular decision matrix is shown in Table 4.

Triangular distributions are useful in decision-making because the DMs can be easily specified by three parameters: the minimum (L), maximum (H), and most probable (M) value. As a result, triangular numbers are generated from the individual assessments of the DMs. Lets $\tilde{a}(l_{ij}^k, m_{ij}^k, u_{ij}^k)$ be an element of matrix, representing the group performance rating of an alternative $A_i (i = 1, 2, \ldots, m)$ attribute $C_j (j = 1, 2, \ldots, n)$ specified by k^{th} DMs. Aggregation of the DM preferences is described below [11]:

$$l_{ij}^k = \min_k x_{ij}^k \tag{14}$$

$$m_{ij}^k = \sqrt[k]{\prod_{k=1}^{k} x_{ij}^k} \tag{15}$$

$$u_{ij}^k = \max_k x_{ij}^k \tag{16}$$

The fuzzy decision matrix is normalized by using a linear scale transformation. Using the Eqs. (14)–(16), a triangular fuzzy number that represents fuzzy data is generated, as shown in Table 5.

Following the Fuzzy TOPSIS procedure, data is calculated. The relative distance to the optimal solution was estimated using the weight criterion. Then, the alternatives according to the relative closeness were ranked as shown in Table 6.

The results indicate plant A is assumed to be the best appropriate plant in the northeastern province than among the 3 plants. Further, plant B is the second one that is very close to the first preference. Considering the weight criterion, the weight of C1 and C6 are what the specialists are concerned with the most out of the 7 criteria respectively.

Table 4 The aggregated triangular decision matrix

Plant	Criteria						
	C1	C2	C3	C4	C5	C6	C7
A	(3, 4.68, 5)	(3, 3.57, 4)	(4, 4.18, 5)	(4, 4.78, 5)	(3, 3.09, 4)	(3, 4.13, 5)	(3, 3.57, 4)
B	(3, 4.35, 5)	(3, 3.84, 5)	(4, 4.18, 5)	(4, 4.78, 5)	(3, 3.37, 4)	(3, 3.70, 5)	(3, 3.57, 4)
C	(3, 3.54, 5)	(4, 4.37, 5)	(4, 4.18, 5)	(4, 4.78, 5)	(3, 3.27, 4)	(3, 4.25, 5)	(3, 3.57, 4)

Table 5 Triangular decision matrix

Plant	Criteria						
	C1	C2	C3	C4	C5	C6	C7
A	(0.6, 0.94, 1)	(0.6, 0.71, 0.8)	(0.8, 0.84, 1)	(0.8, 0.96, 1)	(0.75, 0.62, 1)	(0.6, 0.83, 1)	(0.75, 0.71, 1)
B	(0.6, 0.87, 1)	(0.6, 0.77, 1)	(0.8, 0.84, 1)	(0.8, 0.96, 1)	(0.75, 0.67, 1)	(0.6, 0.74, 1)	(0.75, 0.71, 1)
C	(0.6, 0.71, 1)	(0.8, 0.87, 1)	(0.8, 0.84, 1)	(0.8, 0.96, 1)	(0.75, 0.65, 1)	(0.6, 0.85, 1)	(0.75, 0.71, 1)

Table 6 Rank the preference order

Plant	TOPSIS index	Rank
A	0.4999	1
B	0.4900	2
C	0.4799	3

4 Conclusions

Nowadays, Thailand is using more electricity to develop utilities, economic growth, and improve the quality of life of society. For this reason, fuel is being imported for use in the production of power. Consequently, the government has promoted the use of biomass as a fuel for producing power. Thailand is a country with a large amount of agricultural land, low fuel imports, and a lower risk of varying fuel consumption proportions.

Raw materials are one of the factors that affect the success of biomass power plants. This study aimed to select the raw material plant for biomass power in the northeastern region of Thailand. Selecting plant criteria are criteria that affect the success of biomass power plants. The 7 criteria were calculated by the AHP method. Then, three sugar factories that supply bagasse to the biomass power plant are compared by using Fuzzy TOPSIS. The results showed that Plant A and Plant B are in the first and second ranks in this study. It is in line with the major criteria of concern; specialists care about the price and quality. It is reasonable and related because the price of raw materials must be suitable for the quality of the raw materials. However, Plant C is also suitable since all 3 have very similar index values. Therefore, it can be seen that entrepreneurs can choose raw materials from all three raw material plants.

Raw materials are one of the key elements for biomass power plants and must be properly chosen. Decision making is very difficult. If there is no method appropriately, they may not be able to choose the right alternative for their plant. Therefore, this study can be used as a guide for selecting the raw materials for biomass power plants in different locations for entrepreneurs.

Acknowledgements This research was financially supported in part by Department of Industrial Engineering and Management, Faculty of Engineering and Industrial Technology, Silpakorn University.

References

1. Global Energy Prices—statistics & facts. https://www.statista.com/topics/1323/energy-prices/#topicHeader__wrapper. Accessed 10 Aug 2022
2. World Energy Outlook 2021. https://iea.blob.core.windows.net/assets/4ed140c1-c3f3-4fd9-acae-789a4e14a23c/WorldEnergyOutlook2021.pdf. Accessed 10 Aug 2022
3. Anderson, J., Fergusson, M., Valsecchi, C.: An overview of global greenhouse gas emissions and emissions reduction scenarios for the future. Eur. Parliam. **2**, 11 (2007)
4. Scarlat, N., Prussi, M., Padella, M.: Quantification of the carbon intensity of electricity produced and used in Europe. Appl. Energy **305**, 117901 (2022)
5. Abdul, D., Wenqi, J., Tanveer, A.: Prioritization of renewable energy source for electricity generation through AHP-VIKOR integrated methodology. Renew. Energy **184**, 1018–1032 (2022)
6. Thai energy situation Year 2021. https://www.eppo.go.th/epposite/index.php/th/energy-information/energy-status/year?orders%5bpublishUp%5d=publishUp&issearch=1&orders%5bpublishUp%5d=publishUp&issearch=1. Accessed 12 Aug 2022
7. Wang, T.C., Lin, Y.L.: Accurately predicting the success of B2B e-commerce in small and medium enterprises. Expert Syst. Appl. **36**(2), 2750–2758 (2009)
8. Krohling, R.A., Pacheco, A.G.: A-TOPSIS–an approach based on TOPSIS for ranking evolutionary algorithms. Procedia Comput. Sci. **55**, 308–317 (2015)
9. Chrysafis, K.A., Theotokas, I.N., Lagoudis, I.N.: Managing fuel price variability for ship operations through contracts using fuzzy TOPSIS. Res. Transp. Bus. & Manag. 100778 (2022)
10. Glickman, T.S., Xu, F.: The distribution of the product of two triangular random variables. Stat. Probab. Lett. **78**(16), 2821–2826 (2008)
11. Bayram, H., Şahin, R.: A simulation based multi-attribute group decision making technique with decision constraints. Appl. Soft Comput. **49**, 629–640 (2016)

Solving Supplier Selection for the Photovoltaic System Using Fuzzy Analytic Hierarchy Process

Peerapop Jomtong, Noppakun Sangkhiew, Jaruwan Jankong, Tawiwan Sareebot, Suphachai Yingcharoen, and Choosak Pornsing

Abstract The purpose of this research is to study and analyze the decision-making process considering supplier for the photovoltaic system by using Fuzzy Analytic Hierarchy Process (FAHP) calculation technique used in Multiple Criteria Decision-Making (MCDM). In this research, there are eight criteria: Price (C_1), Financial and Reliability (C_2), Service (C_3), System technology (C_4), Experience (C_5), Maintenance and Repair (C_6), Supply Capacity (C_7), and Quality & Warranty policy (C_8). From this research, factors that affect the decision-makers such as chief executives and engineers are discovered. The criterion most weight is Price (C_1) with weight of 29.56% following by Financial and Reliability (C_2) with weight of 14.53%. Service (C_3) criterion is ranked thirdly important with the weight of 12.74%, and supplier III is likely to be chosen and is the most beneficial one with weight at 39.05%. The number of these weights can be obtained from the experts' judgment in the form of subjective judgment and used as a guidance in prioritizing and making decision on which supplier selection. All of these are the ones to advance the sustainable development of the solving supplier selection for the photovoltaic system.

Keywords MCDM · FAHP · Photovoltaic system · Sustainable

1 Introduction

Electricity is one of the most essential infrastructures and a primary factor that runs the world, either in communication, transportation, agriculture, or industries. As time passes, there is an increasing need for stable electricity and easy access to it. People make decisions every day about both significant and minor matters. It is essential that

P. Jomtong (✉) · N. Sangkhiew · C. Pornsing
Department of Industrial Engineering and Management, Faculty of Engineering and Industrial Technology, Silpakorn University, Nakhon Pathom 73000, Thailand
e-mail: Peerapop_jomthong@hotmail.com

P. Jomtong · J. Jankong · T. Sareebot · S. Yingcharoen
Department of Biomedical Engineering, Faculty of Health Sciences, Christian University, Nakhon Pathom 73000, Thailand

M. L. Kolhe (ed.), *Renewable Energy Systems and Sources*,
https://doi.org/10.1007/978-981-99-6290-7_7

the decisions made are logical enough to generate and ensure the good outcomes, as well as, to find alternatives, and to come up with information that is beneficial for the organization or the community as a whole and is consistent with the rules and decisions that well-timed [1, 2].

Multiple Criteria Decision-Making method is the consolidation of alternative assessment and the comparison of possible alternatives in different factors [3]. The comparisons of each alternative are measured by assessing their appeal according to each criterion, prioritize the reliability in ranking in order to determine the importance of each factor [4].

In this study, the researchers use the Fuzzy Analytic Hierarchy Process technique [5]. The FAHP method uses problem-solving and analyzing the factors and alternatives in the decision-making of supplier for the photovoltaic system: with eight criteria for supplier selection. The researcher lead to Fuzzy Analytic Hierarchy Process which is complex solutions but that are simple to understand with Multiple Criteria Decision-Making calculation so that we can find out the best and most appropriate criteria and alternative. Therefore, the main aim of the current research is to select the best sustainable suppliers for the photovoltaic system of case study.

2 Methodology

2.1 Fuzzy Analytical Hierarchy Process

The Analytic Hierarchy Process (AHP) is a structured technique based on mathematics and behavioral psychology for organizing and analyzing complicated decisions. It was created by Thomas L. Saaty in the 1970s. The AHP is a method of "measurement through pairwise comparisons and relies on the judgments of experts to derive priority scales" [6]. Even though the AHP scale simplifies the process to choose factor and provides data on dominance, there are defects that happen when comparison matrices are set up, and data unpredictability cannot be simply obvious in discrete levels. When the characteristics of factor is rising in a hierarchy, increasingly matchings between attributes need to be applied. However, the fuzzy set theory was created by Zadeh and has gained popularity in comparison, it can be used for the uncertainty of expert considerations [7]. Fuzzy Analytic Hierarchy Process method is presented by Triangular membership function. FAHP can be set as triple $X = (a, b, c)$, which defines a membership function as shown in Fig. 1 and Eq. (1) [8],

$$\mu(x) = \begin{cases} \frac{x-a}{b-a} & \text{if } a \le x \le b \\ \frac{c-x}{c-b} & \text{if } b \le x \le c \\ 0 & \text{if } x \le a \text{ or } x \ge c \end{cases} \tag{1}$$

In this paper, triangular membership function will be applied in order to compare a priority scale between each criterion as shown in Table 1 [9].

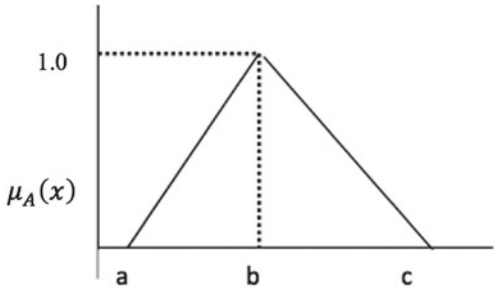

Fig. 1 Triangular membership function

Table 1 Point scale of FAHP

Definition	AHP of saaty	Fuzzy triangular	Reciprocal fuzzy
Equal importance	1	1, 1, 1	1, 1, 1
Intermediate values	2	1, 2, 3	1, 1/2, 1/3
Moderate importance	3	2, 3, 4	1/2, 1/3, 1/4
Intermediate values	4	3, 4, 5	1/3, 1/4, 1/5
Strong importance	5	4, 5, 6	1/4, 1/5, 1/6
Intermediate values	6	5, 6, 7	1/5, 1/6, 1/7
Very strong importance	7	6, 7, 8	1/6, 1/7, 1/8
Intermediate values	8	7, 8, 9	1/7, 1/8, 1/9
Extreme importance	9	9, 9, 9	1/9, 1/9, 1/9

Figure 2, The problem will be decomposed into a multi-level hierarchy. At "Problem identification", the objective is to choose suitable supplier. At "Criteria", the main criteria are $C_1, C_2, C_3, \ldots, C_n$. At "Alternative", the alternatives are Supplier 1 (S_1), Supplier 2 (S_2), Supplier 3 (S_3) [10].

$$A = \begin{bmatrix} 1 & \cdots & a_{1n} \\ \vdots & \ddots & \vdots \\ \frac{1}{a_{n1}} & \cdots & 1 \end{bmatrix} \tag{2}$$

$$a_{ij} = \begin{cases} 5 \text{ Criterion } i \text{ is Favored with criterion } j \\ 1 i = j \\ \frac{1}{5} \text{ Criterion } j \text{ is Favored with criterion } i \end{cases} \tag{3}$$

In the next step, we use the Consistency Ratio (CR) checking method created by Thomas L. Saaty. Which determined the CR as show in Eqs. (4)–(5).

$$CI = \frac{(\lambda_{\max} - n)}{n - 1}. \tag{4}$$

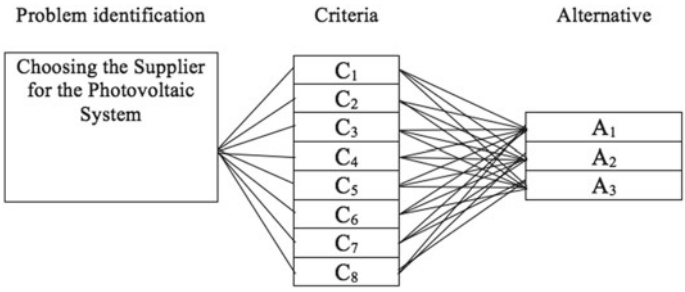

Fig. 2 Structured AHP model for supplier selection

Table 2 List of RI values

n	3	4	5	6	7	8	9	10
RI	0.52	0.89	1.11	1.25	1.35	1.40	1.45	1.49

$$CR = \frac{CI}{RI} \tag{5}$$

when, λ_{max} is the largest eigenvalue of matrix, n is a dimension of matrix and Random Index (RI), that depends on n [11], as shown in Table 2.

If the CR is less than or equal 0.01, the decision is acceptable. However, if it is not, the analyst must redo the whole process [12].

2.2 The Criteria

In this study, there are eight criteria: Price (C_1), Financial and Reliability (C_2), Service (C_3), System technology (C_4), Experience (C_5), Maintenance and Repair (C_6), Supply Capacity (C_7), and Quality & Warranty policy (C_8). Also, there are three suppliers to be selected.

3 Results

3.1 Weight of Criteria

The research started with the review of a secondary information which journal some clues of Supplier Selection and Photovoltaic System for the criteria. The results of the suggested strategy for choosing a photovoltaic system supplier. The pairwise

Table 3 Pairwise comparison matrix of criteria—FAHP

Criterion	C_1	C_2	C_3	C_4	C_5	C_6	C_7	C_8
C_1	(1, 1, 1)	(2, 3, 4)	(2, 3, 4)	(3, 4, 5)	(2, 3, 4)	(2, 3, 4)	(3, 4, 5)	(3, 4, 5)
C_2	(1/2, 1/3, 1/4)	(1, 1, 1)	(1, 1, 1)	(1, 1, 1)	(1, 1, 1)	(2, 3, 4)	(1, 2, 3)	(3, 4, 5)
C_3	(1/2, 1/3, 1/4)	(1, 1, 1)	(1, 1, 1)	(1, 2, 3)	(1, 2, 3)	(1, 1, 1)	(2, 3, 4)	(1, 1, 1)
C_4	(1/3, 1/4, 1/5)	(1, 1, 1)	(1/2, 1/3, 1/4)	(1, 1, 1)	(1/2, 1/3, 1/4)	(1/2, 1/3, 1/4)	(1, 2, 3)	(1, 1, 1)
C_5	(1/2, 1/3, 1/4)	(1, 1, 1)	(1/2, 1/3, 1/4)	(2, 3, 4)	(1, 1, 1)	(1, 1, 1)	(1, 1, 1)	(1, 2, 3)
C_6	(1/2, 1/3, 1/4)	(1/2, 1/3, 1/4)	(1, 1, 1)	(2, 3, 4)	(1, 1, 1)	(1, 1, 1)	(1, 1, 1)	(1, 2, 3)
C_7	(1/3, 1/4, 1/5)	(1, 1/2, 1/3)	(1/2, 1/3, 1/4)	(1, 1/2, 1/3)	(1, 1, 1)	(1, 1, 1)	(1, 1, 1)	(1, 1, 1)
C_8	(1/3, 1/4, 1/5)	(1/3, 1/4, 1/5)	(1, 1, 1)	(1, 1, 1)	(1, 1/2, 1/3)	(1, 1/2, 1/3)	(1, 1, 1)	(1, 1, 1)
Weight	**29.56**	**14.53**	**12.74**	**7.57**	**10.95**	**10.55**	**7.15**	**6.95**
CR	**8.26%**							

comparison matrix of eight criteria, that are Triangular membership function, is shown in Table 3.

Table 3 shows the weight of each criterion through the form of percentage. Therefore, it can be seen that the criteria 1 (price) is the most important criteria. But, at the other hand, criteria 8 (quality & warranty policy) is the lowest important criteria for this research. The consistency ratio (CR) is 8.26%, which is acceptable mathematically.

3.2 Weight of Alternatives

Next step, the experts rated in each criterion comparing with the alternatives to Photovoltaic System Supplier. The results can be found in Tables 4, 5, 6, 7, 8, 9, 10 and 11.

Tables 4, 5, 6, 7, 8, 9, 10, and 11 show the weight of importance of each alternative in the prioritization of the Photovoltaic System and Consistency Ratio values for each criterion. It is normalized matrix and the eigenvector weight calculated per relation are placed and introduced. Using the results from Table 3 (shows the weight of importance of criteria), it is now possible to generate matrix C. The columns in matrix C are put into order in the order of the criteria determined in Table 3: C1, C2, C3, C4, C5, C6, C7, C8. Performing the multiplication of matrix and the vector weight,

Table 4 Shows the comparisons of three suppliers with regard to Price (C_1)

C_1	I	II	III	Weight
I	(1, 1, 1)	(2, 3, 4)	(2, 3, 4)	58.88
II	(1/2, 1/3, 1/4)	(1, 1, 1)	(1, 1, 1)	20.56
III	(1/2, 1/3, 1/4)	(1, 1, 1)	(1, 1, 1)	20.56
CR	4.69			

Table 5 Shows the comparisons of three suppliers with regard to financial and reliability (C_2)

C_2	I	II	III	Weight
I	(1, 1, 1)	(1/2, 1/3, 1/4)	(1/3, 1/4, 1/5)	13.23
II	(2, 3, 4)	(1, 1, 1)	(1, 1, 1)	41.21
III	(3, 4, 5)	(1, 1, 1)	(1, 1, 1)	45.56
CR	4.53			

Table 6 Shows the comparisons of three suppliers with regard to service (C_3)

C_3	I	II	III	Weight
I	(1, 1, 1)	(1/3, 1/4, 1/5)	(1/4, 1/5, 1/6)	10.36
II	(3, 4, 5)	(1, 1, 1)	(1, 1, 1)	43.11
III	(4, 5, 6)	(1, 1, 1)	(1, 1, 1)	46.53
CR	2.57			

Table 7 Shows the comparisons of three suppliers with regard to system technology (C_4)

C_4	I	II	III	Weight
I	(1, 1, 1)	(1/4, 1/5, 1/6)	(1/2, 1/3, 1/4)	11.60
II	(4, 5, 6)	(1, 1, 1)	(1, 2, 3)	56.41
III	(2, 3, 4)	(1, 1/2, 1/3)	(1, 1, 1)	31.99
CR	9.23			

Table 8 Shows the comparisons of three suppliers with regard to experience (C_5)

C_5	I	II	III	Weight
I	(1, 1, 1)	(1/2, 1/3, 1/4)	(1/5, 1/6, 1/7)	9.73
II	(2, 3, 4)	(1, 1, 1)	(1/3, 1/4, 1/5)	22.18
III	(5, 6, 7)	(3, 4, 5)	(1, 1, 1)	68.09
CR	8.20			

Table 9 Shows the comparisons of three suppliers with regard to maintenance and repair (C_6)

C_6	I	II	III	Weight
I	(1, 1, 1)	(1, 1, 1)	(1, 1, 1)	32.72
II	(1, 1, 1)	(1, 1, 1)	(1, 1/2, 1/3)	27.33
III	(1, 1, 1)	(1, 2, 3)	(1, 1, 1)	39.95
CR	9.56			

Table 10 Shows the comparisons of three suppliers with regard to supply capacity (C_7)

C_7	I	II	III	Weight
I	(1, 1, 1)	(3, 4, 5)	(1, 1, 1)	44.25
II	(1/3, 1/4, 1/5)	(1, 1, 1)	(1/3, 1/4, 1/5)	11.50
III	(1, 1, 1)	(3, 4, 5)	(1, 1, 1)	44.25
CR	2.53			

Table 11 Shows the comparisons of three suppliers with regard to quality & warranty policy (C_8)

C_8	I	II	III	Weight
I	(1, 1, 1)	(1/2, 1/3, 1/4)	(1/3, 1/4, 1/5)	13.23
II	(2, 3, 4)	(1, 1, 1)	(1, 1, 1)	41.21
III	(3, 4, 5)	(1, 1, 1)	(1, 1, 1)	45.56
CR	4.53			

the preference vector for the three supplier structures may be obtained, according to the following relation.

3.3 Alternatives Evaluation

The pairwise comparison matrix of eight criteria in case of the FAHP (Triangular) is shown in Tables 3, 4, 5, 6, 7, 8, 9, 10, and 11.

$$x = Cw = \begin{bmatrix} 58.88 & 13.23 & 10.36 & 11.60 & 9.73 & 32.72 & 44.25 & 13.23 \\ 20.56 & 41.21 & 43.11 & 56.41 & 22.18 & 27.33 & 11.50 & 41.21 \\ 20.56 & 45.56 & 46.53 & 31.99 & 68.09 & 39.95 & 44.25 & 45.56 \end{bmatrix} \begin{bmatrix} 29.56 \\ 14.53 \\ 12.74 \\ 7.57 \\ 10.95 \\ 10.55 \\ 7.15 \\ 6.95 \end{bmatrix}$$

$$= \begin{bmatrix} 30.13 \\ 30.82 \\ 39.05 \end{bmatrix} \tag{6}$$

Based on the results from (6), it can be stated that, using FAHP (Triangular) method, the supplier III is to be chosen as the most suitable candidate and happened to be the most beneficial one, according to Tables 3, 4, 5, 6, 7 and 8, as the consistency ratio of FAHP (Triangular) is less than 10%.

4 Conclusion

This research really has an application of Fuzzy Analytic Hierarchy Process for the photovoltaic system supplier selection, the research of an electronic manufacturing services company. There were eight criteria and three companies. Clearly, it really was burdensome to take a decision sensibly without the enabling of the fancy decision-making tool, Fuzzy Analytic Hierarchy Process.

In this research, the criterion with the most weight is Price (C_1). The supplier III should be the first among all alternatives with consistency ratio value of less than 10%, which means it is a non-bias decision-making under subjective judgments and is considerably a justified decision-making process.

To sum up, Fuzzy Analytic Hierarchy Process used in this research can support decision-making in case that there are several criteria and alternatives and reduce the parallel comparison procedure which can confuse the experts during the rating step. The Fuzzy Analytic Hierarchy Process is an effective technique for making decisions. It can manage on both that are continuous and discrete.

Acknowledgements This article was supported in part by the Silpakorn University Research, Innovation and Creative Fund.

References

1. Wu, D.: Intelligent systems for decision support. University of Southern California (2009)
2. Lu, J., Ruan, D.: Multi-objective group decision making: methods, software and applications with fuzzy set techniques **6** (2007)
3. Phudphad, K., Watanapa, B., Krathu, W., Funilkul, S.: Rankings of the security factors of human resources information system (HRIS) influencing the open climate of work: using analytic hierarchy process (AHP). Procedia Comput. Sci. **111**, 287–293 (2017)
4. Abastante, F., Corrente, S., Greco, S., Ishizaka, A., Lami, I.M.: A new parsimonious AHP methodology: assigning priorities to many objects by comparing pairwise few reference objects. Expert Syst. Appl. **127**, 109–120 (2019)
5. Kabir, G., Sumi, R.S.: Power substation location selection using fuzzy analytic hierarchy process and PROMETHEE: a case study from Bangladesh. Energy **72**, 717–730 (2014)
6. Saaty, T.L.: Decision making with the analytic hierarchy process, Int. J. Serv. Sci. (2008)
7. Zadeh, L.: Fuzzy sets. Inform. Control **8** (1965)
8. Mandal, S.N., Choudhury, J.P., Chaudhuri, S.B.: In search of suitable fuzzy membership function in prediction of time series data. Int. J. Comput. Sci. Issues **9**(3), 293–302 (2012)
9. Wichapa, N., Khokhajaikiat, P.: Solving multi-objective facility location problem using the FAHP and goal programming: a case study on infectious waste disposal centers. Oper. Res. Perspect. **4**, 39–48 (2017)
10. Aşchilean, I., Badea, G., Giurca, I., Naghiu, G.S., Iloaie, F.G.: Choosing the optimal technology to rehabilitate the pipes in water distribution systems using the AHP method. Energy Procedia **112**, 19–26 (2017)
11. Huda, M., Okajima, K., Suzuki, K.: Identifying public and experts perspectives towards large-scale solar PV system using analytic hierarchy process. Energy Procedia **142**, 2554–2560 (2017)
12. Galankashi, M.R., Helmi, S.A., Hashemzahi, P.: Supplier selection in automobile industry: a mixed balanced scorecard–fuzzy AHP approach. Alex. Eng. J. **55**(1), 93–100 (2016)

Induction Stove Implementation for Sustainable Clean Energy Consumption: A Literature Study

Dania Latifa Rizky, Retno Wulan Damayanti, and Pringgo Widyo Laksono

Abstract Sustainable and clean energy is a big issue in several countries, including Indonesia. This oversized issue is why the Indonesian government focuses highly on prioritizing clean and sustainable energy, and an example of the efforts implemented is the conversion of 3 kg Liquefied Petroleum Gas (LPG) gas stoves to induction stoves. This program was considered due to its ability to reduce the 3 kg LPG gas subsidy budget, large quantities of carbon gas emissions, and fossil fuel usage. The first sector targeted was households because they are the primary consumers of the 3 kg LPG cylinders. However, this program's success requires studying the process of implementing an induction cooker for sustainable, clean energy consumption. Therefore, this study explores previous literature on induction stoves and their implementation in Indonesia and several other countries. Data were collected using a systematic literature review approach. The results showed that induction stove technology has great potential to reduce CO_2 emissions and the effect of greenhouse gases, which strongly supports the consumption of sustainable and clean energy. However, several challenges are associated with the conversion process in several countries, especially developing ones. This has led to the continuous formulation of strategies to accommodate these challenges, some of which can be implemented in Indonesia's induction cooker conversion program.

Keywords Induction stoves · Clean energy · LPG · Conversion program

D. L. Rizky (✉) · R. W. Damayanti · P. W. Laksono
Faculty of Engineering, Industrial Engineering Study Program, Sebelas Maret University, Jl. Ir. Sutami 36A, Surakarta 57126, Indonesia
e-mail: danialatifa97@student.uns.ac.id

R. W. Damayanti
e-mail: rwd@ft.uns.ac.id

P. W. Laksono
e-mail: pringgo@ft.uns.ac.id

M. L. Kolhe (ed.), *Renewable Energy Systems and Sources*,
https://doi.org/10.1007/978-981-99-6290-7_8

1 Introduction

Issues related to sustainable and clean energy have become important to several countries in recent years. This is indicated by the efforts to develop efficient and low-carbon equipment in addition to the production and utilization of clean and renewable energy [1]

The government of the Republic of Indonesia issued the National Energy Policy in Presidential Regulation Number 79/2014 to mandate the continuous usage of clean energy by lowering the carbon level in the country. The government currently has a target of reducing carbon emissions by nearly 400 million tons by 2030, which is almost five times the increase to the 64.4 million tons of CO_2 reduced in 2020. It has also been projected that renewable energy will supply 23% of primary needs by 2025 and 31% by 2050.

Several low-carbon recommendations made by the government to be implemented in 2020–2045 in other energy fields are also focused on encouraging the transition to renewable energy sources, increasing efficiency, and increasing the amount of biofuel usage [2]. The utilization of electricity sourced from renewable energy sources (EBT) and supported by digital technology is perceived to be the best solution to provide equitable access to clean energy in remote areas, ensure more efficient and sustainable management, reduce carbon emissions, and increase energy security.

One of the efforts made by the Indonesian government to encourage the energy transition is the appointment of PT PLN (Persero), which is the State Electricity Company to promote the use of induction cookers in 2017. This is based on the plan to convert 18% of gas stoves into induction stoves by 2050 through electrification, clean energy, and reduction of LPG usage [3]. PT PLN (Persero) followed up on these efforts in 2018 and 2019 by promoting discounts on power enhancements to encourage the switch from gas to induction stoves by households.

It was discovered that only 0.1% of PT PLN (Persero) customers have used induction cookers up to 2022, and only 5% were sold in Indonesia from 2018 to 2019. This is probably due to the lack of knowledge on the advantages of this new method of cooking compared to gas stoves, and this means PT PLN (Persero) needs to encourage Indonesian people, especially households, to use induction stoves [4].

An in-depth study is, therefore, required to determine the potential usage of induction cookers as a form of sustainable clean energy consumption in Indonesia to support the conversion program implemented by the government. This study serves as an initial stage to explore and map previous studies on induction cookers in Indonesia and several other countries. This is necessary to provide an overview and orientation for further research needed to ensure the successful implementation of the conversion program to support clean energy in Indonesia.

2 Methodology

This study was conducted using the systematic literature review (SLR), which involves identifying, reviewing, evaluating, and interpreting all available studies [5]. The method is one of the important stages required to initiate research and the literature study was achieved by collecting data and information related to induction stoves and energy efficiency directly from research journals on the *Scopus and Google Scholar databases.*

The keywords used *include* induction stove, energy efficiency, and induction heating. They were used to obtain studies with induction stove theme based on the following inclusion criteria:

- articles published between 2016 and 2022
- written in the English language
- focus on induction stoves and sustainable environment
- relevant, accredited, reputable, and attractive.

The journals that match these inclusion criteria were determined using the steps highlighted in Fig. 1 and retrieved for further analysis. The primary data obtained from the literature review were used in this study to make inferences and recommendations.

3 Findings

The summaries of journals related to induction cookers obtained from the literature review are presented in the following Table 1.

The search on Scopus and Google Scholar showed the research developments in the induction stove field for the last 8 years, from 2016 to 2022 and studies were observed to have increased over the years with the trend expected to increase in 2022 because the use of induction stoves is increasingly being encouraged in Indonesia.

It was discovered from Table 1 that the journals sampled vary widely with 17 observed to have different research designs and types such that 9 represented by 53% use quantitative and 47% or 8 use qualitative research designs. This means most of the studies prefer the quantitative approach in studying induction cooker efficiency and clean energy. The table also shows that a research instrument is required in the studies to collect data and experimental instruments were mostly adopted to determine the benefits of an induction stove in reducing greenhouse gas emissions due to their ability to produce more precise data compared to other instruments. This was indicated by the fact that 8 journals used the experimental method, 3 used questionnaires, and 2 journals used literature review, 2 journals used comparative studies, as well as surveys and interviews in a row. The findings also showed that 3 journals discussed carbon emissions, 6 focused on energy consumption, 1 focused

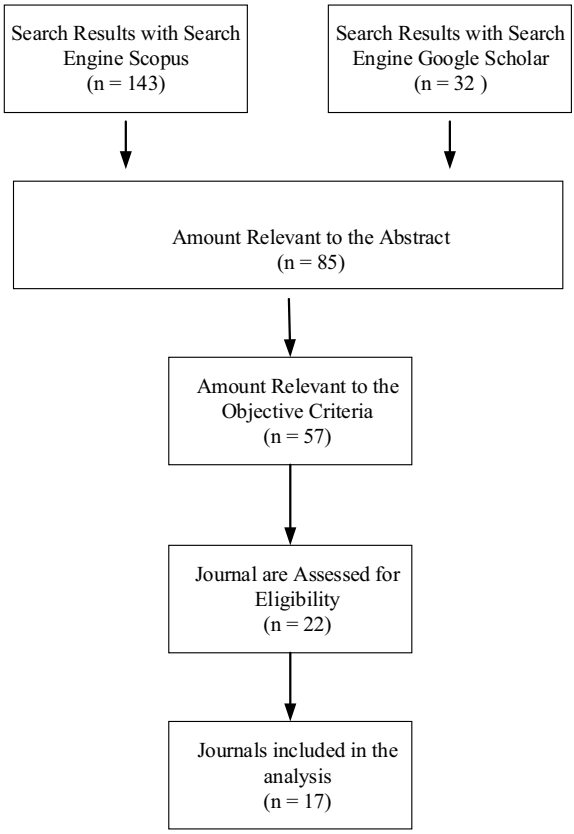

Fig. 1 Research flowchart

on cost and benefit, 5 on intervention and promotion of induction cookers usage, and 2 evaluated the potential use of induction cookers.

Suryati et al. [6] mentioned three scenarios to reduce greenhouse gases (GHG) in household activities in Medan City, with the first being the installation of solar panels on the roof of the house, the second is to replace the LPG stove with an induction stove, and the third is to use CH4 and household composting as a source of electrical energy. Further research was also recommended because the first and second scenarios require relatively high intervention costs. After all, households in rural India generally use traditional mud stoves as their primary cooking technology and LPG stoves as the secondary. Moreover, the switch from firewood to electricity only interested 5% of the respondents because most rural households are low-income earners [8].

Ugye et al. [12] also showed that induction stove is an efficient cooking technology and that electricity is cheaper for cooking. It was further stated that these stoves have better energy efficiency and lower operating costs compared to conventional electric and LPG stoves. They are also better in terms of time and energy consumption but have a shorter lifespan because electronic components are easily damaged by heat

Table 1 Results of the literature review study

Research/ Year	Subject	Instruments	Data analysis	Results	Country
Suryati et al. [6] 2021	Greenhouse gases	Questionnaire	IPCC (International Panel Climate Change) GHG emission calculation method	GHGs from household activities in Medan City can be reduced by installing solar panels on the roofs of houses, replacing LPG stoves with induction	Indonesia
Noverita and Mussry [7] 2020	Switching induction cooker from LPG	Surveys and interviews	Analytical descriptive	Marketing capabilities in CRM, NPD, and brand management need to be improved stoves, utilizing CH4 as a source of electrical energy, and household composting	Indonesia
Banerjee et al. [8] 2016	1000 rural households	Surveys and interviews	Undefined	Induction cookers will have limited potential in reducing fuelwood and LPG consumption if included	India
Zhou et al. [9] 2017	Greenhouse gases	Experiment	Analytical descriptive	1. Enhancing the gas supply pressure can eliminate the effect of altitude on the heat input There is a large heat loss and higher thermal efficiency during incomplete combustion in Lhasa 2. Oxygen-lacking conditions promote the formation of carbon monoxide and lower flame temperatures reduce the emission of nitrogen oxides	China

(continued)

Table 1 (continued)

Research/ Year	Subject	Instruments	Data analysis	Results	Country
Ramadhan and Ulfa [4] 2020	Promotion of induction cookers to household	Questionnaire	Analytical descriptive	The application of cognitive intervention methods can significantly increase the number of inductive stove users in Indonesia	Indonesia
Chhetri et al. [10] 2021	Infrared stove, induction cooker, LPG	Experiment	Analytical descriptive	Electric cooking is better for the environment because it can reduce greenhouse gas emissions	Bhutan
Tiandho et al. [11] 2021	Induction cooker	Literature review	Analytical descriptive	Induction hobs have better energy efficiency and lower operating costs	Indonesia
Ugye et al. [12] 2019	Induction cooker	Comparative studies	Analytical descriptive	An induction cooker is an efficient cooking technology and electricity is cheaper for cooking	South Africa
Tiandho et al. [13] 2021	Induction cooker and electric filament stove	Experiment	Analytical descriptive	Induction cookers have higher energy efficiency compared to Fiamen electric stoves	Indonesia
Kim et al. [14] 2017	Induction hob and gas stove	Questionnaire	Analytical descriptive	There are convenience and safety benefits for consumers using induction stoves instead of gas stoves	South Korea
Engineers et al. [15] 2019	Energy efficiency of induction cooker	Experiment	Analytical descriptive	Induction stoves are not significant harmonic sources, therefore, they do not generate a considerable increment of harmonic distortion levels in the residential sector	Ecuador

(continued)

Table 1 (continued)

Research/ Year	Subject	Instruments	Data analysis	Results	Country
Aisyah et al. [16] 2020	Induction cooker	Experiment	Analytical descriptive	Induction electric stoves are the most efficient because halogen and electric coils need more time to reach the boiling temperature of water	Indonesia
Im et al. [17] 2019	Induction cooker energy consumption	Comparative studies	Analytical descriptive	Induction cookers have the potential to reduce energy demand and greenhouse gas emissions	South Korea
Martínez et al. [18] 2017	CO_2 emissions and the economic impact of induction stove implementation	Experiment	Analytical descriptive	LPG-to-induction cooker conversion program can help reduce government subsidies	Ecuador
Hakam et al. [19] 2022	Induction cooker	Literature review	Descriptive	The application of induction stoves for cooking is more economical compared to LPG stoves in several scenarios tested in the study	Indonesia

(continued)

Table 1 (continued)

Research/ Year	Subject	Instruments	Data analysis	Results	Country
Anggono et al. [20] 2022	Costs and benefits of LPG stoves and electricity-based cooker	Experiment	Analytical descriptive	The policy can significantly reduce the energy cost for cooking on poorer households while relatively wealthy household undergoes higher energy costs for cooking because many of them are still using the subsidized LPG 3 kg. For them, the energy cost of the induction stove will be lower than the energy cost of the unsubsidized LPG 12 kg	Indonesia
Aemro et al. [21] 2021	Energy consumption, energy costs, efficiency, energy outputs/ inputs, Net Present Value (NPV), and heat transfer behavior of two electric resistance cookstoves	Experimental	Analytical descriptive	The pressure cookers provide a lower energy difference between output and input, higher water boiling efficiency and lower energy costs, whereas locally manufactured products resulted in higher energy difference, lower water boiling efficiency, and higher energy cost. Concerning NPVs, the single hot plate presents a better cost–benefit ratio compared with the other cookstove options	Ethiopia

[10]. Induction stoves are considered superior to other types in the aspect of carbon emissions. Moreover, electric cooking is better for the environment due to its ability to reduce greenhouse gas emissions and this means individual end users can benefit from cleaner and energy-efficient technological solutions at the micro level [10]. This means the conversion of LPG stoves to induction cookers can be one of the policy options to be considered by the Government of the Republic of Indonesia to achieve energy sustainability and reduce carbon emissions [11].

Ethiopia has specific policies and strategies recommended for adapting and promoting clean electronic cooking solutions, namely, developing clean cooking policies and strategies, increasing supply and demand, gender as a key component in implementing and promoting clean cooking, as well as energy access in remote areas with using solar power [21].

Some of the challenges associated with its implementation include misunderstanding, funding, accessibility, and weak institutional frameworks. The use of electricity as a cheap and efficient cooking fuel is very essential, and this is the reason Ugye et al. [12] suggested the adoption of subsidies, awareness campaigns, and application of large energy users as catalysts to encourage the use of induction cooking. Moreover, Ramadhan & Ulfa [4] stated that the application of cognitive intervention methods can significantly increase the number of induction cooker users in Indonesia, thereby, leading to a "good" category. This can be achieved through different media outlets including posters, videos, discussions, and promotions as well as other incentives such as the addition of more power and implementation of new installments to increase the number of PT PLN (Persero) customers beyond these induction stoves.

The studies conducted in Indonesia such as the proposed policy of migrating from LPG stoves to induction stove are economically feasible. This policy will reduce energy costs for cooking in households that are 450 VA and 900 VA customers by replacing imported energy with locally produced electricity [20]. Aisyah et al (2021) stated that people currently switching from liquefied gas-fueled to induction stoves perceive that induction stoves have higher efficiency than others.

However, its high operating power is a challenge that needs to be resolved to achieve the sustainable energy targets set in Indonesia [13]. The challenges that will be experienced are the need for grouping or installing special power lines for induction cookers in homes that have power below 2200 VA, rejection from people who are not used to using induction cookers, and LPG retailer or distributors who will certainly lose their business [20]. The majority of households are low-power electricity customers, thereby, indicating the need to reduce the price of induction cookers on the market [11].

Therefore, to achieve energy sustainability and reduce carbon emissions, converting LPG stoves to induction stove can be one of the policy options that can be implemented by the Government of the Republic of Indonesia through PT PLN (Persero). PT PLN (Persero) needs to strengthen Customer Relationship Management through a value delivery network and complaint handling, New Product Development through features and sales team, and Brand Management through its marketing communications. This is necessary because most customers represented by 63.36% are interested in using induction cookers but only a few, 15.7%, are willing to switch

[11]. Moreover, a business ecosystem needs to be built through the proposed government regulation to further encourage induction cooker innovation from producers and ensure a cooperation program to implement promotions [7]. Revocation of the 3 kg LPG gas subsidy, providing induction stove, cooking utensils and electrical installation for free, and large-scale campaigns can encourage people to voluntarily use induction stove [20].

The 17 studies reviewed showed that the transition from LPG to induction cookers has several challenges in different countries and this makes it difficult to reduce CO_2 emissions, thereby, leading to increased greenhouse gases. This means the government needs to participate in the process of launching the conversion program, issue regulations to support and ensure the use of induction cookers by the public, and strengthen marketing capabilities through complaint services, feature explanations, and marketing communications.

4 Conclusion

The literature review conducted showed that the research method that is widely used is an experiment because it can obtain more precise data compared to other instruments. Induction stove is an environmentally friendly technology that can help maintain sustainable clean energy but its adoption is faced with several challenges such as the non-willingness of people to switch from gas stoves because they think the operating costs of induction stoves are high. Therefore, the government needs to issue appropriate regulations to support and ensure the use of induction cookers and strengthen the capability of the customer relationship management department in value delivery networks and customer complaint handling processes.

References

1. Kusumadewi, T., Limmeechokchai, B.: Energy Procedia **138**, 955–960 (2017)
2. Sugiyono, A., Anindhita, Fitriani, I., Wahid, L., Adiarso: Indonesia energy outlook 2019: The impact of increased utilization of new and renewable energy on the national economy (Jakarta: Center of Assessment for Process Industry and Energy Agency for the Assessment and Application Technology) (2019)
3. Badan Pengkajian dan Penerapan Teknologi: Outlook Energi Indonesia 2019: Dampak Peningkatan Pemanfaatan Energi Baru Terbarukan Terhadap Perekonomian Nasional (2019)
4. Ramadhan, A.S., Ulfa, E.A.: Increasing the number of inductive stove users in Indonesia using cognitive intervention model to support industry 4.0 implementation at PT PLN (Persero). IOP Conf. Ser. Mater. Sci. Eng. **1096**(1), 012105 (2021). https://doi.org/10.1088/1757-899x/1096/1/012105
5. Triandin, E., Jayanatha, S., Indrawan, A., Putra, G.W., Iswara, B.: Metode systematic literature review untuk Identifikasi Platform dan Metode Pengembangan Sistem Informasi di Indonesia. IJIS Indones. J. Inf. Syst. **1**(2), 63–77 (2019)

6. Suryati, I., et al.: The mitigation strategy for reducing greenhouse gas emissions from household activities in Medan city. IOP Conf. Ser. Earth Environ. Sci. **802**(1) (2021). https://doi.org/10.1088/1755-1315/802/1/012034
7. Noverita, R., Mussry, D.J.S.: Proposed PT PLN (Persero) marketing capability to realize induction stove as a preferable option for LPG substitution and electrifying lifestyle growth. ICBMR **160**, 36–44 (2020). https://doi.org/10.2991/aebmr.k.201222.006
8. Banerjee, M., Prasad, R., Rehman, I.H., Gill, B.: Induction stoves as an option for clean cooking in rural India. Energy Policy **88**, 159–167 (2016). https://doi.org/10.1016/j.enpol.2015.10.021
9. Zhou, Y., Huang, X., Peng, S., Li, L.: Comparative study on the combustion characteristics of an atmospheric induction stove in the plateau and plain regions of China. Appl. Therm. Eng. **111**, 301–307 (2017). https://doi.org/10.1016/j.applthermaleng.2016.09.095
10. Chhetri, R., Lham, P., Chhetri, D.: Analysis of infrared stove, induction cooktop and LPG for cooking selective dishes in Bhutan, pp. 0–6 (2021). https://doi.org/10.13140/RG.2.2.28555.21288
11. Tiandho, Y., Indriawati, A., Putri, A.K., Afriani, F.: Induction stoves: an option for clean and efficient cooking in Indonesia. IOP Conf. Ser. Mater. Sci. Eng. **1034**(1), 012068 (2021). https://doi.org/10.1088/1757-899x/1034/1/012068
12. Ugye, R., Kolade, A., Abdullahi, A.J.: Comparative studies of cooking fuels and the need to harness induction cooking: South Africa as a case study. Am. J. Eng. Res. (AJER) **2006**(8), 155–161 (2019). www.ajer.org
13. Tiandho, Y., Afriani, F.: Comparison of efficiency and carbon emissions of filament electric stoves and induction electric stoves. J. Neutrino **14**(1), 12–19 (2021). https://doi.org/10.18860/neu.v14i1.13008
14. Kim, H.J., Lim, S.Y., Yoo, S.H.: Are Korean households willing to pay a premium for induction cooktops over gas stoves? Sustainability **9**(9) (2017). https://doi.org/10.3390/su9091546
15. E. Engineers, I.E. Commission, E. Regulation, C. Agency, C. Average, I. Duration: Impact of induction stoves penetration over power quality in Ecuadorian households **50160**(2011), 1–8 (2019)
16. Aisyah, S., Triani, M., Rasgianti, R.: Energy efficiency analysis for various type of electric cooker. J. Phys. Conf. Ser. **1869**(1), 012175 (2021). https://doi.org/10.1088/1742-6596/1869/1/012175
17. Im, H., Kim, Y.: The electrification of cooking methods in Korea—Impact on energy use and greenhouse gas emissions. Energies **13**(3) (2020). https://doi.org/10.3390/en13030680
18. Martínez, J., Martí-Herrero, J., Villacís, S., Riofrio, A.J., Vaca, D.: Analysis of energy, CO2 emissions and economy of the technological migration for clean cooking in Ecuador. Energy Policy **107**, 182–187 (2017). https://doi.org/10.1016/j.enpol.2017.04.033
19. Hakam, D.F., Nugraha, H., Wicaksono, A., Rahadi, R.A., Kanugrahan, S.P.: Mega conversion from LPG to induction stove to achieve Indonesia's clean energy transition. Energy Strat. Rev. **41**, 100856 (2022), November 2021. https://doi.org/10.1016/j.esr.2022.100856
20. Anggono, T., Ruslan, I., Anditya, C., Cendrawati, D.G., Irsyad, M.I.A.: Assessing the feasibility of migration policy from LPG stoves to induction stoves in Indonesia. IOP Conf. Ser. Earth Environ. Sci. **1041**(1), 0–8 (2022). https://doi.org/10.1088/1755-1315/1041/1/012039
21. Aemro, Y.B., Moura, P., de Almeida, A.T.: Experimental evaluation of electric clean cooking options for rural areas of developing countries. Sustain. Energy Technol. Assess. **43**, 100954 (2021), June 2020. https://doi.org/10.1016/j.seta.2020.100954

Estimation of Aircraft Engine Gas Emission by Mining ADS-B Data for Peninsular Malaysia Airspace

M. Mustaffa, N. A. Aini, S. Ahmad, and R. Ghazali

Abstract Aircraft engines release greenhouse gases that are comparable to those emitted from the combustion of fossil fuels, raising significant environmental concerns regarding their global and ground-level air quality impacts. With the escalating demand for air transport worldwide, air traffic has resulted in various issues and consequences for the global and national environments. The International Civil Aviation Organization (ICAO) has identified several pollutants in their database, including hydrocarbon (HC), carbon monoxide (CO), and nitrogen oxides (NOX). To estimate the gas emissions from aircraft engines, this study focused on gathering and analyzing aircraft movement data within the Kuala Lumpur Flight Information Regions (KLFIR) of Peninsular Malaysia, specifically limiting the analysis to the northern region. To accomplish this, a web-based application was developed, and a data mining approach was employed. The methodology comprised data collection and optimization, pre-processing and post-processing, database design, web application data analysis, and engine gas emission calculation, following the framework established by a prior study. The data utilized for this study were collected from existing equipment in the laboratory and obtained from freely available online services, specifically focusing on the year 2019. Through the data mining approach using ADS-B data, the analysis successfully estimated aircraft emissions, with nitrogen oxides (NOx) accounting for the highest emission count at 82% of the total, while carbon monoxide (CO) and hydrocarbon (HC) emissions were the lowest at 13 and 15%, respectively.

Keywords Aircraft engine emission · ADS-B data · Chemtrail · Data mining · Traffic density · Environmental pollution

M. Mustaffa · N. A. Aini (✉)
Fakulti Sains Gunaan, Universiti Teknologi MARA, 40450 Shah Alam, Selangor, Malaysia
e-mail: nazli2005@uitm.edu.my

S. Ahmad
Fakulti Kejuruteraan Mekanikal, Universiti Teknologi MARA, 40450 Shah Alam, Selangor, Malaysia

R. Ghazali
Fakulti Senibina, Perancangan & Ukur, Universiti Teknologi MARA, 40450 Shah Alam, Selangor, Malaysia

M. L. Kolhe (ed.), *Renewable Energy Systems and Sources*,
https://doi.org/10.1007/978-981-99-6290-7_9

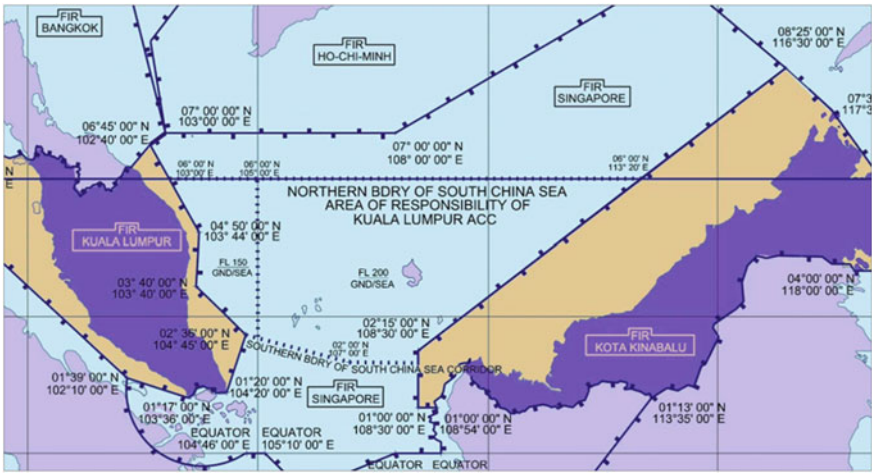

Fig. 1 Kuala Lumpur flight information regions [3, 4]

1 Introduction

Aircraft engines emit greenhouse gases similar to those produced from the combustion of fossil fuels. These emissions give rise to significant environmental concerns about their global impact and their impact on ground-level air quality [1]. As the global demand for air transport continues to rise, air traffic has led to problems and impacts on global and national environments. The pollutants identified in the International Civil Aviation Organization (ICAO) database include hydrocarbon (HC), carbon monoxide (CO), and nitrogen oxides (NOX) [2].

This study will estimate aircraft engine gas emission by collecting and analyzing aircraft movement data in Peninsular Malaysia airspace [3] or also known as Kuala Lumpur Flight Information Regions (KLFIR) as in Fig. 1 and limit the area of study to the northern region of Peninsular. A web-based application was developed, and a data mining approach was used to accomplish this objective.

2 Background

Automatic Dependent Surveillance Broadcast (ADS-B) is a surveillance technology that enables aircraft to broadcast important information to neighboring aircraft and nearby ground stations as shown in Fig. 2 [3, 5]. Air Traffic Services (ATS) relies on this information to manage air traffic in such a way as to prevent collisions between aircraft to provide this service. ATS has relied on radar surveillance or primary radar to provide this position information [6]. ADS-B is a surveillance application transmitting parameters such as ID, position, velocity, and operational status via a

digital data link introduced by ICAO [7]. Samples of decoded data are shown in Fig. 3.

Meanwhile, traffic density is relative to the traffic existence domain in the space or area as a time-varying and was introduced as a tool for identifying the safety and efficiency of air traffic [1, 8]. Air traffic density also refers to the degree of congestion of traffic in a sector of airspace. Estimation of aircraft engines' gas emissions is part of the study in traffic density [9–11].

Several studies have been using a data mining approach on ADS-B data. Probabilistic models were proposed from extracted ADS-B data using a genetic algorithm for cluster analysis [12]. There is also a study on ADS-B data to derive an accurate meteorological model and use it to determine aircraft performance parameters including a study of aviation impacts on the atmosphere. There is also a study on the ASEAN region to the estimated amount of air pollutants such as NOX and CO_2 due to air traffic activity implementation in the region [13]. A methodology has also been developed in the framework of the MEET (methodologies for estimating air pollutant emissions from transport) Project to estimate emissions for air traffic [14].

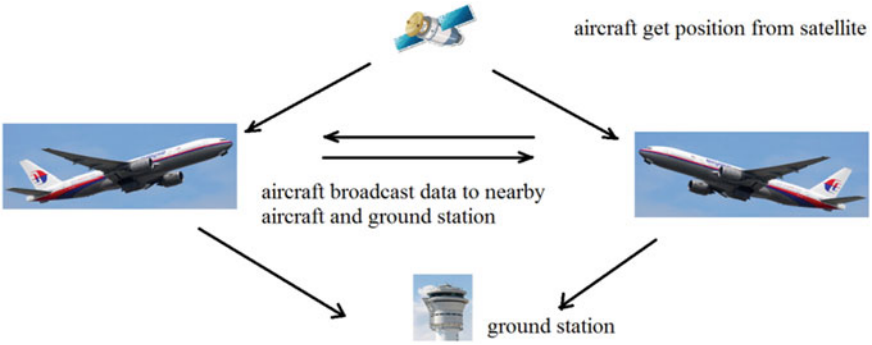

Fig. 2 Basic concept of ADS-B transmission [3]

```
3,MSG,6,0,0,8A07C9,0,2019/12/31,16:35:00.508,2019/12/31,16:35:00.508,,,,,,,2441,0,0,0,0
4,MSG,5,0,0,8A07C9,0,2019/12/31,16:35:00.514,2019/12/31,16:35:00.514,,37975,,,,,,0,,0,0
5,MSG,5,0,0,750288,0,2019/12/31,16:35:00.535,2019/12/31,16:35:00.535,,15700,,,,,,0,,0,0
```

Fig. 3 Sample of decoded ADS-B data [19]

3 Methodology

We divided our approach into data collection and optimization, pre-processing and post-processing, database design, web application data analyzer, and engine gas emission calculation adapting the framework from the previous study [15–17].

This study will only use collected for the year of 2019 data from existing equipment in our laboratory and also data downloaded from free online services [3, 18]. As we know, ADS-B messages provide only basic information about a given aircraft. To complement the ADS-B data, other relevant information about aircraft was retrieved from external open sources or any online service, which are often scattered across different systems and applications. Open internet sources can provide general aircraft data such as flag, aircraft type, number of engines and type of engine used, wake turbulence, and other construction details.

In general, raw data may contain up to 22 data fields separated by commas with up to 8 transmission types and all data collected were initially in CSV format. We only consider data for message type 3, which contains the position of the aircraft besides other information such as the ICAO number of the aircraft, time stamp, and altitude. We group data into the ICAO number of each aircraft and then into aircraft types or models. All data were then exported to our SQL database, which also stored all raw and analyzed data for the system.

A web-based front-end application was developed for the study and was divided into three main categories as web;

- Static Data—information of aircraft such as ICAO, aircraft type and model, number of engines and type, wake turbulence, fuel.
- Dynamic Data—information such as coordinates, height, speed, vertical rate, heading.
- Analyzed Data—module specifically to perform analyzing data such as number of traffics, traffic trajectory, and engine gas emission.

From the decoded data, we analyzed each aircraft on its ICAO number and flight time recorded in the system. Then, to estimate the engine emission, we are using an approach proposed by the ICAO [20]. Equation 1 was used to estimate the pollutant emissions, which are hydrocarbon (HC), carbon monoxide (CO), and nitrogen oxides (NOx) as;

$$E = t \times FF \times EI \times NE \tag{1}$$

where:

E—Total Emission of pollutant product by aircraft in kilogram (kg).

t—Time duration of the flight in seconds (s).

FF-Fuel flow, in kilogram per second (kg/s) for each engine used on aircraft.

EI—Emission index for the pollutant in kilograms per pollutant of fuel, for each engine used on aircraft.

NE—Number of engines on aircraft.

4 Result and Discussion

The web application that has been developed managed to analyze a total of 307,621 numbers of aircraft for the year 2019 with monthly average aircraft of 25,635. Trends f aircraft numbers as in Fig. 4 are ranging between 16,364 and 34,907 aircraft. Data for March 2019 were selected for detailed analysis due to its highest number of aircraft.

To estimate the aircraft engine gas emission, we use sample data for March 2019 as shown in Fig. 5. The gas emission for individual aircraft was calculated based on the aircraft model. Table 1 shows the top most common aircraft model in our data. We used Eq. 1 to calculate the emission of individual models using flight time, fuel flow (FF), and Emission Index (EI) for pollutants.

Then the systems calculate the monthly total engine gas emission of all aircraft for March 2019 which resulted in total gas emission of 65,795,135 kg, an average of 2,141,056 kg daily and 1,936 kg per flight as listed in Table 2 and Fig. 6. Nitrogen oxides contribute most of the total emission, and carbon monoxide is estimated as the second highest followed by the lowest total emission type which is a hydrocarbon. Total emissions for each of these pollutants are seen fluctuated throughout the month.

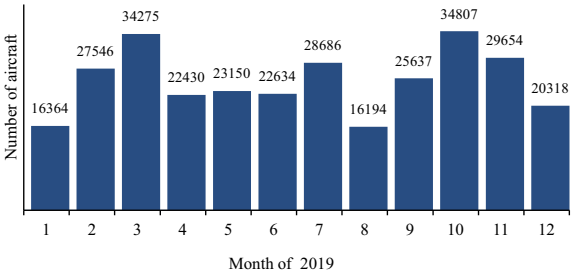

Fig. 4 Monthly number of aircraft for the year 2019

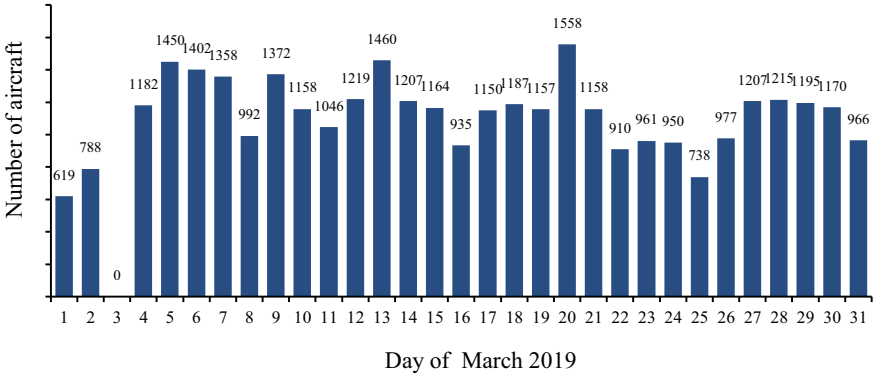

Fig. 5 Daily number of aircraft for March 2019

Table 1 Emissions for common aircraft engine emissions for March 2019

Model	Fuel flow (kg/h)	Total aircraft	Total time (s)	Emissions index	Total (kg)	
					Pollutant	All
Airbus A320	2.64	242	2,004,420	HC:0.0005 CO:0.0019 NO_X:0.0317	5,291 20,108 335,491	360,891
Boeing B737	2.75	220	1,489,800	HC:0.0015 CO:0.0029 NO_X:0.0205	12,290 23,762 167,974	204,028
Airbus A330	6.46	112	402,900	HC:0.0061 CO:0.0081 NO_X:0.08	31,753 42,164 416,437	490,355

Table 2 Engine gas emissions for March 2019

	Engine emission/kg	HC	CO	NO_X
Total	65,795,135	2,126,611	6,269,744	57,976,388
Average per day	2,141,056	2212	6524	60,329
Average per aircraft	1,936	2,201	6,490	1,691

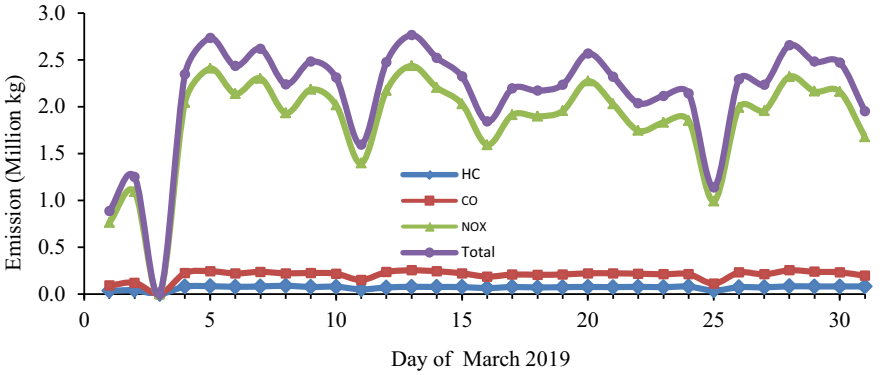

Fig. 6 Daily aircraft engine gas emission by type for March 2019

We are using the emission index for HC, CO, and NO_x based on what has been used by other studies [21–23] and assumed that the values of fuel flow and emission index are identical for the same aircraft model such as B737-200, B737-300 was assumed to have the same FF and EI.

The total monthly emission of aircraft engine emission was then further calculated using the same method for all months of 2019, which is shown in Fig. 7.

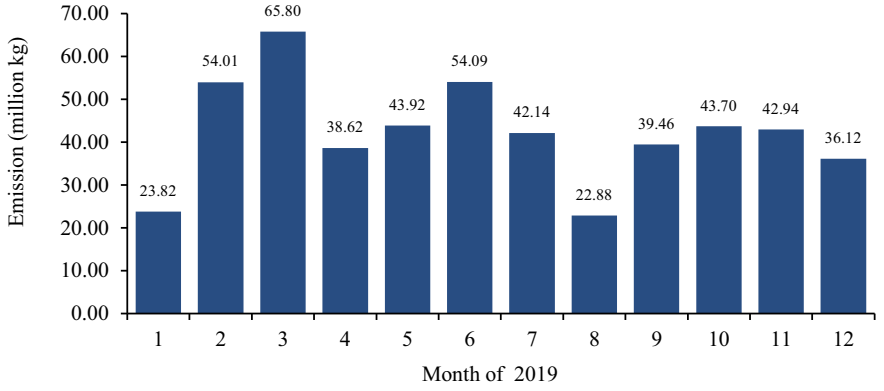

Fig. 7 Total monthly aircraft engine gas emissions of 2019

5 Conclusion

The aircraft emissions were successfully analyzed and estimated from ADS-B data by using a data mining approach. The emission of NOx is the highest emission count, 82% of total aircraft emissions. In the meantime, the lowest emissions are CO and HC, which contribute 13% and 15%, respectively. Therefore, it can be concluded that the system application successfully analyzed and estimated engine gas emissions for Peninsular Malaysia airspace from ADS-B data. As a suggestion for future works, we would suggest adding a module of the system that would enable estimating other pollutants such as SO_X, CO_X, and CH_X [16, 17].

Acknowledgements This research was supported by UiTM Lestari Grant Number 600-RMC/MyRA 5/3/LESTARI (125/2020). The author would like to thank the Office of Research Management Centre (RMC) and also the Faculty of Applied Sciences, UiTM Shah Alam, Malaysia for sponsoring the research.

References

1. Standards, B., et al.: Introduction to the ICAO engine emissions databank. Easa **II**, 1–6 (2008)
2. Zhang, M., Huang, Q., Liu, S., Li, H.: Assessment method of fuel consumption and emissions of aircraft during taxiing on airport surface under given meteorological conditions. Sustainability **11**(21) (2019). https://doi.org/10.3390/su11216110
3. Mustaffa, M., Ahmad, S., Nor, R.M., Zahari, N.H.B.: Preliminary study on air traffic density of Peninsular Malaysia using visual flight path trajectories from Automatic Dependent Surveillance-Broadcast (ADS-B) data. Int. J. Eng. Technol. **7**(4) (2018)
4. Nusyirwan, I.F., Mohd Rohani, J.: Study of air traffic over KLFIR. IOP Conf. Ser. Mater. Sci. Eng. **270**(1) (2017). https://doi.org/10.1088/1757-899X/270/1/012033
5. Zhang, J., Liu, W., Zhu, Y.: Study of ADS-B data evaluation. Chin. J. Aeronaut. **24**(4), 461–466 (2011). https://doi.org/10.1016/S1000-9361(11)60053-8

6. Francis, R.: Air traffic surveillance in remote and oceanic airspace using orbital detection of automatic dependent surveillance—broadcast (Ads-B) signals, pp. 8–9 (2009)
7. Song, J.H., Oh, K.R., Kim, I.K., Lee, J.Y.: Application of maritime AIS (Automatic Identification System) to ADS-B (Automatic Dependent Surveillance—Broadcast) transceiver. In: ICCAS 2010—International Conference on Control, Automation and System, pp. 2233–2237 (2010). https://doi.org/10.1109/iccas.2010.5669842
8. Ramin, A., Mustaffa, M., Ahmad, S.: Prediction of marine traffic density using different time series model from AIS data of Port Klang and Straits of Malacca. Trans. Marit. Sci. **9**(2) (2020). https://doi.org/10.7225/toms.v09.n02.006
9. Elliott, M.P.: A methodology for determining aircraft fuel burn using air traffic control radar data, p. 49 (2011). https://smartech.gatech.edu/handle/1853/39614
10. Khadilkar, H., Balakrishnan, H.: Estimation of aircraft taxi fuel burn using flight data recorder archives. Transp. Res. Part D Transp. Environ. **17**(7), 532–537 (2012). https://doi.org/10.1016/j.trd.2012.06.005
11. Price, T., Probert, D.: Environmental impacts of air traffic. Appl. Energy **50**(2), 133–162 (1995). https://doi.org/10.1016/0306-2619(95)92629-8
12. Marsh, R., Ogaard, K.: Mining heterogeneous ADS-B data sets for probabilistic models of pilot behavior. In: 2010 IEEE International Conference on Data Mining Workshops, vol. 113, pp. 606–612, December 2010. https://doi.org/10.1109/ICDMW.2010.34
13. Aneeka, S., Zhong, Z.W.: NOX and CO2 emissions from current air traffic in ASEAN region and benefits of free route airspace implementation. J. Appl. Phys. Sci. **2**(2), 32–36 (2016). https://doi.org/10.20474/japs-2.2.1
14. Zabaglia, V.N., Roma, I.: Air pollutant emissions estimate from global air traffic in airport and in cruise : methodology and case study. In: 11th International Scientific Symposium on "Transport Air Pollution" 19–21 June 2002—Grazer Congress, June 2002 (2002). https://www.researchgate.net/publication/236892570%0AAir
15. Cho, C., Kang, S., Kim, M., Hong, Y., Jeon, E.C.: Uncertainty analysis for the CH4 emission factor of thermal power plant by Monte Carlo simulation. Sustainabiltiy **10**(10) (2018). https://doi.org/10.3390/su10103448
16. Starik, A.: Gaseous and particulate emissions with jet engine exhaust and atmospheric pollution. Adv. Propuls. Technol. High-Speed Aircr. **150**(15), 1–22 (2008)
17. Song, S.K., Shon, Z.H.: Emissions of greenhouse gases and air pollutants from commercial aircraft at international airports in Korea. Atmos. Environ. **61**, 148–158 (2012). https://doi.org/10.1016/j.atmosenv.2012.07.035
18. Tabassum, A., Semke, W.: Assessing the effect of ADS-B message drop-out in detect and avoid of unmanned aircraft system using Monte Carlo simulation. Safety **4**(4) (2018). https://doi.org/10.3390/safety4040049
19. Cohen, B., Smith, A.: Implementation of a low-cost SSR/ADS-B aircraft receiver decoder (SY-100). In: 17th DASC. AIAA/IEEE/SAE. Digital Avionics Systems Conference. Proceedings (Cat. No.98CH36267), vol. 2, pp. F44/1–F44/8 (2002). https://doi.org/10.1109/DASC.1998.739828
20. Kurniawan, J.S., Khardi, S.: Comparison of methodologies estimating emissions of aircraft pollutants, environmental impact assessment around airports. Environ. Impact Assess. Rev. **31**(3), 240–252 (2011). https://doi.org/10.1016/j.eiar.2010.09.001
21. Lee, D.S., et al.: Aviation and global climate change in the 21st century. Atmos. Environ. **43**(22–23), 3520–3537 (2009). https://doi.org/10.1016/j.atmosenv.2009.04.024
22. Koudis, G.S., Hu, S.J., Majumdar, A., Jones, R., Stettler, M.E.J.: Airport emissions reductions from reduced thrust takeoff operations. Transp. Res. Part D Transp. Environ. **52**, 15–28 (2017). https://doi.org/10.1016/j.trd.2017.02.004
23. Irvine, D., Budd, L., Ison, S., Kitching, G.: The environmental effects of peak hour air traffic congestion: the case of London Heathrow Airport. Res. Transp. Econ. **55**(x), 67–73 (2016). https://doi.org/10.1016/j.retrec.2016.04.012

Building Energy Efficiency Optimization and the Cost-Benefit Analysis

Framework of Optimizing Building Energy Consumption in Temperate Climates Based on Life Cycle Cost Analysis. Case Study: Residential Building in Cairo, Egypt

Doaa El-Beheiry, Zeyad El Sayad, and Tarek Farghaly

Abstract Energy retrofitting is considered an innovative way to improve energy performance of the existing building and improve the indoor environment. It can be more cost-effective than building a new facility. Since Egypt has experienced a surge in electricity demand over the past 10 years due to the quickly rising number of air-conditioned buildings, it is important to initiate energy conservation retrofits in order to reduce energy consumption and reduce the cost of heating and cooling. This study aims to introduce the real energy-saving potential of retrofitting an existing building, since, energy retrofitting is considered as an effective solution of high energy consumption and thermal discomfort. The objective of this study is to conduct a framework to investigate the effect of suitable retrofitting interventions on residential buildings' cooling energy in the climate of Cairo, which is one of the highest expanding urban communities, using one of the existing energy modeling techniques. Then, to assess the different interventions of the energy retrofitting via life cycle cost analysis and finally optimize a retrofitting scenario through a combination of measures. The results showed that retrofitting strategies on the building envelope could have high potential in reducing the energy consumption levels of residential buildings in Cairo. It is also cleared that not necessarily the option with the highest energy reduction is the most economical solution, sometimes due to its high cost, it doesn't provide an appropriate payback period and, hence, it becomes an uneconomical solution.

Keywords Energy retrofitting · U-value · Simulation · Life cycle cost analysis

D. El-Beheiry (✉) · Z. El Sayad · T. Farghaly
Architectural Engineering, Alexandria University, Alexandria, Egypt
e-mail: doaa.elbeheiry@pua.edu.eg

Z. El Sayad
e-mail: zelsayad1@alex.edu.eg

T. Farghaly
e-mail: tarek.farghaly@alex.edu.eg

M. L. Kolhe (ed.), *Renewable Energy Systems and Sources*,
https://doi.org/10.1007/978-981-99-6290-7_10

1 Introduction

One of the most popular research areas today is the building energy efficiency. The major reason for this direction is that the building sector accounts for around 36% of energy demand in the world. The focus is on the implementation of energy conservation technologies and the optimization [1]. Enhancement of the buildings using different energy conservation measures provides direct potential savings as well as reduced energy consumption. The energy-efficient measures connected to the building envelope have the greatest impact on energy efficiency in terms of passive energy reduction for heating, cooling, and lighting [2]. It is also crucial to highlight that, in order to improve the energy efficiency of existing buildings, the most recognizable ones are: window replacement, facade insulation, roof insulation, and new sealing to reduce ventilation losses [3].

Urbanization in Egypt is taking a sharp hike with two thirds of Egypt's total population are now living in urban areas. Egypt has a building stock of about 12 million buildings where 60% are in the residential sector. More than 60% of the total electricity consumption in the country is attributed to residential, commercial, and institutional buildings [4]. A recognizable increase in electricity demand is expected over the next 5 years with a growth rate of 8%.

According to [5], building energy retrofit is a challenging multilateral problem that requires a complete integrated team approach. There are two main objectives of such an approach, which are; minimizing the energy consumption while maximizing the economic benefits. They are generally conflicting and hence, multi-objective optimization is recommended [6]. Therefore, life cycle cost analysis (LCCA) is used as a measuring tool to assess the effect of the retrofitting and determine whether it is economical or not. It helps to define an optimized model in terms of energy and cost. The LCCA strikes a balance between the upfront financial investment and the ongoing costs of owning and operating the facility.

This study aims to define an optimization framework for buildings in terms of energy and cost. The research has attempted to use one of the existing energy modeling software—Design Builder to calculate the amount of energy used by an existing residential building in Cairo, Egypt and implement a number of different retrofitting scenarios since the most important issue when determining an optimal retrofit scenario is to define a combination of measures that can be effective and reliable on the long term [7]. Then, assess the different scenarios of the energy retrofitting via life cycle cost analysis in order to find the optimum solution.

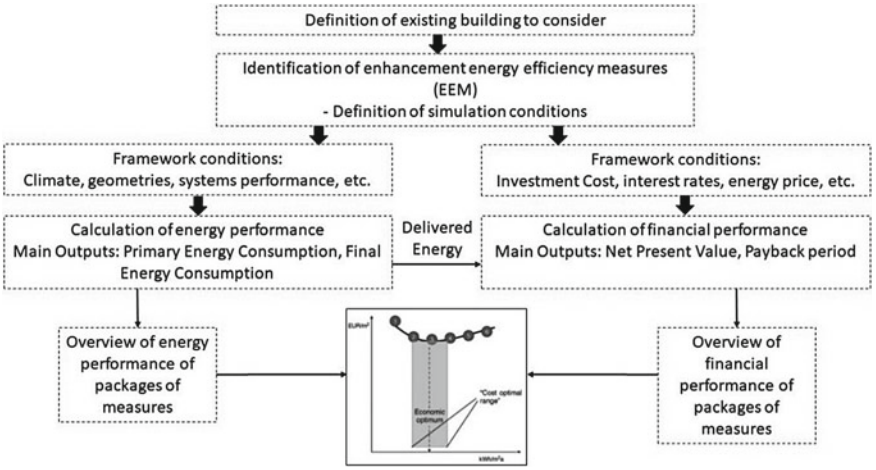

Fig. 1 The flowchart of cost-optimal methodology. *Source* [8]

2 Methodology

2.1 Cost Optimal Methodology

According to Fig. 1, cost optimal technique strives to set up minimal energy performance standards and energy efficiency measures that are both cost and energy effective. It has four key components. First, it establishes reference buildings, which can be either residential or non-residential buildings and are reflective of their functionality, geographic location, and indoor and outdoor temperature conditions. The second step is to specify the energy efficiency measures (EEMs) that will be evaluated. Then, evaluate the reference building's final and main energy requirements as well as the energy requirements after applying the specified energy efficiency measures. Finally, determine the net present value and payback period of the various packages in order to determine which one has the lowest payback period and, as a result, represents the cost-optimal level [8]. This calculation should be done during the predicted economic lifetime applied to the reference building.

2.2 Description of Case Study

The general atmosphere of Egypt is known for having a dry, hot climate (Köppen classification: BWh), with extremely high sun radiation the majority of the year [9]. There are eight regions in Egypt. Nowadays, the region of Cairo and Delta is Egypt's economic and financial heart. Around 90% of the population live in Egypt's part of the Nile Basin and 50% in the delta itself [10]. El-Sheikh Zayed City is situated

Fig. 2 El-Sheikh Zayed residential building. *Source* Google Earth

about 20 km from Lebanon Square in the Mohandiseen district of Giza. The city is located in Cairo and Delta climatic zone. It is divided into 17 residential districts, with four neighborhoods in each district. The selected case study is considered as one of the repetitive prototypes in El-Sheikh Zayed. It is located in 304,663.74 m E 3,323,826.11 m N. The building is composed of three stories with the same layout (Fig. 2).

The building's roof is composed of 30 mm concrete tiles, 20 mm mortar, 50 mm sand, 150 mm reinforced concrete, 20 mm mortar, and 15 mm plaster, with a U-value of 3.049 W/m^2.K. The external walls are composed of 20 mm plaster, 20 mm mortar, 200 mm brickwork, 20 mm mortar, and 15 mm plaster, with a U-value 1.703 W/m^2.K. For the internal walls, they are either plastered from both sides or they are covered with ceramic tiles in case of bathroom and kitchen. All windows are composed of aluminum frame and 3 mm single clear glass. As shown in Fig. 3, the plan of this residential building is composed of two flats each of 100m^2.

2.3 Model Validation

The verification and validation of computer simulation model were described by [11] as: "The process of gathering evidence to establish that the computational implementation of the mathematical model and its associated solution are correct". For the acceptable difference between projected and measured (actual) data, Kaplan and Canner [12] presented suggestions for the simulation of environmental parameters where it is deemed adequate when the monthly difference is less than 15–25%

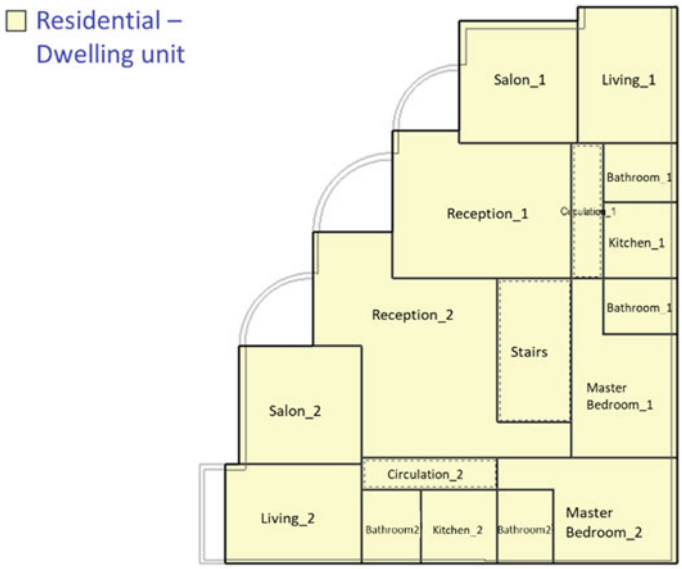

Fig. 3 Plan of residential building using Design Builder

monthly. Monthly energy consumption was taken into account during this computational simulation process for base model validation compared to that of real electricity bill, and the difference was found to be 4%, so it is an acceptable percentage according to [12].

2.4 Simulation of Selected Apartment Block

Energy Plus, a computerized dynamic simulation tool for building thermal performance, and Design Builder (DB), its user-friendly interface, accounts for all the major theories of heat transfer that directly affect energy use and indoor thermal comfort. To accomplish the goal of the research, DB in its second version (V.2.2.5.004) has been used. First of all, the specified weather file was defined to the program in order to identify the exact location and weather data. All parameters were introduced after drawing the complete model of the building including the openings and the surroundings. The model shown in Fig. 4 was then identical to the real building. Simulation was selected to be done in August since the air temperature reaches its maximum leading to a recognizable increase in the energy consumption due to cooling load.

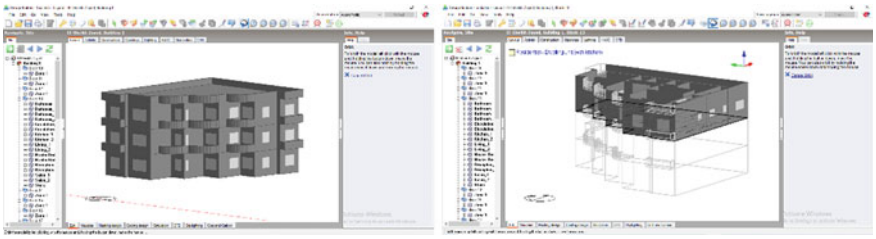

Fig. 4 Design Builder model for the residential building

2.5 Simulation of Selected EEMS

One of the critical ways of reducing energy through retrofit is the use of thermal insulation. Thermal insulation was found to reduce the U-value of a wall between 34 and 61% [13]. Hence, four retrofitting interventions were implemented. First: improvement on the building envelope with thermal insulation through roof insulation with examining different insulation types, chosen as the most popular insulation types and known for their high insulation effectivity. Second: improvement on the building envelope with thermal insulation through exterior wall insulation. Third: improvement on the openings with energy-efficient windows using different glazing types. Fourth: improving air infiltration rate. According to Table 1, applying different retrofitting interventions on the building envelope can greatly enhance the building energy efficiency and can cause a great reduction in the overall energy consumption.

3 LCCA Calculations for Different EEMs

It is worth mentioning that all these retrofitting interventions have been assessed only in terms of energy reduction and still they need to be assessed using the life cycle cost analysis tool in order to examine whether they are economical or not. Therefore, LCCA is used to evaluate the cost-effectiveness of these interventions. In LCCA, two primary metrics are to be calculated; life cycle costs of each alternative and its payback over a certain study life. The alternative with the shortest payback period is considered as the most economical solution [14]. One of the major defects in the LCCA is that many assumptions are to be made over the life cycle cost calculations in order to generate enough data to produce results [15]. The basic formula is as follows:

$$LCC = C + PV_{\text{Recurring}} - PV_{\text{Residual-Value}} \tag{1}$$

where;—*LCC* is the life cycle cost.

—*C* is the construction cost (hard and soft costs).

Table 1 The effect of each intervention on the energy consumption

EEMs	Description	U-value (W/m^2 K)	Percentage of energy reduction
Roof insulation	Nano silica aerogel 10 mm	0.753	33.44
	Expanded polystyrene 10 mm	1.834	20.86
	Vacuum insulation panel 10 mm	1.374	25.91
External wall insulation	Nano silica aerogel 10 mm	0.44	15.65
	Expanded polystyrene 10 mm	1.243	9.05
	Vacuum insulation panel 10 mm	0.92	14.42
Energy efficient windows	Double blue 6 mm/6 mm Aerogel	3.094	12.69
	Double blue 6 mm/ 13 mm Aerogel	2.511	12.85
	Double Low-E 6 mm/ 6 mm Aerogel	1.761	14.4
Improving air infiltration rate	Sealing around windows and doors	–	14.3

—$PV_{\text{Recurring}}$ is the present value of all recurring costs (utilities, maintenance, replacements, service, added values, etc.).

—$PV_{\text{Residual-Value}}$ is the present value of the residual value at the end of the study life (note: this is recommended to to be 0 L.E considering that the building won't be sold in the future).

3.1 Time Value of Money

– Eliminating Inflation where inflation is reducing the value or of money over time;

$$\text{Discount Rate} = \frac{1 + \text{Nominal Rate}}{1 + \text{Inflation Rate}} \tag{2}$$

According to the Central Bank of Egypt, discount rate and the escalation rate were calculated from the average of 6 years 2016–2022 and were found to be 13.88 and 14.2%, respectively [16].

– The Basic Discounted Equation;

$$PV = \frac{F_Y}{(1 + \text{DISC})^Y} \tag{3}$$

where PV is the present value (in Year 0).
—F_Y is the value in the future (in Year Y).
—DISC is the discount rate.
—Y is the number of years in the future.

– Escalation Rates like discount rates are adjusted to remove the effects of inflation from goods and services;

$$\text{Cost}_{\text{Year-Y}} = \text{Cost}_{\text{Year-0}} * (1 + \text{ESC})^Y \tag{4}$$

where;—$\text{Cost}_{\text{Year-Y}}$ is the cost at Y years into the future.
—$\text{Cost}_{\text{Year-0}}$ is today's cost (at Year 0).
—ESC is the escalation rate.
—Y is the number of years into the future.

3.2 Payback Analysis for the Applied EEMs

According to the applied LCCA of the three options of the roof insulation, their payback periods are lower than the base case at a certain point (Fig. 5). For Option 1 "aerogel insulation", the payback was found to be 3 years. For Option 2 and Option 3 "polystyrene and vip", the payback was found to be 2 and 3 years, respectively.

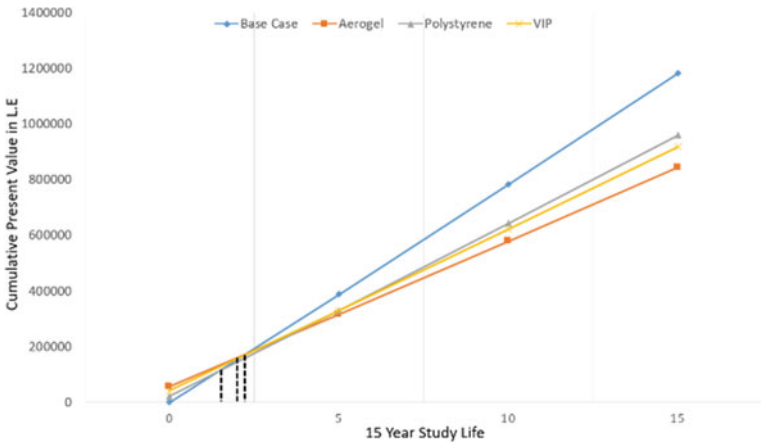

Fig. 5 Payback analysis of the three options of roof insulation

Table 2 Payback Period for the applied EEMS

EEMs	Description	Payback Period
Roof insulation	Nano silica aerogel 10 mm	3 years
	Expanded polystyrene 10 mm	2 years
	Vacuum insulation panel 10 mm	3 years
External wall insulation	Nano silica aerogel 10 mm	5.5 years
	Expanded polystyrene 10 mm	3.5 years
	Vacuum insulation panel 10 mm	5 years
Energy efficient windows	Double blue 6 mm/6 mm aerogel	13 years
	Double blue 6 mm/13 mm aerogel	14 years
	Double Low-E 6 mm/6 mm aerogel	14 years
Improving air infiltration rate	Sealing around windows and doors	2.5 years

Payback calculation is then done for the rest of the applied EEMS, calculating the payback period for each applied intervention. Table 2 clarifies the payback period for each one where some of them have a very long payback period consequently they are considered as an economical option in terms of the monetary value.

4 Discussion with Optimized Scenario

This research has introduced a framework for optimizing building energy consumption and examined this framework on a selected case study with specific conditions. It analyzed a residential building in El-Sheikh Zayed, Cairo using computer simulation. Four different interventions were assessed to define how this changes the way the building consumes energy and satisfies comfort conditions. It has been found that the roof and wall insulation in addition to improving air infiltration rate can greatly enhance the thermal comfort (Fig. 6) and hence decrease the building energy consumption. Concerning the energy-efficient windows, they gave the least energy consumption reduction despite their low U-Value. The payback period for each intervention is then examined. The highest payback periods were given by the energy efficient windows due to their high initial cost and low percentage of energy reduction, while, the shortest payback period was given by the polystyrene insulation for both roof and wall insulation due to its low initial cost, but it is important to clarify that it isn't necessary the shortest payback period is the most optimum solution.

According to [7], the most important issue when determining an optimal retrofit scenario is to define a combination of measures that is effective and reliable in the long term. An optimized solution was then introduced to the selected case study where a combination of measures was applied using nano-silica aerogel for the roof and wall insulation as it has given the highest energy reduction percentage accompanied with improving air infiltration rate through sealing around windows and doors. This has led to 56% energy reduction and a payback period of less than 2.5 years (Fig. 7).

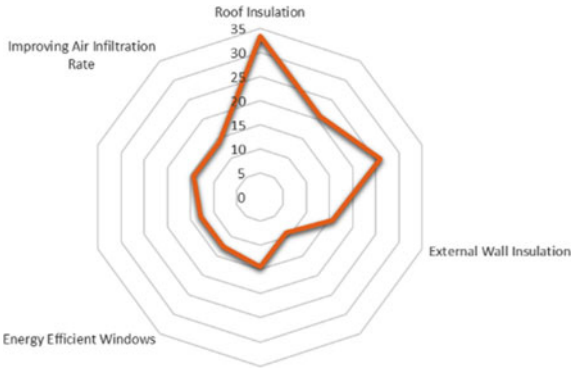

Fig. 6 Radar chart for percentage of energy reduction of the selected interventions

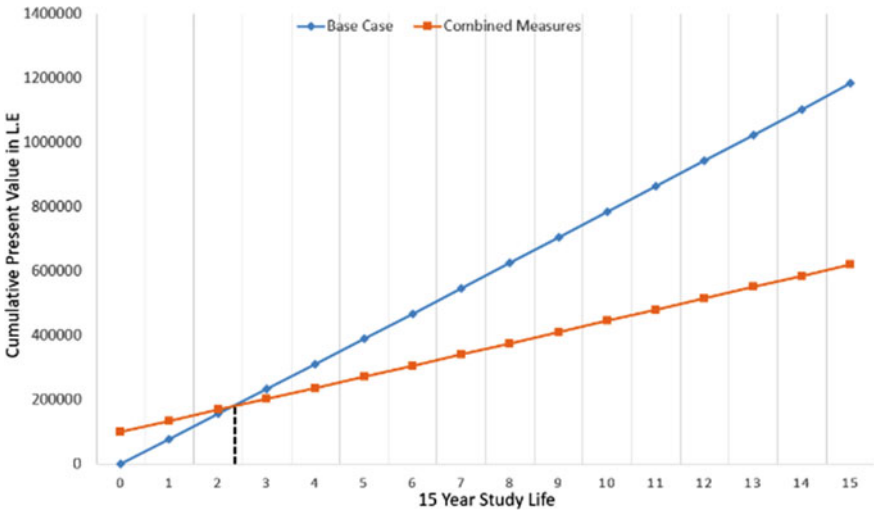

Fig. 7 Payback analysis of the optimal retrofitting scenario

5 Conclusion

Building energy efficiency and energy retrofitting have become imperative in the process of construction and design in order to conserve resources for future generations as well as providing a healthy environment for coexistence and the economic benefit, which is one of the most important dimensions that underpin any project. In conclusion, a properly fitted insulating material at its ideal thickness could not only lessen heat transfer through building envelopes but also achieve obvious benefits to the economy and environment. Therefore, designers and builders in hot arid and temperate nations could use the applied framework to help enhance the building

energy consumption and reach an optimized solution to apply on the building envelope components. According to this, it is recommended to encourage the retrofitting process due to the great already built areas in Egypt, which will always remain as a constraint against any step forward.

References

1. Wang, B., Xia, X.: Optimal maintenance planning for building energy efficiency retrofitting from optimization and control system perspectives. Energy Build. **96**, 299–308 (2015)
2. Ferrara, M., Monetti, V., Fabrizio, E.: Cost-optimal analysis for nearly zero energy buildings design and optimization: a critical review. Energies **11**(6), 1478 (2018)
3. Galante, A., Pasetti, G.: A methodology for evaluating the potential energy savings of retrofitting residential building stocks. Sustain. Cities Soc. **4**, 12–21 (2012)
4. Hanna, G.B.: Energy efficiency building codes and green pyramid rating system. Int. J. Sci. Res. 3055–3060 (2013)
5. Hopfe, C.J., Augenbroe, G.L., Hensen, J.L.: Multi-criteria decision making under uncertainty in building performance assessment. Build. Environ. **69**, 81–90 (2013)
6. Nguyen, A.T., Reiter, S., Rigo, P.: A review on simulation-based optimization methods applied to building performance analysis. Appl. Energy **113**, 1043–1058 (2014)
7. Murray, S.N., Walsh, B.P., Kelliher, D., O'Sullivan, D.T.J.: Multi-variable optimization of thermal energy efficiency retrofitting of buildings using static modeling and genetic algorithms–a case study. Build. Environ. **75**, 98–107 (2014)
8. Becchio, C.: Assessment of energy and cost effectiveness in retrofitting existing buildings. Politecnico di Torino, Torino, Italia (2013)
9. Mahmoud, A.H.A.: An analysis of bioclimatic zones and implications for design of outdoor built environments in Egypt. Build. Environ. **46**(3), 605–620 (2011)
10. Haars, C., Lönsjö, E.M., Mogos, B., Winkelaar, B.: The uncertain future of the Nile Delta. NASA/GSFC: Greenbelt, MD, USA (2016)
11. Schwer, L.E.: Guide for verification and validation in computational solid mechanics (2009)
12. Rahman, Md.M., Rasul, M.G., Khan, M.M.K.: Energy conservation measures in an institutional building in sub-tropical climate in Australia. Appl. Energy **87**(10), 2994–3004 (2010)
13. Walker, R., Pavía, S.: Thermal performance of a selection of insulation materials suitable for historic buildings. Build. Environ. **94**, 155–165 (2015)
14. Reidy, R., Davis, M., Gould, S., Regina, C.: Guidelines for Life Cycle Cost Analysis. Stanford University, Land and Buildings, Stanford, California (2005)
15. Alexandersson, J.: Life cycle cost analysis of two high temperature cooling systems supplied by geothermal energy. A case study in Sant-Cugat, Spain. KTH—Royal Institute of Technology, Stockholm, Sweden (2022)
16. Central Bank of Egypt. www.cbe.org.eg, https://www.cbe.org.eg/en/pages/Search.aspx?k=inflation%20rate. Accessed 30 Oct 2022

An Assessment of the Profit Gained Based on the Use of Roof Cooling Devices in Chengdu

Haonan Wang

Abstract This paper aims to evaluate how much money could be saved by using a radiative cooling appliance mounted on the roofs if it is widely used in Chengdu. In 2018, Chinese people consumed electric energy in air conditioning most, arriving at 34% of the total use in that field in the whole world with a sharp increment. Meanwhile, Chinese refrigeration electricity consumption represented above 15% of total electricity consumption. The energy shortage impacts a lot, from national development to the living for the public. In fact, some people used to invent some devices like roof cooling technology, which could decrease the temperature in the house to replace the air conditioner in refrigeration for energy saving and decrease people's expenditure. Therefore, the author plans to establish a model to gain a function of the number of the temperature decreased in this way by its theory and provided physical functions and plug the collected data on Chengdu into the formula to judge whether this radiative cooling technology could bring profit to Chengdu public for a long time through another model established based upon the calculation methods and data. In the end, the author finds that the roof cooling device is beneficial to the citizens living in Chengdu in the economic aspect.

Keywords Radiant energy · Roof cooler · Chengdu · Refrigeration

1 Introduction

Chinese total social electricity consumption maintained growth with different ranges from 2015 to 2020 [1–6]. Nowadays, the Chinese electric energy shortage has been a huge challenge, and some cities in northeastern China governments have adopted measures to limit the use of electricity [7]. The research of Bloomberg New Energy Finance (BNEF) shows in 2018, Chinese citizens consumed the electrical energy in air conditioners most among all the countries around the world at 34% [8], keeping a

H. Wang (✉)
The University of Southampton, Southampton, UK
e-mail: hw11n22@soton.ac.uk

M. L. Kolhe (ed.), *Renewable Energy Systems and Sources*,
https://doi.org/10.1007/978-981-99-6290-7_11

stable ascend. Meanwhile, the Chinese National Development and Reform Commission spokesman named Men Wei indicated that Chinese refrigeration electricity consumption represented above 15% of total electricity consumption [9], and air conditioning electricity load accounts for three-fifths of whole electricity in large and intermediate cities in China in summer [10].

To address the difficulty of the energy shortage in cooling, some scientists used to invent various devices like radiance cooling technology, which could decrease the temperature in the house to replace the air conditioner in refrigeration for decreasing the citizens' electricity bills. The author established a model for gaining a formula with decreasing temperatures while using seven-layer cool roof devices, relying on the theories and some provided physical functions. Subsequently, the author plugged the gathered data from governmental institutions such as the Chinese National Energy Administration and Chengdu Meteorological Network into the formulas modeled to evaluate whether this radiative cooling technology could bring profits to the Chengdu public in a decade.

Cool roofs are roofs that can reflect high solar [11]. Doctor Raman used the cool roof apparatus made from a seven-layer structure, which consists of two layers of HfO_2 and SiO_2 and one layer of Si, Ag, and Ti, like in Fig. 1, having strong reflexes via an apparent window during both daytime and night as the roof cooler to do the research. By contrast, the normal radiance cooling device can be only sure to drop the temperature at night, but in the daytime, it needs to refer to the intensity of sunlight and wavelength. For the device having seven layers, owing to its materials, it can provide the equipment with reflectance arriving at 97%. This is why it reduces the impact of the heating radiative cooler by the sun, which leads to the fact that these appliances decrease the temperature by 5 °C in the daytime at the average level [12].

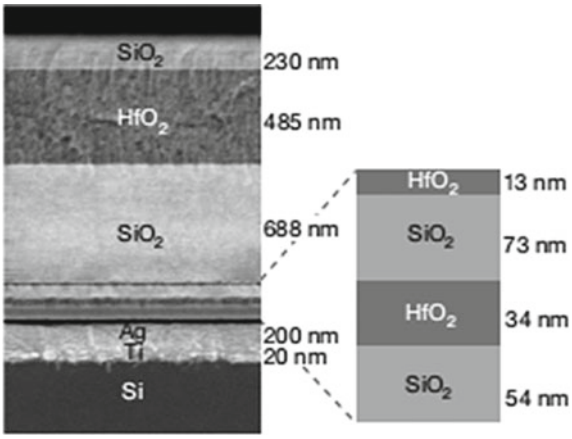

Fig. 1 The cooler device layout [12]

2 Research

This research has a model to calculate the value of the decreased temperature after using the roof coolers, being also a segment of another model used to compute the number of payments with the wide use of this equipment for the next calculation. In this way, the money saved could be figured out successfully by comparing the gap between two types of payment in cooling from gathered data from interviews and documents.

2.1 Models

The first model is to compute the temperature decreased after using coolers in the daytime. In order that in the layer of energy, Function 1 is gained, precisely, the right hand of Function 1 is divided into four separate parts, having four different functions, which could be subdivided into Function 2 to Function 5 for calculating in the area of A and at the temperature of T, with spectral emissivity λ and angle Θ, depending on the angle and the orientation of the cooler laid on the rooftops (usually 30° towards the south). Since the cooler is affected by three kinds of radiance powers, and they are solar irradiance power, atmospheric radiance power, and the power lost in conduction and convection in the whole process. To be specific, Function 2 represents the amount of the energy radiated out through the cooler, including the volume of the hemisphere with angle Θ and area A and the spectral radiance of blackbody IBB (T, λ). Meanwhile, some energy is lost in the equipment. According to Function 4, in area A, the energy is lost on both the inside and outside of the cooler. As a result, the lost energy is impacted by two types of temperature, owing to the process of conduction and convection. By contrast, the last two Functions 3 and 5 display the impact of two factors, which leads to the fact that the cooling effect rises. Functions 3 and 5 both stem from Kirchhoff's radiate rule, and Functions 2 and 4 refer to Planck's law. The values of the parameters and varieties, such as Planck's constant, Boltzmann's constant, speed of light, and the wavelength in these equations, could be found on the website and calculator.

$$P_{\text{cool}}(T) = P_{\text{rad}}(T) - P_{\text{atm}}(T_{\text{amb}}) - P_{\text{sun}} - P_{\text{cond+conv}} \tag{1}$$

$$P_{\text{rad}}(T) = A \int d\Omega \cos\theta \int_0^{\infty} d\lambda I_{BB}(T, \lambda)\epsilon(\lambda, \theta) \tag{2}$$

$$P_{\text{atm}}(T_{\text{amb}}) = A \int d\Omega \cos\theta \int_0^{\infty} d\lambda I_{BB}(T_{\text{amb}}, \lambda)\epsilon(\lambda, \theta)\epsilon_{\text{atm}}(\lambda, \theta) \tag{3}$$

$$(P_{\text{cond+conv}}(T, T_{\text{amb}}) = Ah_c(T_{\text{amb}} - T) \tag{4}$$

$$P_{\text{sun}} = A \int_0^{\infty} d\lambda \epsilon(\lambda, \theta_{\text{sun}}) I_{AM1.5}(\lambda) \tag{5}$$

In the condition of California, Raman calculated that the apparatus was able to reduce 4.9 °C with an error margin (about 0.15 °C) [12]. In contrast, in Chengdu, one of the Chinese lowest sunshine intensity regions, there is lower solar radiance and atmospheric radiance compared with California, which is a place in the desert and in similar altitude and latitude conditions, which means the result that the cooler can drop at least 4.9 °C while being the same arrangement is able to evaluate [13].

Under conservative estimates, the result of five degrees Celsius is used for evaluating the profits in the next step, regarding the lack of radiance data in Chengdu.

Based on the value of the temperature decreased via using roof coolers, the second model, which is for computing the profits bought from roof coolers in Chengdu can be established. The profit P is equal to the total cost of air conditioners before using roof coolers named C_{a1} minus the total cost of new devices (C_t) as shown in Function 6. In Function 7, it illustrates that the cost of air conditioners is equal to the total energy use (C_{es}) multiply the ratio of the cooling energy consumed by Chengdu people accounting for the total electricity consumption in society (R_1) multiplied the price of energy per degree multiplied the unit price per kWh (P_1).

$$P = C_{a1} - C_t \tag{6}$$

$$C_{a1} = C_{es} \times R_1 \times P_1 \tag{7}$$

However, the payment of the condition using the new devices in Chengdu is much complicated. It needs to be mainly divided into three sections.

$$C_t = C_{a2} + C_m + C_p + C_i \tag{8}$$

The first section is about the spending on air conditioners after using roof coolers, as some of the Chengdu residents cannot stand the indoor temperature, in spite of the condition that the indoor temperature has already decreased by 5 °C. For instance, some citizens are used to turning on the air conditioner when the temperature is 30 °C, which means if the natural temperature is above 35 °C, they will also use air conditioners, although the cooler can help to reduce 5 °C, and this part of the cost named C_{a2} cannot be ignored, and it is equal to the value of C_{a1} multiple the number of days using air conditioners after using this equipment divide the number of days before using the coolers, and Function 9 is given.

$$C_{a2} = C_{a1} \div \left(\sum P_{t1} N_{t1} \div \sum P_{t2} N_{t2} \right) \tag{9}$$

The second section is the cost for materials per device named C_m/N, which is to make roof coolers. In Fig. 1, the volume of the raw materials of the metals and

compounds in the seven-layer construction separately and some aluminum and wood as the parts of the cooler could be obtained. Subsequently, the volume, density, and unit price of each section are used to figure out the price of raw materials of an individual appliance. Thereafter, it is easy to compute the final result via using the unit price multiple the number of the devices, which could be solved by computing the living area per person living in Chengdu multiple by the number of the population of Chengdu, which is to evaluate that the area of the roofs divides by the average number of the layers of buildings in Chengdu divide the field of the coolers (1 square meter). Nevertheless, because the equipment is set on the rooftop, the region is larger than the area used to be lived by people in one layer, which means when we calculate the area of the rooftop, its value should be raised. Thus, Function 10 to Function 13 could be gained.

$$C_m/N = C_{\text{str}} + C_w + C_{al} \tag{10}$$

$$C_{\text{str}} = \sum_{n=7} V_n P_n \rho_n \tag{11}$$

$$C_w = V_w \times p_w \times \rho_w \tag{12}$$

$$C_{al} = V_{al} \times p_{al} \times \rho_{al} \tag{13}$$

In considering the labor cost, which is also the third section, the compound of production cost and installation cost called C_p and C_i, respectively, also determines the final cost. The function could solve the two costs that a worker's salary is divided by the working time divided by the working efficiency of the worker in their own field. Based upon these costs, the price in the market usually doubles the entire cost computed before due to some costs in the factory, such as rent and water and electricity bills and delivery costs, and Function 14 is shown below.

$$C_p + C_i = S_f \div N_1 + S_I \div N_2 \tag{14}$$

2.2 Result

To compare the cost difference between using air conditioning and roof coolers in cooling in Chengdu, the two costs should be computed through collected data separately. As a result, in the first part, the payment of individuals in Chengdu when they do not have roof coolers is needed to be evaluated. After that, in the second part, the entire bill of the residents who own the coolers and live in Chengdu will be computed.

Firstly, the total cost of air conditioners before using roof coolers can be figured out by the total energy use multiple the ratio of the cooling energy consumed by Chengdu people contributing to the total energy use in society multiple the price of energy per degree and multiples the unit price per KWH, which is also the value of C_{a1}. In 2020, State Grid Sichuan Corporation indicated that Chengdu citizens consumed 72.543 billion KWH electricity in the whole society [14]. The average unit price of electricity was about 0.6 yuan per KW (Sichuan Development and Reform Commission) [15]. At the same time, cooling accounted for 15% of total electricity consumption. Thus, C_{a1} equals 0.15 times 72.543 times 0.6, and the result is approximately 6.53 billion yuan in total. The population in Chengdu has approached 20.93 million, and there are only 2.49 people per family [16], so each citizen should pay 312 yuan for air conditioning annually at the average level.

$$C_{a1} = 0.15 \times 72.543 \times 0.6 = 6.53 \,\text{billion} \tag{7-1}$$

$$C_{a1}/N = 0.15 \times 72.543 \times 0.6/20.93 \,\text{million} = 312 \,\text{yuan} \tag{7-2}$$

When these people have roof cooling equipment, their bills are mainly in three aspects. Now, the value of C_{a1} has already been computed. However, the amount of the spending of the people in Chengdu paying for air conditioners after using coolers (C_{a2}) is still needed. To cope with that, the author designed interviews with just one question, that is, what is the temperature outside you would like to turn on the air conditioner in summer with my friends, classmates, teachers, and my relatives who live in Chengdu in five different age groups with the same number of males and females (five males and females in each age group and 50 people in total) through calling, sending messages and talking face to face. The five age groups are 10–24, 25–39, 40–54, 55–69, and more than 70 as shown in Table 1. Table 1 demonstrates that all the interviewees (50 of 50) turned on the air conditioners from 30 to 35 °C, among which 28 of 50 people preferred open the air conditioner when the temperature arrived at 30 °C followed by 8 people at 32 °C, 5 people at both 31 and 33 °C, 3 people at 34 °C and one person at 35 °C.

Table 1 The temperature at which people are willing to turn on air conditioners

Male						Female				
T (°C)	10–24	25–39	40–54	55–69	>70	10–24	25–39	40–54	55–69	>70
30	5	5	3	2	2	4	4	1	1	1
31	0	0	1	0	0	0	0	1	1	2
32	0	0	1	0	1	1	1	1	2	1
33	0	0	0	2	2	0	0	0	0	1
34	0	0	0	1	0	0	0	2	0	0
35	0	0	0	0	0	0	0	0	1	0

There is an assumption that all the residents in Chengdu turn on air conditioners on this distribution so that the value of the ratio of the number of days that the air conditioners being on after they use this equipment and that of before using the coolers is computed by checking the temperature meeting the air conditioning situation of Chengdu public. In the years 2020 and 2021, Chengdu experienced 145 days of hot weather, which is equal to or above 30 °C, including 31 days with 30°, 33 days with 31°, 27 days with 32°, 20 days with 33°, 19 days with 34°, 9 days with 35°, 2 days with 36°, 3 days with 37° and 1 day with 40°, respectively [17].

In this case, after using cooling devices, the number of people who open air conditioners at the temperature of 30 °C accounts for 56% of the total number of people living in Chengdu. They are still necessary to open air conditioners for 15 days per 2 years, which is 3/29 as many as the frequency before using the coolers so that the ratio could be figured out. Meanwhile, all the values of the counterparts in different temperatures are able to calculate, being 1/19 in the temperature of 31 °C, 4/81 in the temperature of 32 °C, 1/54 in the temperature of 33 °C, 1/34 in the temperature of 34 °C and 1/15 in the temperature of 35 °C and then multiply their respective share of the population to acquire the ration of the number of days that people used air conditioning before and after using roof coolers and it equals 0.076. Consequently, the value of C_{a2} is equal to the value of C_{a1} multiple 0.076, and the result is 0.496 billion yuan in total or 23.71 yuan per person, like Function 9-1 and Function 9-2 below.

$$C_{a2} = 6.53 \times (0.56 \times 3/29 + 0.1 \times 1/19 + 0.16 \times 4/81 + 0.1 \times 1/54 + 0.6 \times 1/34 + 0.2 \times 1/15) = 0.486 \text{ billion yuan} \quad (9\text{-}1)$$

$$C_{a2}/N = 0.486/0.02093 = 23.71 \text{ yuan} \quad (9\text{-}2)$$

From Fig. 1 as shown before, the volume of the metals and compounds in the seven-layer structure could be ignored owing to their height, which means their prices are very low despite their high prices per unit. Besides, the wood and aluminum, as non-core parts of the device, also have adequately low prices because the apparatus does not need more than 10 g of aluminum due to the lack of space, so the cost of major materials is almost the same as the cost of the wood being at most 10 yuan considering its weight, which is used to support the cooler that is a cylinder with diameter 3.4 inches (8.6 cm) and the author assesses that it is about 0.01 cubic meters and the hypothetical unit price of woods (1500 yuan per cubic meter) which is higher than the market [12]. Therefore, the material cost per device is about 10 yuan.

$$C_{\text{str}} \approx 7 \times 3.14 \times 1000 \times 10 \times 0.08 \times 0.08 \times 10 - 7 \approx 0 \text{ yuan} \quad (11\text{-}1)$$

$$C_w \approx 0.01 \times 0.6 \times 1500 = 9 \text{ yuan} \quad (12\text{-}1)$$

$$C_{al} \approx 10 \times 20 \div 1000 = 0.2 \text{ yuan} \quad (13\text{-}1)$$

$$C_m/N = 9 + 0.2 = 9.2\,\text{yuan} \tag{10-1}$$

Unfortunately, the highest part of this equipment is the labor cost. It is generally acknowledged that such sophisticated devices are too difficult and time-consuming to make. Hence, the limitation of manpower and technology leads to the fact that the cost of the device is higher than the counterparts of other products produced by assembly lines due to the precision of the materials. If we have a large factory with 10 million yuan for bills and 10 million for other places and 150 staffs having annual salaries of 200,000 yuan on average which is able to produce 3000 coolers per day per line and there are ten lines for production. In this situation, the factories could produce 3000 multiple 10 multiple 300 days as 9 million coolers and the cost per cooler equals the costs of the composition of salaries, bills and other costs divided the number of coolers, which are 5.6 yuan each. In fact, the author made a conservative estimate because the diameter of a cooler is about 10 cm. It means abundant coolers can be produced in one process, so the factory could produce more coolers, and the salaries are higher than 90% of relevant technicians (159.4 thousand yuan annually) [18].

$$\begin{aligned}(C_p + C_i)/N &\approx (200000 \times 150 + 10000000 + 10000000) \div (10 \times 300 \times 3000) \\ &\approx 5.6\,\text{yuan}]\end{aligned} \tag{14-1}$$

Afterward, the value of how many coolers each Chengdu citizen uses ought to be calculated. Actually, it is reckoned that layers of buildings multiply the area of the living space per person in Chengdu medially. The author assumes that the number of layers of buildings in Chengdu is 10 at the average level. Some information indicates that Chengdu people own 44 m^2 to live in and at most 6 m^2 of public area per person in 2018 [19]. Based on these values, the result that each Chengdu resident should buy 5 coolers per person at most can be found, which spends 5 multiple 15.6 yuan, which is the composition of the two categories of cost, which are the cost of production and the cost of materials totally. The reason why the cost of installation can be ignored is that installing these appliances does not depend on technology because they work automatically and a worker just takes half an hour to install a mass of coolers on a rooftop. Thus, each cooler does not pay little money in this field.

Therefore, the individual cost after using roof coolers is the cost of air conditioning after using roof coolers plus the cost of roof coolers per person as Function 15 shown, that is, 5 multiple 15.6 (C_p and C_m) plus 23.71 (C_{a2}) at most, which is 101.71, and the marketing price doubling or tripling the cost of the equipment, so each person perhaps will spend 179.71 to 257.71 yuan (C_F/N) on cooling in a year finally, being lower than the cost before using the devices, as Function 15, Function 15-1, and Function 15-2 shown.

Finally, the profit for each person is C_{a1} per person minus C_t per person, being in the range of 54.29 to 132.29 yuan in the first year as Function (6-1) shown.

$$C_t/N = C_{a2}/N + (C_p + C_i)/N + C_m/N = C_{a2}/N + n \times ((C_p + C_i)/N + C_m/N) \tag{15}$$

$$C_t/N = 23.71 + 5 \times 15.6 = 101.71 \text{ yuan} \tag{15-1}$$

$$\begin{aligned} 5 \times 15.6 \times 2 + 23.71 = 179.71 \text{ yuan} < C_F/N < 5 \times 15.6 \times 4 + 23.71 \\ = 257.71 \text{ yuan} \end{aligned} \tag{15-2}$$

$$312 - 257.71 = 54.29 \text{ yuan} < P/N < 312 - 179.71 = 132.29 \text{ yuan} \tag{6-1}$$

3 Discussion

This research is to evaluate the profit brought by roof coolers for residents in Chengdu by models. The results of the first model represent that using roof coolers is able to drop the temperature by 5 °C, and the results of the second model indicate that, in the first year, citizens living in Chengdu could economize approximately 100 yuan after utilizing roof coolers. In addition, in the next years, the households without these devices should pay 312 yuan per year constantly, while the others just need to pay 23.71 yuan per year as the value of C_{a2} in common until the devices break down, that is, as time increases, the people who have roof coolers can get more profits. When the coolers are able to work for a decade successfully, they could reduce about 10 times C_{a1}/N minus 9 times C_{a2}/N minus C_t/N as Function (6-2) shown.

$$\begin{aligned} 10 \times 312 - 9 \times 23.71 - 257.71 = 2648.9 \text{ yuan} < P10 \text{ year} \\ = 10C_{a1}/N - 9C_{a2}/N - C_t/N < 10 \\ \times 312 - 9 \times 23.71 - 179.71 \\ = 2726.9 \text{ yuan} \end{aligned} \tag{6-2}$$

A means to bring more benefits is that, in a dense population area such as skyscrapers, train stations, and airports, each person would allocate a lower number of devices so that they could have less cost in purchasing cooling devices because one person has 44 square meters generally, but it is per square meter that, in these zones, accommodates at least one person normally. For instance, in Chongqing Jiangbei International Airport, as the symbolization of the user of the radiative cooling system, there is a cooling system with similar principles being used to save energy and spending, which also contributes to the target of national carbon–neutral standards [20].

Meanwhile, it is difficult to produce roof coolers on a large scale in Chengdu in a short time since the factories need to manufacture about 104.65 million devices (five devices per person), and it is almost impossible for factories in Chengdu to

accomplish the tasks. Hence, the best order to provide cooling equipment is from densely populated regions to unpopulated regions.

4 Conclusion

Overall, this work finds that the cooling devices are able to bring profits in saving the fees used in the air conditioning to the users in Chengdu, especially compared with the profit gained per person in the first year (54.29–132.29 yuan), profit per person in 10 years is far more (2648.9–2726.9 yuan). However, the burden of production is great, so it is almost impossible to provide for all the residents in Chengdu. Consequently, there are three suggestions to governments and films to decrease the negative impact. Firstly, the governments in Chengdu need to encourage relevant corporations to produce such products. Simultaneously, the governments require massive investments on technical personnel to improve productivity since the industrial base is also a significant place where development is needed since the yields impact the cost of production directly because faster production leads to lower staff costs and other costs and considering reducing the power consumption and the economic burden of residents in Chengdu. Thus, the economic spending and time costs are reduced in this way. Secondly, the enterprises involved in producing these devices should guarantee the quality of the equipment, leading to longer use of these devices so that users could save more money, and it is convinced that local people need to take care of these appliances with the related policies put forward by the governments, which makes the life of the appliances extend. Finally, the order in which devices are sold from densely populated regions to unpopulated regions should be adopted by the providers to meet the refrigeration demands of more people in order to reduce more people's electricity bills much more quickly, and then the region with low population density could be considered as the residents living in such region may not gain profit after using the cooling devices. In this way, some electrical energy is saved and some people particularly living in the densely populated area could save much more electricity fees when the roof cooler is used in a proper scale.

Because of the lack of precise data, the values of the unit prices and volume of the materials of equipment are assessed or estimated. Additionally, some risk factors like the impact of high wind and rain on the coolers mounted on the rooftop and the influence of thieves are overlooked, perhaps resulting in inestimable demands in real life. Consequently, the actual situation and theoretical calculation may bring distinct results, which means a further study after using this type of device in Chengdu is needed for gaining a more precise result to meet the accurate range of population density under the condition that the use of the equipment is profitable and finding the methods to protect the devices should also be paid attention.

References

1. China National Energy Administration: The National Energy Administration released the electricity consumption in 2015, 15 January 2016 (2016). http://www.nea.gov.cn/2016-01/15/c_135013789.htm. Accessed 5 Dec 2021
2. China National Energy Administration: In 2016, electricity consumption increased by 5.0% year on year, 16 January 2017 (2017). http://www.nea.gov.cn/2017-01/16/c_135986964.htm. Accessed 5 Dec 2021
3. China National Energy Administration: National Power Industry statistics in 2017, 22 January 2018 (2018). http://www.nea.gov.cn/2018-01/22/c_136914154.htm. Accessed 5 Dec 2021
4. China National Energy Administration: The National Energy Administration released statistics on the country's power industry in 2018, 18 January 2019 (2019). http://www.nea.gov.cn/2019-01/18/c_137754977.htm. Accessed 5 Dec 2021
5. China National Energy Administration: The National Energy Administration released statistics on the country's power industry in 2019, 20 January 2020 (2020). http://www.nea.gov.cn/2020-01/20/c_138720881.htm. Accessed 5 Dec 2021
6. China National Energy Administration: The National Energy Administration released statistics on the country's power industry in 2020, 20 January 2021 (2021). http://www.nea.gov.cn/2021-01/20/c_139683739.htm. Accessed 5 Dec 2021
7. China dotcom corporation: People's quick review: in many places, power cuts imposed to ensure that ordinary people's lives are not restricted, 27 September 2021 (2021). https://news.china.com/socialgd/10000169/20210927/40095003_8.html. Accessed 13 Nov 2022
8. The Beijing News: Does China use more electricity than any other country in the world? It is really hot, 10 July 2019 (2019). https://www.bjnews.com.cn/detail/156194721514360.html. Accessed 5 Dec 2021
9. The website of the Central People's Government of the PRC: The action plan for green and efficient refrigeration was issued, 19 June 2019 (2019). http://www.gov.cn/xinwen/2019-06/19/content_5401443.htm. Accessed 13 Nov 2022
10. Economy Daily: The implementation of the new national energy efficiency standard for air conditioners is encouraging the promotion of green and energy-saving products, 22 July 2020 (2020). http://www.ce.cn/cysc/zgjd/kx/202007/22/t20200722_35373425.shtml. Accessed 5 Dec 2021
11. Gentle, A., Aguilar, J., Smith, G.: Optimized cool roofs: integrating albedo and thermal emittance with R-value. Sol. Energy Mater. Sol. Cells **95**(12), 3207–3215 (2011)
12. Raman, A.P., Anoma, M.A., Zhu, L., Rephaeli, E., Fan, S.: Passive radiative cooling below ambient air temperature under direct sunlight. Nature **512**(7528), 540–544 (2014)
13. Yang, X., et al.: Geography 1 Compulsory, 3rd edn., pp. 8–13. People's Education Press, Beijing (2020)
14. Chuanguan News: Interpretation of the Chuanguan. The growth rate of electricity consumption in Chengdu ranks first among the top ten cities in GDP, 8 February 2021 (2021). https://cbgc.scol.com.cn/news/817568. Accessed 5 Dec 2021
15. Sichuan Development and Reform Commission: Notice of Development and Reform Commission of Sichuan Province on adjusting the price of catalog sales in our province, 26 October 2021 (2021). http://fgw.sc.gov.cn//sfgw/tzgg/2021/10/26/594d6fc8bb804a1eae4363607c4988c5.shtml. Accessed 5 Dec 2021
16. Chengdu Bureau of Statistics: Chengdu 7th National Census Bulletin [1] (No.1), 27 May 2021 (2021). http://gk.chengdu.gov.cn/uploadfiles/070332020803/2021052715194162.pdf. Accessed 13 Nov 2022
17. Global Weather Website: Historical weather in Chengdu. (n.d.). https://lishi.tianqi.com/. Accessed 5 Dec 2021
18. Ministry of Human resource and Social Security of China: Information from the 2020 corporate compensation survey, 19 November 2021 (2021). http://www.mohrss.gov.cn/SYrlzyhshbzb/laodongguanxi_/fwyd/202111/t20211119_428286.html. Accessed 5 Dec 2021

19. Sichuan Bureau of statistics, Sichuan Statistical Yearbook 2018 Beijing. China Statistics Press (2019)
20. Zhou, W.: Application of HVAC system in air conditioning energy saving in terminal building—a case study of T3A terminal building of Chongqing Jiangbei International Airport and its comprehensive transportation hub. Low Carbon World **5**, 134–135 (2021)